WHITE PAPER
CINEMATOGRAPHY TECHNICAL STUDY
June 2026

A Study of the DZO Arles Lenses

Instrumental Evaluation and Perceptual Analysis
WHITE PAPER
DZO Arles Lenses

By Alfonso Parra Cinematographer AEC
Featuring an Interview with Adriana Bernal, ADFC

1- Introduction and Methodology

In this article, we analyze the optical performance of selected DZO Arles lenses, with particular emphasis on resolution, contrast, and the overall consistency of the lens set, in the context of the production of the feature film *Indeleble*. The film's cinematography was directed by Adriana Bernal, ADFC, and it was produced by Sagitario Films under the direction of Jairo Estrada. The lenses analyzed in detail are the 35, 50, 75, 100, 135, and 180 mm focal lengths. The 14, 21, and 25 mm lenses are also included in specific sections devoted to resolution analysis.

All tests were performed using a Sony Burano camera recording at a resolution of 8632 × 4856 pixels in a 1.77 (16:9) aspect ratio, at 24 fps with a 1/48 s shutter speed, using the X-OCN LT codec. Post-production was carried out in DaVinci Resolve Studio, while the technical analysis was conducted using Imatest and ImageJ.

Although the article examines the optical characteristics of each lens individually, readers interested in an overall assessment of the lens set may refer directly to the section *Overall Evaluation of the DZO Arles Lens Set* (*p. 68*).

Scope and Limitations of the Study

The results presented in this study should be interpreted within the specific experimental conditions under which the measurements were obtained. Although the methodology was designed to ensure repeatability and internal consistency, the objective was not to establish absolute or universal characteristics of the lenses, but rather to characterize their behavior within a controlled and clearly defined testing framework.

All laboratory measurements were performed using a single camera platform (Sony Burano), recording in the X-OCN LT format under standardized optical conditions. The analyses were conducted at a single working aperture (T4), selected as a representative operating point that allowed consistent comparison across the entire lens set while minimizing the influence of aperture-dependent aberrations. Optical performance is expected to vary at wider or narrower apertures, particularly with respect to field curvature, the balance of aberrations, contrast transfer, and out-of-focus rendering.

Similarly, all measurements were obtained at a single focus distance. Consequently, the results should not be interpreted as a characterization of lens performance throughout the entire focusing range. Variables such as close-focus performance, infinity focus, or optical changes associated with the movement of internal lens groups may partially modify some of the characteristics described here and fall outside the scope of the present study.

The relationship established between the instrumental measurements (MTF, PSF, chromatic aberration, geometric distortion, and other optical parameters) and visual perception should likewise be understood within its intended scope. While the measurements characterize the physical behavior of the optical system, the final appearance of a cinematographic image is influenced by numerous additional factors, including lighting design, exposure, shot composition, the camera's internal image processing, color management, post-production, display technology, and viewing conditions. Consequently, the perceptual interpretations developed throughout this study should not be understood as direct causal relationships, but rather as visual tendencies that are consistent with the measured optical behavior, whose final manifestation will always depend on the combined influence of the variables involved in the construction of the cinematic image.

The feature film *Indeleble*, photographed by Adriana Bernal, ADFC, using the DZOFilm Arles lens set, is incorporated into this research as a **case study** that allows the instrumental observations to be examined alongside their manifestation in a real cinematographic production. Its inclusion is not intended to provide experimental validation of the laboratory measurements, but rather to explore how objectively measured optical characteristics may become evident in images produced under real production conditions. In this sense, the observations derived from the production complement the technical characterization of the lenses by providing a cinematographic interpretation of the results, without seeking to establish universal relationships applicable to every production context.

Within these boundaries, the study provides a coherent and reproducible characterization of the optical behavior of the DZOFilm Arles lens set, integrating objective measurements with a reflection on their visual translation into cinematographic language. Rather than establishing an absolute ranking of optical quality, the results contribute to an understanding of how each focal length organizes resolution, contrast, aberrations, and spatial rendering, offering a useful framework for both technical evaluation and creative decision-making in cinematography.

As a possible direction for future research, this methodology could be extended to include different apertures, focus distances, camera platforms, and sensor formats, as well as the evaluation of additional lens systems using the same testing protocol. Such work would make it possible to investigate the influence of these variables on both optical performance and visual perception under a broader range of shooting conditions, while facilitating comparisons between different families of cinema lenses.

Observations on Resolution Analysis

Our objective is to evaluate the resolution delivered by the lenses as a function of focal length and aperture, as well as its distribution between the center of the image and the peripheral areas.

Resolution was measured using the Imatest ISO 12233:2017 Edge SFR (eSFR) Photographic Chart, which evaluates spatial frequency response through slanted-edge and frequency-pattern analysis.

The measured resolution results from the combined influence of multiple factors, including the image sensor and the recording codec. Any change to these elements would affect the absolute values obtained; however, the relative values and the comparisons between them remain valid references for evaluating the optical performance of the lens set.

The following analysis examines each focal length individually, beginning with the 35 mm lens. The wider-angle lenses could not be evaluated with the same level of precision in this study; however, they are included in the overall evaluation presented in Section 8.

The following MTF curves are presented at both the 50% and 30% contrast thresholds, measured at different locations across the image field.

Resolution is expressed in LW/PH (Line Widths per Picture Height), except in Section 8, where values are reported in cycles per pixel (cyc/pixel). For reference, the theoretical resolution limit of the imaging system without aliasing is:

$$Nyquist = \frac{\text{Picture Height}}{2}$$

$$Nyquist = \frac{4856}{2} = 2428 \text{ LW/PH}$$

Evaluating lenses using both MTF50 and MTF30 provides complementary information about image sharpness. MTF50 represents the spatial frequency at which contrast has fallen to 50%. Because it is sensitive to high spatial frequencies, it is closely related to the lens's ability to resolve fine detail. In practical terms, a high MTF50 generally translates into a sharper, better-defined image, particularly noticeable in theatrical projection, where fine textures can be more readily perceived by the audience.

MTF30, by contrast, corresponds to the spatial frequency at which contrast falls to 30% and better describes lens performance at mid-range spatial frequencies, which play a greater role in human visual perception. For this reason, MTF30 is more closely associated with perceived sharpness, image volume, and the sense of solidity in objects—qualities that become especially important when viewing content on streaming platforms or smaller displays, where extremely fine detail is less critical. Comparing these two parameters provides insight not only into the amount of resolution a lens delivers, but also into how it distributes contrast across the spatial frequency spectrum. Two lenses may exhibit similar MTF50 values while differing in MTF30, producing images with distinct visual characteristics: one offering greater texture separation, the other a softer rendering with greater tonal continuity.

For feature films intended for both theatrical exhibition and streaming platforms, this distinction is particularly relevant. MTF50 ensures that the image retains sufficient detail for large-format projection, while MTF30 contributes to good visual clarity and consistency under more typical viewing conditions. Evaluating both parameters together therefore provides a more complete assessment of a lens's real-world optical performance across different exhibition environments.

Adriana Bernal ADFC

***Adriana Bernal**: From the very beginning, I wanted the film to have a slightly rougher image—less clinical and less overtly digital. Together with Jorge Román, we developed a heavily desaturated LUT with a bleach bypass–inspired look that significantly increased overall contrast. Had the lenses been excessively sharp or too analytical in the way they rendered fine detail, the final image would probably have felt too harsh and overly contrasty.*

What I found interesting about the Arles lenses is that they maintain good resolution without making the image feel hard or overly crisp. That was also reflected in the technical evaluation: although some focal lengths achieved high resolution values, the contrast transitions remained smooth, and the image never acquired an overly sharp or hyper-detailed appearance. Faces retained plenty of

detail without making skin textures look harsh, while backgrounds preserved a sense of atmosphere and tonal continuity. That combination fit perfectly with the visual language we were looking for.
That said, the final look of the film was never determined by the lenses alone. It was the result of how they interacted with every other element of the image: the lighting, the camera, the exposure strategy, and the color workflow.
For me, there was a very specific balance between three elements: the texture produced by the Sony BURANO operating at EI 3200, the high-contrast lighting approach we developed during production, and the bleach bypass–inspired LUT created for the final grade. Within that combination, the Arles lenses worked extremely well because they introduced a degree of softness and tonal continuity that prevented the overall image from becoming excessively harsh.

2- 35 MM LENS

Keeping the broader context of the study in mind, we begin the individual analysis of each focal length with the 35 mm lens, examining its MTF50 curves at different locations across the image field (Figs. 1–4).

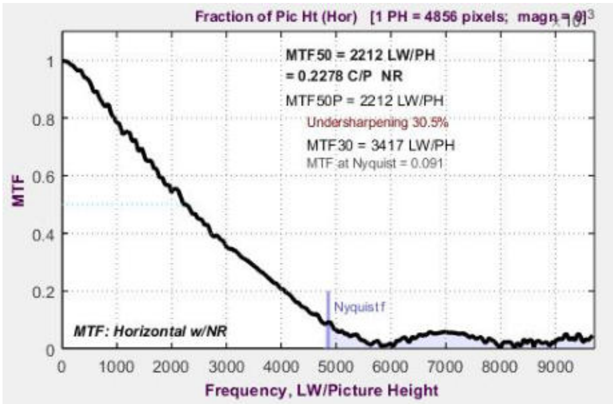

Figure 1. Center of the Image

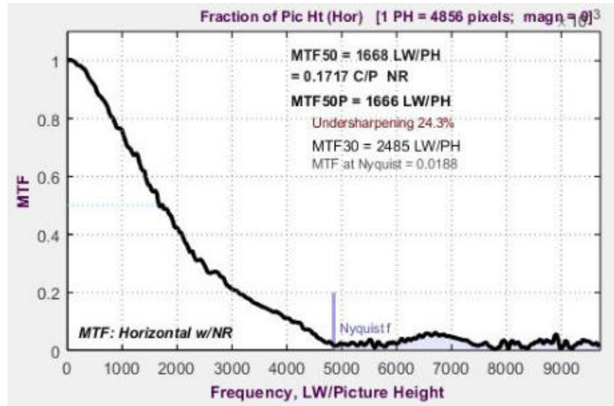

Figure 2. Left Side of the Image

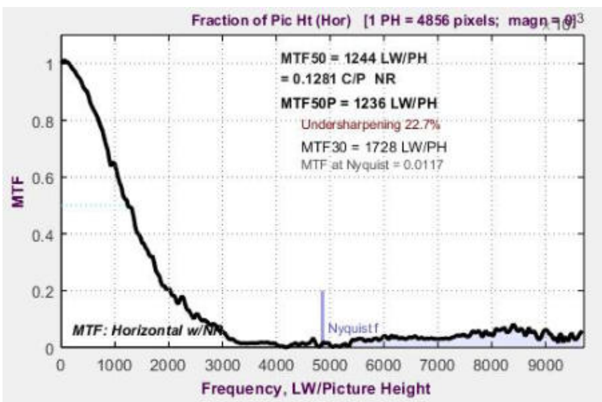

Figure 3. Upper-Left Corner of the Image

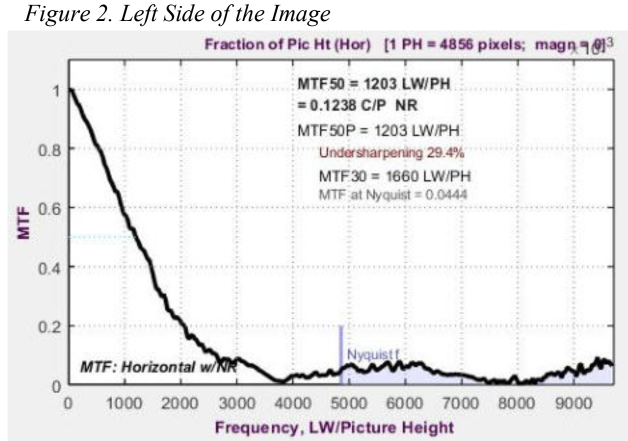

Figure 4. Lower-Right Corner of the Image

Figures 5 and 6 reveal a clear difference in performance between the center of the image and the peripheral regions. At the optical axis, the lens reaches an MTF50 value of 2212 LW/PH, placing it very close to the limit imposed by the sensor under this test configuration. This indicates excellent optical performance and a high resolving capability at the center of the image.

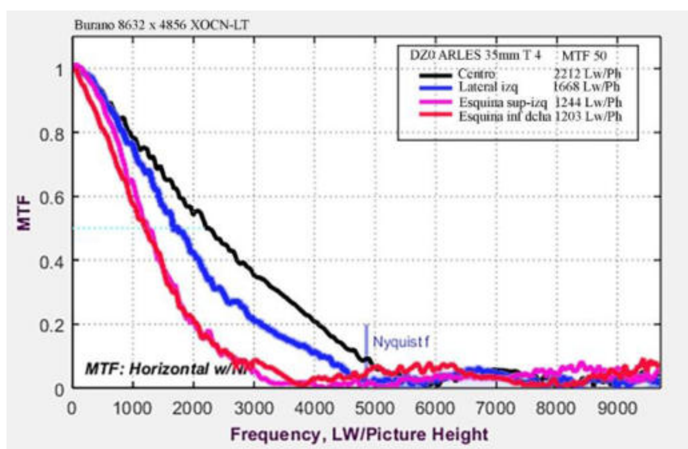

Figure 5. Comparison of the MTF50 Curves

Moving toward the lateral regions of the image, resolution decreases progressively to approximately 1668 LW/PH, before falling further in the corners, where it reaches values of about 1200–1250 LW/PH. Although this reduction is significant, it occurs in a smooth and gradual manner, without irregularities or abrupt transitions, indicating a well-controlled optical design with consistent performance across the entire image field (*Table 1, Figure 7*).

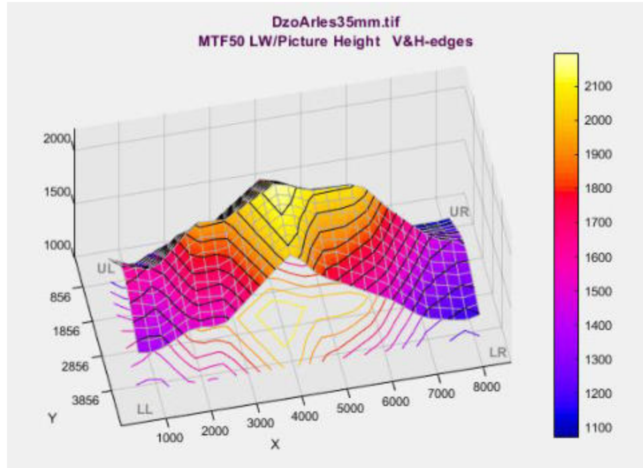

Figure 6. Three-dimensional MTF50 (LW/PH) map of the 35 mm lens at T4, showing a consistent radial distribution, with peak performance at the center of the image and a progressive falloff toward the corners, characteristic of a well-corrected wide-angle

The shape of the MTF curves reinforces this interpretation. At the center of the image, contrast transfer remains high over a broad range of spatial frequencies, whereas in the peripheral regions it declines more rapidly, particularly in the corners, where high-frequency contrast falls off sooner. This behavior is characteristic of wide-angle lenses, in which off-axis aberrations—such as astigmatism and field curvature—have a greater influence on image quality.

Relative to the camera sensor, whose Nyquist limit is approximately 2428 LW/PH, only the center of the image approaches this theoretical threshold, while the rest of the image field falls progressively below it. The result is an image with a highly resolved center and progressively softer edges, concentrating the perception of sharpness along the optical axis while allowing the periphery to provide a gradual transition in detail. Rather than representing a limitation, this controlled falloff contributes to a natural sense of depth and separation between subject and background. Within the DZO Arles lens set, the 35 mm ranks among the highest-performing focal lengths in terms of resolution while maintaining excellent consistency across the image field.

35 MM LENS	LW/PH 50%
CENTER	2212
LEFT SIDE	1668
UPPER-LEFT CORNER	1244
LOWER-RIGHT CORNER	1203

Table 1

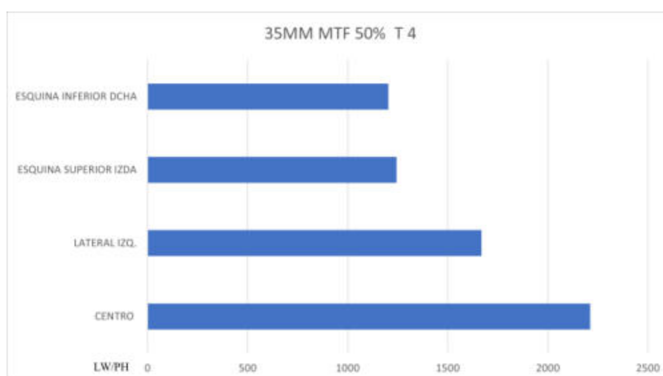

Figure 7.

Table 2 and Figure 8 present the MTF30 values.

35 MM LENS	LW/PH 30%
CENTER	3417
LEFT SIDE	2485
UPPER-LEFT CORNER	1728
LOWER-RIGHT CORNER	1660

Table 2

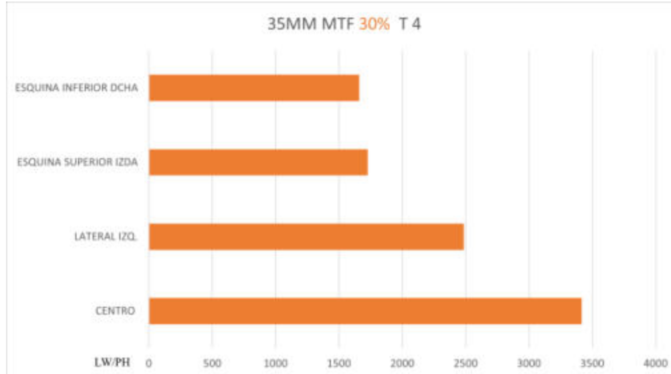

Figure 8

A direct comparison of the MTF50 and MTF30 values across the image field reveals that the spatial performance pattern remains essentially unchanged at both contrast levels. The center consistently delivers the highest resolution, followed by the lateral region and, finally, the corners, where the greatest decline is observed. This indicates that the lens maintains a consistent optical behavior across the spatial frequency spectrum. In practical terms, the image does not change its visual character from the center to the corners; what changes is the amount of resolved information rather than the way contrast is distributed.

At the center of the image, the increase from 2212 LW/PH (MTF50) to 3417 LW/PH (MTF30) reflects a substantial separation between the two metrics. This is characteristic of a lens that not only resolves fine detail effectively but also preserves a high level of contrast at mid spatial frequencies, resulting in an image with a strong sense of presence and solidity. In other words, the image is not simply sharp; it also exhibits rich local contrast.

Moving toward the lateral region, the values decrease to 1668 LW/PH (MTF50) and 2485 LW/PH (MTF30). Although the reduction relative to the center is significant, the relationship between the two metrics remains remarkably stable. This suggests that the loss of resolution is accompanied by a proportional reduction in contrast, without abrupt changes in the overall rendering of the image. The transition is therefore gradual and visually consistent.

In the corners, where MTF50 falls to approximately 1200 LW/PH and MTF30 ranges between 1660 and 1728 LW/PH, the reduction becomes more pronounced. Even so, the relationship between MTF30 and MTF50 remains consistent with that observed across the rest of the image field. This is significant because it indicates that the lens does not introduce anomalous behavior in the outer regions of the image; instead, its resolving power simply decreases in a predictable manner.

Overall, the 35 mm lens exhibits the behavior expected of a well-corrected moderate wide-angle design: high central performance, a progressive falloff toward the edges, and a high degree of consistency between resolution and local contrast. The result is an image with a highly defined optical axis and progressively softer peripheral regions, yet without abrupt discontinuities—an important characteristic in cinematography, where visual continuity between shots is often as important as absolute resolution.

Analysis of the Point Spread Function (PSF) of the 35 mm lens provides a detailed understanding of how light energy is distributed across different regions of the image field and, consequently, helps explain the behavior observed in the MTF curves. At the intermediate image height, located approximately 33.43% of the image field (Fig. 9), the PSF exhibits a compact and relatively symmetrical profile, with major and minor axis dimensions of 3.97 and 3.74 pixels, respectively, and an eccentricity of 0.337. The three-dimensional representation reveals a well-defined, highly concentrated peak, indicating efficient point-image formation and, consequently, strong performance in terms of sharpness and contrast at both medium and high spatial frequencies.

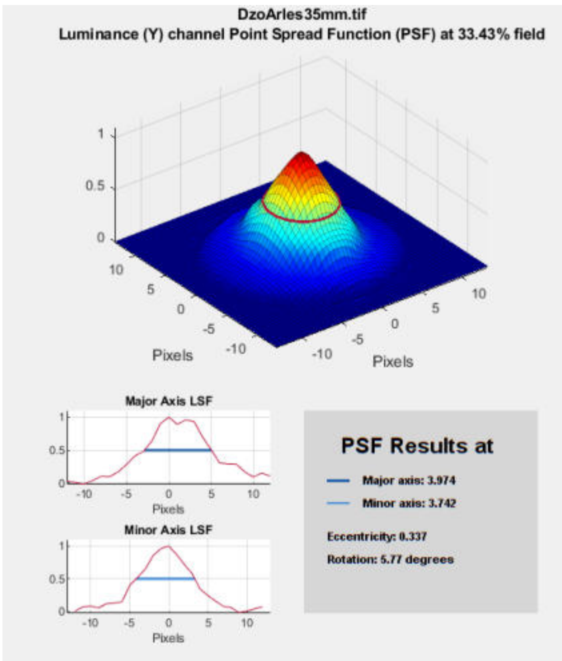

Figure 9

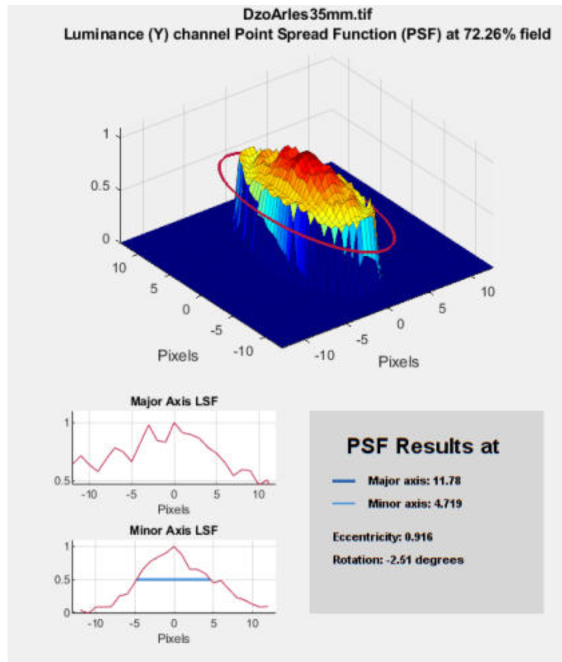

Figure 10

However, toward the periphery of the image field, at approximately 72.26% image height (Fig. 10), the PSF changes markedly. It becomes clearly elongated, taking on a pronounced elliptical shape with major and minor axis dimensions of 11.78 and 4.72 pixels, respectively, and an eccentricity of 0.916. In the three-dimensional representation, this deformation appears as an elongated ridge oriented along a specific direction, revealing an anisotropic distribution of light energy. This behavior is characteristic of off-axis aberrations, primarily astigmatism, which affects image quality differently depending on orientation.

Comparing the two image locations reveals a gradual transition from a compact, concentrated, and efficient point response to a more extended and directional energy distribution. This spatial evolution corresponds directly to the reduction in MTF observed from the center toward the corners of the image. Visually, it results in an image with a well-defined optical axis, while fine detail in the peripheral regions becomes progressively softer and acquires a slight directional character. This smooth, predictable behavior, free from abrupt irregularities, is characteristic of a well-corrected wide-angle lens and forms part of its distinctive visual signature.

Adriana Bernal: *As I mentioned before, the Arles lenses are not exceptionally high-resolution when compared with much more expensive optics. The tests show that the lens set delivers very good central resolution—particularly with focal lengths such as the 35 mm and the 100 mm—while also exhibiting a gradual falloff toward the edges that gives the image its characteristic softer texture.*

For me, that was never a drawback because I was deliberately trying to move away from an image that felt overly clean or excessively sharp. The lenses retain more than enough detail for professional cinema work, but without the overly crisp, clinical rendering that some contemporary lenses can produce.

I also think these lenses have to be understood within the realities of the production environment we work in here in Colombia. Very often, we simply don't have access to optical sets that cost many times more, and in that context, I think the Arles are a very solid option. Their price-to-performance ratio is excellent: they offer good consistency across focal lengths, stable optical performance, and a clearly defined visual character, without reaching price levels that are simply out of reach for many independent or mid-budget productions.

In the end, what mattered to me wasn't achieving the highest possible resolution. What mattered was finding lenses that helped build the atmosphere of the film. And in that respect, the Arles did exactly what I needed them to do.

Adriana Bernal ADFC

Lateral Chromatic Aberration

The following figures present the lateral chromatic aberration measured by Imatest in the peripheral regions of the image.

The lateral chromatic aberration plots (Figs. 11 and 12), measured at two symmetrical locations approximately 75% of the image field, provide an assessment of both the magnitude of the color-channel displacement and its spatial distribution. In both cases, the red, green, and blue channel profiles exhibit the characteristic separation at the edge transition, with the green channel serving as the reference while the red and blue channels are displaced in opposite directions. This pattern is characteristic of lateral chromatic aberration rather than longitudinal chromatic aberration.

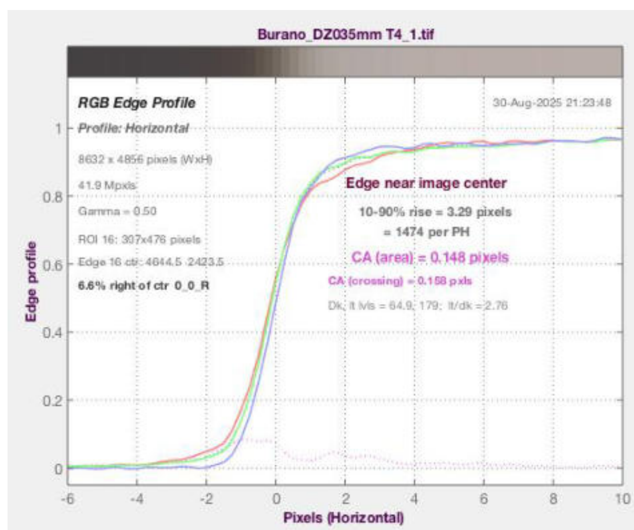

Figure 11. Lateral Chromatic Aberration at the Center of the Image

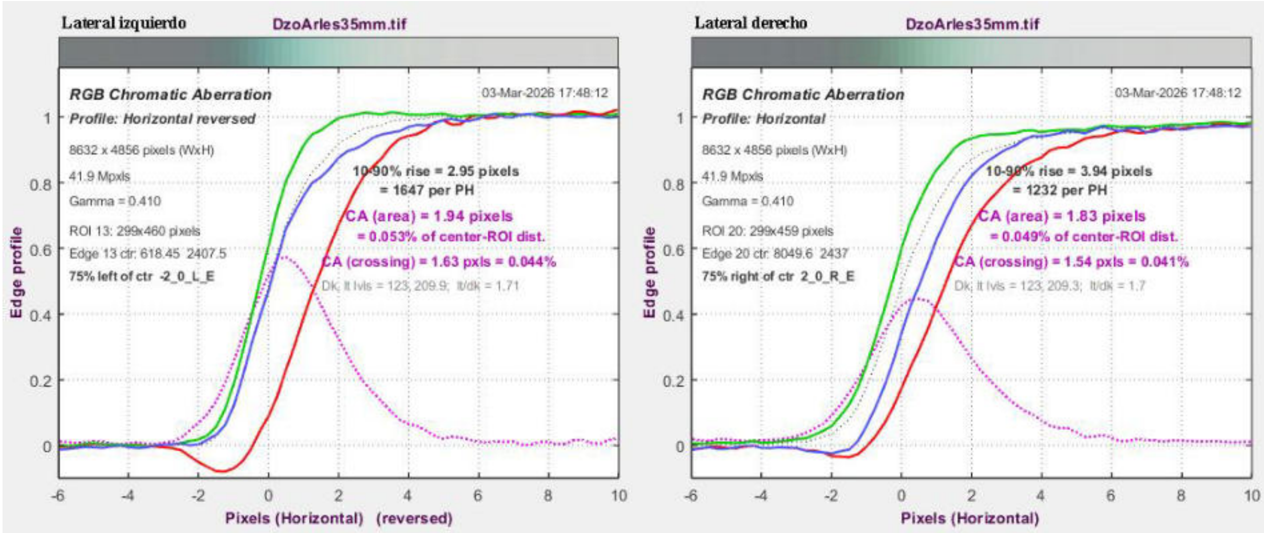

Figure 12. Lateral Chromatic Aberration at the Sides of the Image

Two complementary metrics are used to quantify this displacement. The first, CA (Area), is a perceptual measure of lateral chromatic aberration. It integrates the separation between the color channels across the edge transition and therefore reflects how visible color fringing is in the final image. The second, CA (Crossing), measures the separation between the color channels at the point where each reaches 50% of the black-to-white edge transition (the midpoint of the S-shaped edge profile), providing a geometric measure of the lens's chromatic misregistration.

Quantitatively, the measured values remain low and are very similar on both sides of the image. On the right side, lateral chromatic aberration measures 1.83 pixels for CA (Area) (0.049% of the distance from the image center) and 1.54 pixels for CA (Crossing) (0.041%). On the left side, these values increase only slightly to 1.94 pixels (0.053%) for CA (Area) and 1.63 pixels (0.044%) for CA (Crossing). This small difference indicates a slight asymmetry between the two sides of the image, although it remains well within the normal tolerances expected in a real optical system.

Beyond this minor variation, the most significant finding is the consistency of the lens's behavior. Lateral chromatic aberration remains within a narrow range—approximately 1.5 to 2 pixels—and exhibits no significant irregularities. The channel profiles confirm that the color displacement is concentrated in the region of maximum edge slope, indicating that its visual impact is largely confined to high-contrast transitions.

Taken together with the rest of the analysis, these results indicate that lateral chromatic aberration is not the primary factor responsible for the reduction in resolution toward the peripheral regions of the image. As demonstrated by both the PSF and the MTF measurements, this reduction is mainly associated with off-axis aberrations, particularly astigmatism, together with a directional spread of light energy. In this lens, lateral chromatic aberration is well controlled and plays only a secondary role in its overall optical performance.

From a visual standpoint, these levels of chromatic aberration result in only minimal color fringing along high-contrast edges. Under normal viewing conditions, the effect is rarely perceptible and, if necessary, can be readily corrected during post-production. Overall, the 35 mm lens demonstrates good chromatic correction, consistent with its overall optical performance, while maintaining excellent uniformity across the image field.

The radial chromatic aberration plot (Fig. 13) for the 35 mm lens illustrates how the separation between the color channels increases with distance from the center of the image, providing an overall view of the lens's chromatic behavior across the entire image field. The horizontal axis represents the distance from the image center toward the corner, expressed both as a percentage of the image field and in pixels, while the vertical axis shows the magnitude of the chromatic aberration in pixels. The two main curves represent the displacement between the red and green channels (R–G) and the blue and green channels (B–G), with the green channel serving as the reference.

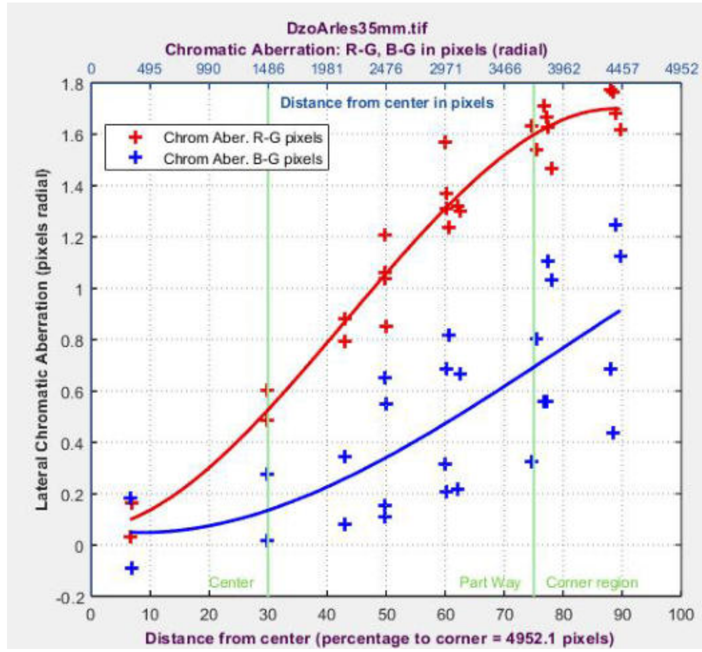

Figure 13

It should be noted that the crosses shown in the plot represent the actual measurements obtained from each Region of Interest (ROI) on the test chart. Each cross corresponds to a discrete measurement of lateral chromatic aberration at a specific location within the image field. The continuous curves represent fitted functions derived from these data points, providing a clearer visualization of the overall trend. The close agreement between the measured data points and the fitted curves indicates a high degree of consistency and uniformity in the lens's behavior, with no significant local variations or notable anomalies. Within the central region of the image—approximately the inner 20% of the image field—lateral chromatic aberration is virtually negligible, with values close to 0–0.1 pixels. This indicates excellent alignment of the color channels and, consequently, the absence of any noticeable color fringing. Moving toward the mid-field region (approximately 40–60% of the image field), channel separation gradually becomes apparent. The red channel progressively diverges, reaching values between 1.0 and 1.4 pixels, while the blue channel exhibits a smaller displacement, typically ranging from 0.3 to 0.7 pixels.

Figure 14. Lateral chromatic aberration of the 35 mm lens. x1500 magnified detail of a lateral perforation from the Vía Stellae test chart, with a slight increase in contrast and saturation to emphasize channel separation.

In the outermost regions of the image, approaching the corners (80–100% of the image field), lateral chromatic aberration reaches its maximum values, with R–G displacement of approximately 1.6–1.7 pixels and B–G displacement between 0.8 and 1.0 pixels (see Table

5). More important than the increase itself—which is expected for lateral chromatic aberration—is the manner in which it develops. The curves exhibit a smooth and regular slope, without irregularities or abrupt transitions, indicating that the aberration is evenly distributed and well controlled across the entire image field.

Another noteworthy characteristic is the difference in slope between the R–G and B–G curves. In this case, the R–G curve increases more rapidly than the B–G curve, indicating that the red channel diverges more strongly from the green channel. This difference not only quantifies the magnitude of the aberration but also determines the dominant color-fringing pattern that will appear in the image, forming part of the lens's chromatic signature (*Fig. 14*).

From a visual perspective, these values result in an image that remains clean at the center, with only a very slight amount of color fringing toward the edges, primarily visible in high-contrast scenes. Since the magnitude of the aberration remains moderate—approximately 1.0 to 1.7 pixels even under the worst-case conditions—its impact on the final image is limited and, if necessary, can be easily corrected during post-production.

Taken together with the rest of the analysis, these results confirm that although lateral chromatic aberration increases toward the image periphery, it is not the primary factor responsible for the reduction in resolution observed near the edges. As demonstrated by both the PSF and the MTF measurements, this degradation is mainly associated with off-axis aberrations, particularly astigmatism, together with a directional spread of light energy. Consequently, the 35 mm lens exhibits excellent chromatic correction consistent with its overall optical performance, maintaining a high degree of uniformity across the entire image field.

It should also be noted that the perceived visibility of lateral chromatic aberration depends on a number of factors, including the capture and display resolution, the nature of the scene content (for example, high-contrast edges versus skin tones), the region of the image being observed (center versus corners), the display size, and the viewing distance—which together determine the viewing angle and the visibility of fine detail—as well as motion itself. In motion-picture applications, for example, lateral chromatic aberration is generally less noticeable in moving shots than in static images.

Geometric Distortion

The geometric distortion analysis of the 35 mm lens (Fig. 15) evaluates how the lens alters the geometry of the scene relative to an ideal rectilinear projection. The primary parameter reported is the SMIA TV distortion, measured at –2.13%, indicating barrel distortion. This produces a slight outward expansion of the image toward the edges of the frame, causing straight lines to appear gently curved.

SMIA TV distortion is a standardized metric that quantifies the maximum geometric deviation of the image from its ideal position,

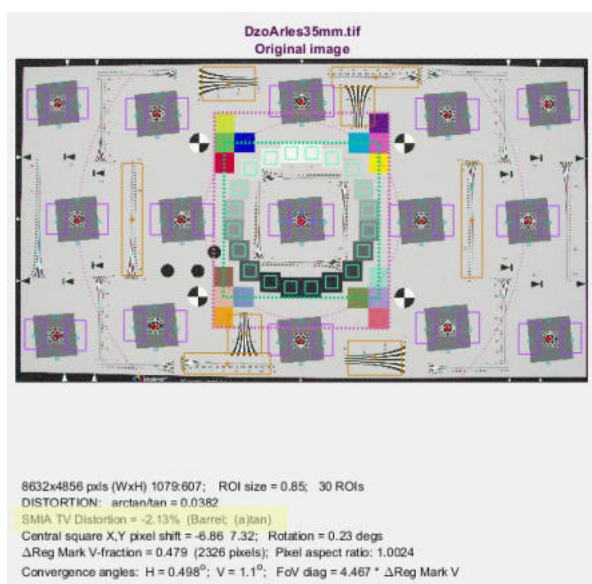

Figure 15

normalized to the Picture Height (PH). In other words, it expresses the displacement of image points near the edges relative to a perfect geometric projection, independently of the sensor resolution. In this case, a value of –2.13% means that the maximum deviation corresponds to approximately 2.13% of the total image height, which, in absolute terms, represents on the order of one hundred pixels in this image format. This metric is particularly useful because it allows the geometric performance of different lenses to be compared on a consistent basis.

Beyond the numerical value itself, the most important aspect is the type of distortion it describes. The measured distortion follows a smooth radial (arc/tan) model, with no evidence of more complex deformation patterns such as moustache distortion. This means that the curvature increases progressively from the center toward the edges of the image while maintaining a smooth and predictable distribution. The center of the image remains virtually free of distortion, whereas the deformation becomes progressively more evident toward the periphery, as is characteristic of this type of lens.

Additional parameters reinforce this interpretation. The small displacement of the optical center (–6.86 / 7.32 pixels) and the negligible image rotation (0.23°) indicate good optical alignment, while the measured pixel aspect ratio (1.0024) confirms that no additional geometric distortion is introduced by the image sensor.

In practical terms, this level of distortion may become visible in scenes containing strong geometric structures—particularly architectural subjects or straight lines located near the edges of the frame. However, its gradual character and moderate magnitude make it largely unobtrusive under typical shooting conditions. Furthermore, because the distortion is smooth and well defined, it can be corrected accurately and efficiently during post-production.

Overall, the geometric performance of the 35 mm lens is fully consistent with what would be expected for this focal length. It exhibits moderate, stable, and easily manageable barrel distortion that does not compromise the structural integrity of the image and remains fully consistent with the overall optical performance observed throughout the rest of the analysis.

Lens Breathing

Both the 35 mm and the 100 mm lenses were evaluated for focus breathing using a quantitative method based on pixel-distance measurements between reference points on a calibrated test chart recorded at different focus positions (in focus and defocused in both directions). The analysis compared the distances between corresponding reference points at the center, intermediate regions, and periphery of the image field *(Fig. 16*).

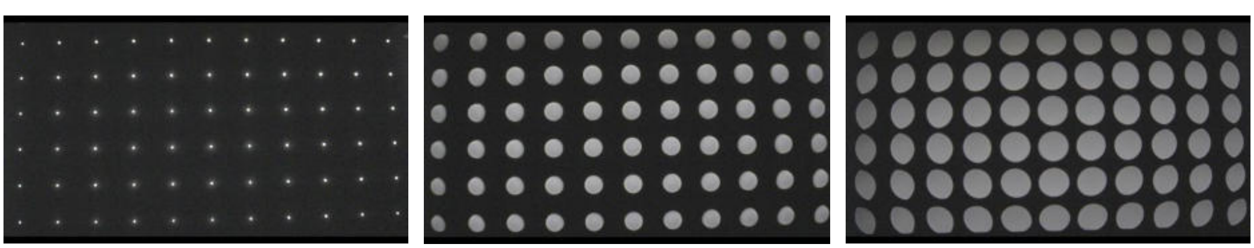

Figure 16. Via Stellae Test Chart at Three Focus Positions

The results show variations consistently below 1%, with no evidence of systematic expansion or contraction of the image, indicating that the measured differences remain within the uncertainty of the measurement. This behavior demonstrates that focus breathing is essentially negligible, with no perceptible changes in framing during focus pulls. The visible differences observed in the out-of-focus images—primarily in the shape and orientation of the blur disks—are attributable to off-axis aberrations rather than to any actual change in image magnification.

The superposition of the three focus positions—the in-focus image together with the defocused images on either side of the focal plane (*Fig. 17*)—provides a clear visualization of the lens's behavior. First, it confirms the stability of the framing: the reference points maintain their relative spacing, with no evidence of image expansion or contraction. In other words, the lens exhibits virtually no focus breathing, as changes in focus do not alter image magnification.

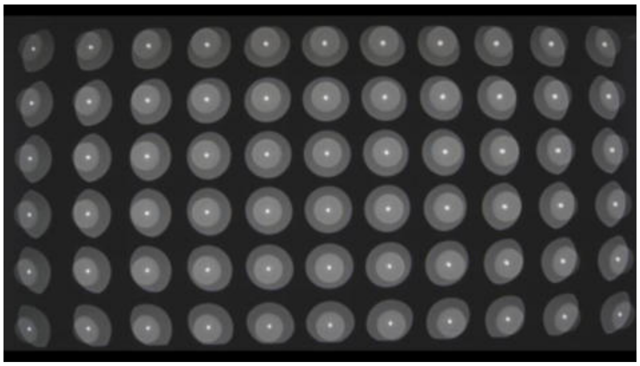

Figure 17

This geometric stability is accompanied by a progressive transformation of the out-of-focus rendering away from the optical axis. Toward the edges of the image, the blur disks become increasingly elliptical and compressed, producing the characteristic cat's-eye bokeh. This phenomenon does not imply a direct loss of illumination or sharpness; rather, it reflects a redistribution of light energy, causing the out-of-focus blur to become more directional and less uniform toward the image periphery.

The comparison between the two defocused images suggests the presence of off-axis aberrations. However, the predominance of mechanical vignetting prevents these aberrations from being isolated with precision. Consequently, phenomena such as astigmatism and field curvature—which were identified in the MTF and PSF analyses—cannot be confirmed directly from these images alone.
The test chart also allows several characteristics of the bokeh to be inferred: it remains uniform near the center of the image and becomes progressively more elliptical toward the edges. Nevertheless, its full aesthetic character can only be appreciated under real shooting conditions.
Overall, the lens combines excellent geometric stability with increasingly complex out-of-focus rendering in the peripheral regions, resulting in a cinematic character that strikes a balanced compromise between optical control and visual expressiveness.

***Adriana Bernal**: I felt the lenses exhibited very little, if any, focus breathing. It wasn't completely absent, but it was never something that concerned us during production or influenced our staging or focus pulls.*
In practice, focus transitions felt very natural, and any change in framing was minimal. I never had the impression that the image expanded or contracted noticeably when pulling focus in either direction.
I also think the overall consistency of the lens set played an important role. The lenses maintained a very consistent visual response across the different focal lengths, and focus breathing never stood out as a defining characteristic of any of them. For the kind of film we were making—with its

emphasis on atmosphere, silence, and careful observation of the characters—that was important because it allowed us to shift focus without drawing attention to the mechanics of the lens itself.

This frame, shot with the 35 mm lens, clearly demonstrates the expansive spatial rendering characteristic of this focal length. The distance between the characters is rendered with remarkable clarity: the foreground figure appears very close to the camera, the central character occupies a distinct spatial plane, and the background recedes noticeably into the distance. Rather than compressing space, the lens organizes the scene through depth.

The 35 mm places the viewer within the scene. The foreground character enters the frame with a strong visual presence, while the running figure and the character aiming the weapon retain their relative positions in space, creating dramatic tension through the relationship between the different planes.

This behavior is consistent with the optical analysis of the 35 mm lens. The MTF measurements show strong central performance with a gradual falloff toward the edges, which in this scene translates into clear emphasis on the main action while preserving sufficient detail throughout the rest of the frame without creating visual competition. The PSF characteristics and the more moderate defocus, compared with the longer focal lengths, allow multiple depth planes to remain simultaneously legible.

Although lateral chromatic aberration is somewhat more pronounced than in the longer focal lengths, it remains well controlled and produces no visible artifacts, even in high-contrast areas such as the outlines of the figures or the texture of the wall. Geometric distortion is also low, allowing the architectural lines of the environment to remain stable and unobtrusive, while the natural perspective of the 35 mm introduces a subtle expansion of objects in the foreground.

Overall, the 35 mm is not intended to isolate the subject but to organize the scene through depth. The image is constructed around the spatial relationships between its elements, creating a strong sense of three-dimensionality in which the dramatic tension arises primarily from the interaction between the different depth planes rather than from shallow depth of field or spatial compression.

Adriana Bernal*: I don't remember noticing any major differences in the bokeh between the longer focal lengths, at least not differences that affected the visual continuity of the film.*

I think the Arles lenses have a very smooth and natural out-of-focus rendering. The defocused areas never draw too much attention to themselves or create an exaggerated separation between the subject and the background. That helped maintain an image that felt more cohesive and less driven by the effect itself.

The technical tests reflected something similar. The lenses exhibit a gradual falloff in contrast together with relatively gentle peripheral resolution, particularly away from the optical axis. As a result, the transition from sharp focus to defocus feels smooth rather than abrupt. Backgrounds retain texture and atmosphere, but without competing with the main subject.

With the longer focal lengths, there was naturally a greater sense of spatial compression and the backgrounds appeared more compact, but the overall character of the out-of-focus rendering remained remarkably consistent. I never felt that any one focal length produced a bokeh that looked fundamentally different from the rest of the set.

Filming of Indeleble

3- 50 MM LENS

MTF Curves at Different Locations Across the Image Field (Figs. 18–21)

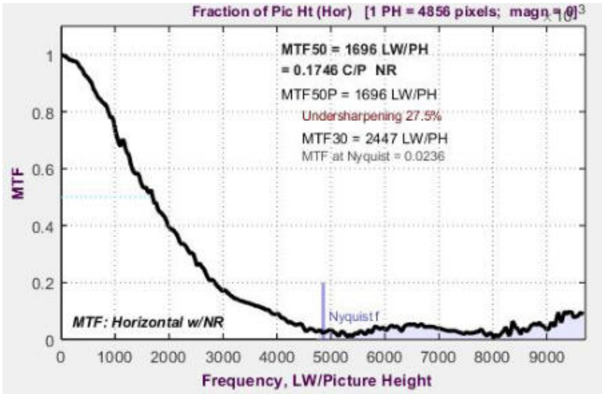

Figure 18. Center of the Image

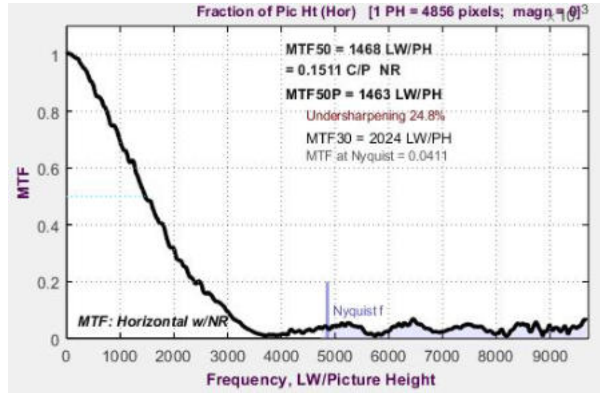

Figure 19. Left Side of the Image

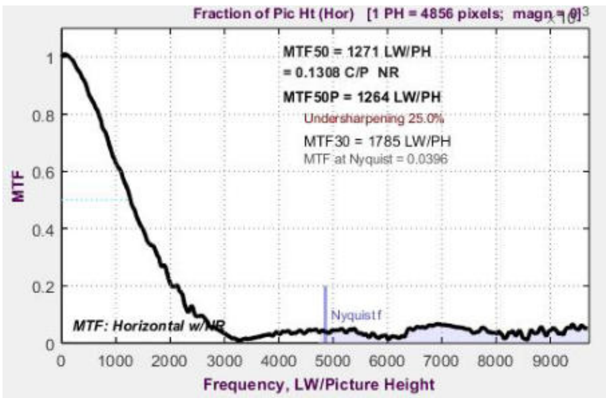

Figure 20. Upper-Left Corner of the Image

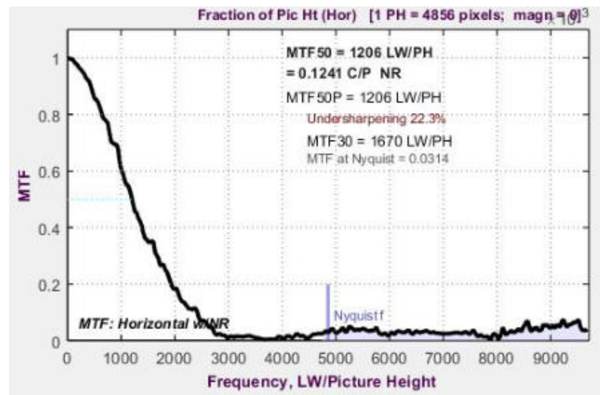

Figure 21. Lower-Right Corner of the Image

The analysis of the 50 mm lens reveals a behavior consistent with that observed in the 35 mm, although with slightly lower overall performance and a more pronounced falloff toward the periphery of the image field. At the center, the lens achieves an MTF50 value of 1696 LW/PH, which is taken as the 100% reference. From this point, resolution decreases progressively with increasing distance from the optical axis. In the left side of the image, the MTF50 value falls to 1468 LW/PH, representing an approximately 13.4% reduction relative to the center. Although moderate, this decrease already indicates a measurable reduction in local contrast away from the optical axis. The degradation becomes more pronounced in the corners: the upper-left corner reaches 1271 LW/PH, corresponding to a 25.1% reduction, while

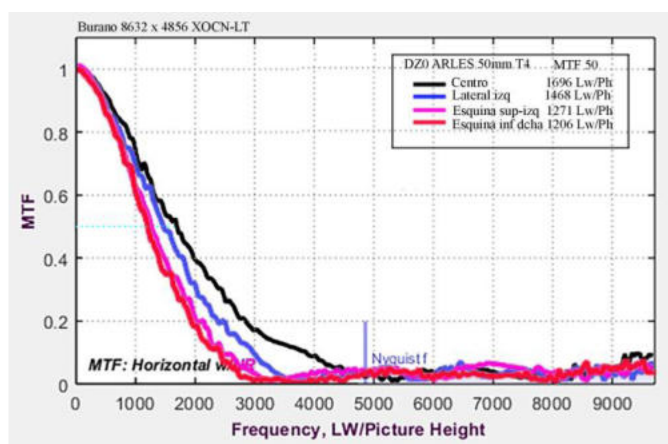

Figure 22

the lower-right corner falls to 1206 LW/PH, representing an overall decrease of approximately 28.9%.
The comparison of the MTF curves (Fig. 22) clearly illustrates this behavior. The central curve exhibits a gradual and relatively stable decline, although the transition toward the mid-spatial frequencies occurs more rapidly than in the 35 mm lens, indicating a lower ability to maintain contrast in this frequency range. Moving toward the peripheral regions of the image field, the curves separate in a smooth and orderly manner, without intersections or irregularities, confirming that the degradation is structural rather than the result of localized anomalies. This pattern is characteristic of performance losses associated with off-axis aberrations, particularly astigmatism and field curvature, which primarily affect the lateral regions of the image and become more pronounced in the corners.

The three-dimensional MTF50 map (Fig. 23) provides a spatial visualization of what is already suggested by the MTF curves: a progressive reduction in resolution from the center toward the periphery of the image field, with a distribution that, although consistent, is less uniform than that observed in the shorter focal lengths. The highest performance is concentrated at the center of the image, where values exceed 1600–1700 LW/PH, forming a relatively well-defined plateau. However, this region of peak performance is not particularly extensive and begins to decline rather rapidly toward the mid-field, producing a steeper surface gradient than that observed in the 35 mm lens.

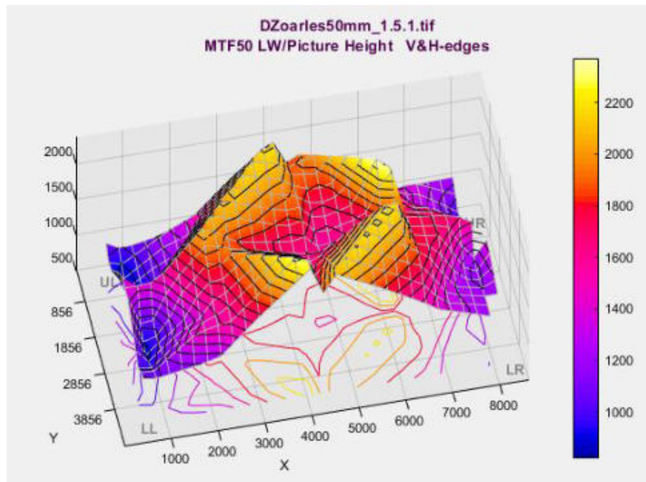

Figure 23

Statistically, the weighted mean MTF50 is 1573 LW/PH, with representative values of 1720, 1708, and 1077 LW/PH for the center, intermediate regions, and corners, respectively, and a minimum value of 773 LW/PH at the least favorable image locations. These data reflect a substantial reduction in performance toward the periphery, consistent with the 25–30% loss already observed in the MTF50 measurements. The map also reveals a slight asymmetry in the spatial distribution of performance, with differences between various regions of the image field becoming more apparent in the corners. Although not severe, this irregularity suggests that the off-axis degradation is not entirely uniform, possibly owing to aberrations such as astigmatism or to minor optical alignment deviations.

The relationship between this map and the MTF curves is straightforward. Whereas the MTF curves describe the response at specific sampling locations, the three-dimensional map illustrates the continuity of that behavior across the entire image field. The progressive separation of the MTF curves is represented here as an inclined surface, where the loss of resolution follows an overall radial pattern while also revealing local variations that cannot be fully appreciated from point measurements alone.

From a practical imaging perspective, this behavior indicates that the 50 mm lens delivers good central definition but exhibits a progressive reduction in sharpness toward the edges that is not entirely uniform. As a result, the image maintains a strong central rendering while displaying some variation in fine-detail rendition across the peripheral regions, particularly in scenes that demand consistently high resolution throughout the frame. Overall, the 50 mm lens demonstrates consistent optical behavior, although it is less spatially uniform than the 35 mm lens. This lower degree of field uniformity may become relevant in applications where consistent sharpness across the entire image field is critical.

Tables 3 and 4, together with Figures 24 and 25, present the MTF50 and MTF30 measurements, respectively.

50 MM LENS	LW/PH 50%
CENTER	1696
LEFT SIDE	1468
UPPER-LEFT CORNER	1271
LOWER-RIGHT CORNER	1206

Table 3

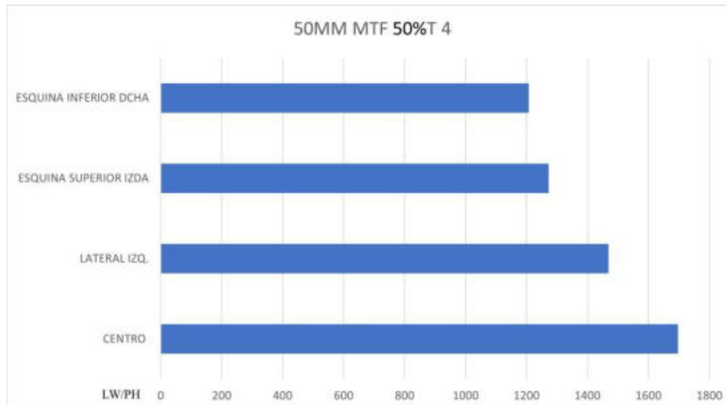

Figure 24

50 MM LENS	LW/PH 30%
CENTER	2447
LEFT SIDE	2024
UPPER-LEFT CORNER	1785
LOWER-RIGHT CORNER	1670

Table 4

Figure 25

Comparing the MTF50 and MTF30 values of the 50 mm lens provides a more refined assessment of its optical performance by complementing resolution measurements with information about contrast at mid-spatial frequencies, which plays a key role in visual perception.

The MTF50 results exhibit the pattern already described: strong central performance followed by a progressive decline toward the image periphery, with losses approaching 30% in the corners. The MTF30 measurements, however, reveal a more nuanced behavior. Although contrast also decreases from the center toward the edges, the falloff is less pronounced and remains at relatively high levels across the entire image field.

This indicates that, while the lens loses some ability to resolve the finest spatial detail (as reflected by MTF50), it preserves contrast at mid-spatial frequencies more effectively (as reflected by MTF30). In practical terms, although the extreme sharpness of the image decreases toward the corners, the overall perception of sharpness remains more consistent than the MTF50 values alone would suggest.

The relationship between these two metrics therefore reveals a characteristic behavior:

- MTF50 describes the decline in technical resolving power.
- MTF30 reflects the greater stability of contrast at mid-spatial frequencies.

Overall, the 50 mm lens produces an image that, although less uniform in terms of absolute resolution, appears perceptually more homogeneous because contrast at mid-spatial frequencies is maintained more consistently across the image field. This helps explain why, under real shooting conditions, the reduction in corner sharpness is often less apparent than the MTF50 values alone might imply.

It is also instructive to examine the radial V/H MTF30 plot (Fig. 26). It should be noted that the differences between the discrete MTF30 values and those shown in the radial plot arise from the calculation method. The former correspond to local measurements obtained from specific regions of the image, whereas the radial representation is based on a weighted average of multiple ROIs together with a regression fit. Consequently, it characterizes the overall behavior of the lens rather than its maximum performance at individual measurement locations.

The radial MTF30 plot introduces a particularly important nuance to what has already been observed from the MTF50 measurements and the average values. Not only does performance decline toward the periphery of the image field, but this decline is not entirely continuous or uniform.

Within the central region of the image (approximately 10–30% of the image radius), the lens reaches its highest values, around 3000–3200 LW/PH, confirming strong performance at mid-spatial frequencies. This is consistent with the previous observations: central contrast at mid-spatial frequencies remains robust and exceeds what would be inferred from the MTF50 measurements alone. From this point onward, the curve declines progressively, but with an important characteristic: the rate of decline increases across the mid-field region (approximately 40–70% of the image radius).

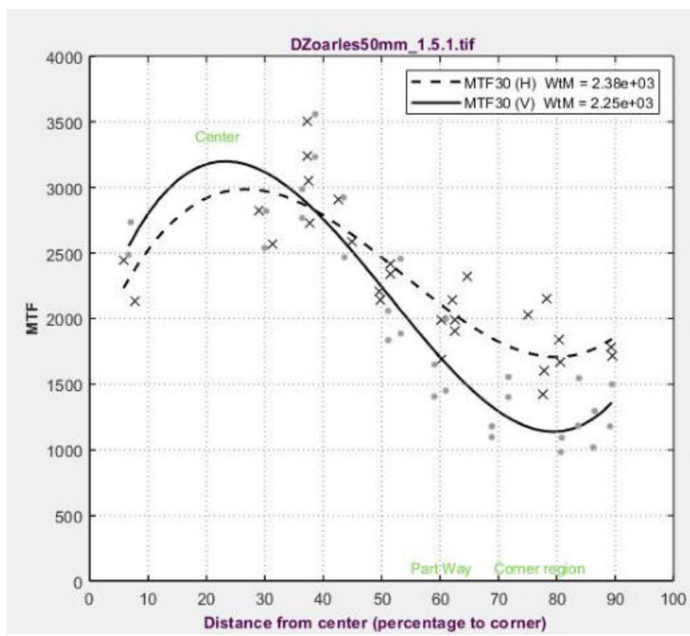

Figure 26

It is within this region that the most significant loss of performance occurs, in excellent agreement with both the three-dimensional MTF50 map and the MTF50 curves. In other words, the lens behavior is defined less by the extreme corners than by the transition from the center toward the intermediate regions of the image field. Indeed, between approximately 70% and 80% of the image radius, the curve reaches its lowest

values—around 1100–1300 LW/PH—confirming a substantial reduction in contrast at mid-spatial frequencies toward the periphery.
An interesting feature, however, appears near the outer edge of the image field (approximately 85–95% of the image radius), where the curve exhibits a slight recovery. This behavior is not typical of a purely radial decline and suggests the influence of phenomena such as field curvature or the interaction between astigmatism and focus, whereby certain peripheral regions may partially coincide with the plane of best focus.

Another key observation is the difference between the horizontal (dashed) and vertical (solid) curves. Although the separation is not large, it becomes clearly noticeable toward the periphery, indicating a moderate degree of astigmatism. In other words, the optical response is not identical for structures of different orientations, a behavior that was already suggested by the slight asymmetry observed in the three-dimensional MTF50 map.
Taken together, this plot confirms and further refines the overall interpretation of the 50 mm lens:

- The lens delivers strong central performance.
- The principal loss of image quality is concentrated in the mid-field region.
- The corners are not always the most critical areas in absolute terms.
- The lens exhibits a degree of anisotropy, meaning that its performance depends on image orientation.

From a perceptual standpoint, this means that the image can retain a convincing impression of sharpness at the center and even in certain peripheral regions, while the transition in detail reproduction is less uniform across the image field. It is precisely this transition—rather than the absolute performance at the corners—that defines the distinctive optical signature of the 50 mm lens within the Arles set.

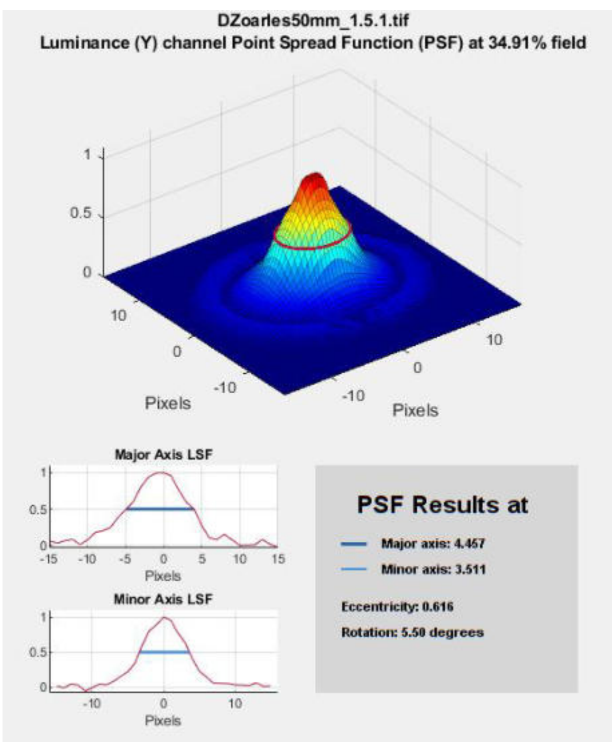

Figure 27

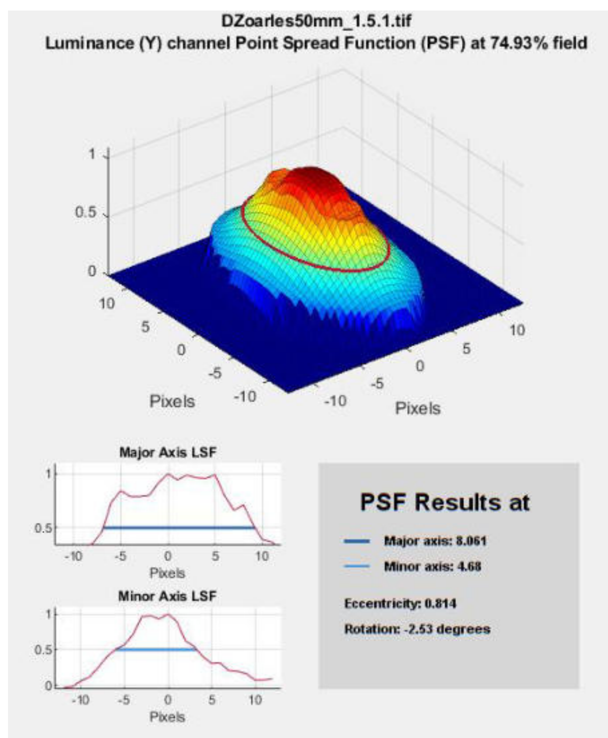

Figure 28

The PSF analysis of the 50 mm lens completes the interpretation of the results presented so far—including the MTF curves, the three-dimensional maps, and the radial distribution—by directly describing how the lens distributes the energy of a point across the image plane.

Near the center of the image (approximately 35% of the image field) (Fig. 27), the PSF remains relatively compact, although it already exhibits slight elongation. The measured major and minor axes (4.457 px and 3.511 px, respectively), together with an eccentricity of 0.616, indicate that the response is no longer perfectly circular. This confirms the presence of a certain degree of anisotropy even at relatively small image heights, a behavior that had already been suggested by the separation between the horizontal and vertical MTF curves. Nevertheless, the light energy remains efficiently concentrated, accounting for the strong central MTF values and the robust contrast at mid-spatial frequencies observed in this region.

The situation changes markedly toward the periphery (approximately 75% of the image field) (*Fig. 28*). Here, the PSF broadens and becomes significantly more distorted, taking on a distinctly elongated elliptical shape with a major axis of 8.061 px, a minor axis of 4.680 px, and an eccentricity that increases to 0.814. This elongation not only indicates a greater spread of light energy but also reveals a pronounced directional dependence, characteristic of astigmatism. The rotation of the major axis (–2.53°) further indicates that this deformation is not aligned with the sensor axes but is instead determined by the optical geometry of the lens.

This behavior provides a direct explanation for the trends observed in both the MTF curves and the three-dimensional MTF map. The reduction in resolution and contrast toward the image periphery is not simply the result of decreased energy concentration, but rather of the way in which that energy is distributed. As the PSF broadens and becomes increasingly elongated, the optical system loses its ability to reproduce fine detail (reflected in the decline of MTF50) while also becoming less effective at preserving contrast at mid-spatial frequencies (as evidenced by the reduction in MTF30 across the intermediate and peripheral regions). Furthermore, the anisotropy observed in the PSF corresponds directly to the separation between the horizontal and vertical curves in the radial MTF plots, confirming the directional nature of the lens's optical performance.

Another important observation is that the degradation is gradual rather than abrupt. The transition from a relatively compact PSF at the center to a markedly elongated response in the peripheral regions closely matches the behavior described previously: the most critical area is not confined to the extreme corners, but rather lies in the transition from the center toward the intermediate regions of the image field, where the greatest loss of optical performance occurs.

From a perceptual standpoint, this behavior means that the 50 mm lens maintains good central definition while introducing a progressive reduction in sharpness accompanied by an increasing directional character in the image toward the edges. As a result, textures become not only softer but also increasingly orientation-dependent, reducing the overall spatial uniformity of the image.

Overall, the PSF analysis provides the physical basis for the observations made throughout this study. The 50 mm lens delivers strong central performance, but its off-axis degradation is dominated by the expansion and deformation of the point spread function, accounting for the lower spatial uniformity together with the progressive loss of resolution and contrast at mid-spatial frequencies described in the preceding analyses.

Lateral Chromatic Aberration

The analysis of lateral chromatic aberration in the 50 mm lens confirms a behavior consistent with that observed in the resolution and PSF analyses: excellent correction at the center of the image, followed by a progressive increase in chromatic displacement toward the periphery, although remaining within moderate levels.

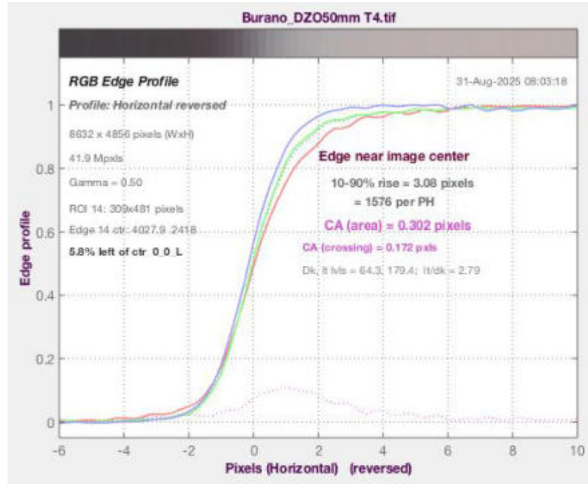

Figure 29. At picture center

At the center of the image (*Fig. 29*), lateral chromatic aberration is virtually negligible. The measured values—CA (Area) ≈ 0.302 pixels and CA (Crossing) ≈ 0.172 pixels—indicate excellent alignment of the RGB channels. The profiles of the three color channels overlap very closely across the edge transition, resulting in an almost complete absence of visible color fringing. This behavior is consistent with the more compact PSF and the strong central MTF values: light energy remains well concentrated, and there is no significant chromatic separation between the color channels.

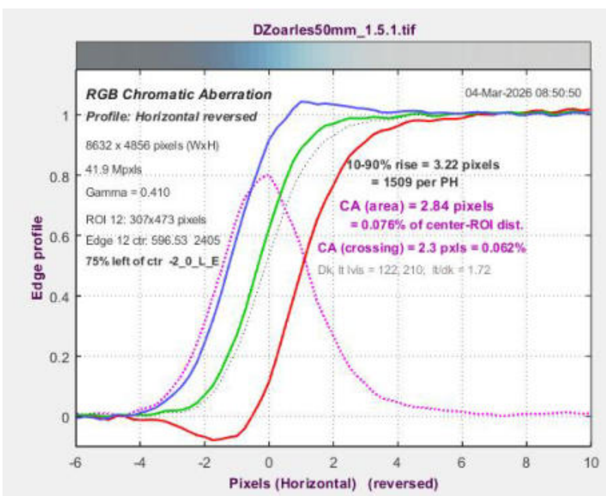

Figure 30. Left Side of the Image.

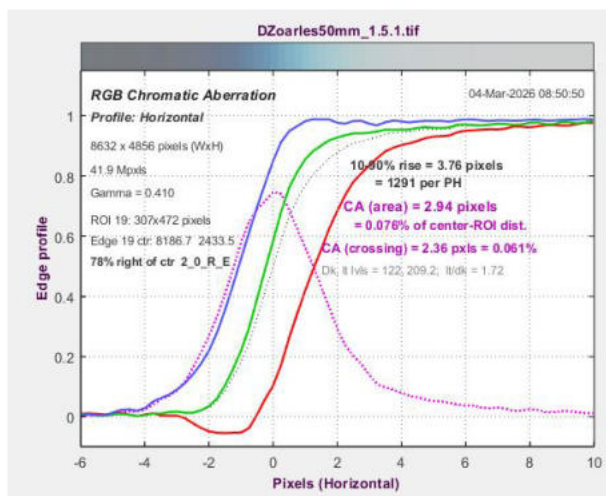

Figure 31. Right Side of the Image

However, moving toward the lateral regions of the image (approximately 75–78% of the image field), the situation changes. Lateral chromatic aberration increases to CA (Area) values of approximately 2.80–2.94 pixels, corresponding to about 0.07% of the distance from the image center, while CA (Crossing) reaches approximately 2.30–2.36 pixels (about 0.06%) (Figs. 30 and 31). This increase reflects a clearly measurable separation between the color channels, visible in the plots as a progressive displacement of the red, green, and blue channel profiles across the edge transition.

Beyond the absolute values, the structure of this separation is particularly significant. The red channel is clearly displaced relative to the green channel, while the blue channel exhibits an

intermediate behavior, indicating that the chromatic aberration is not symmetrical across the three color channels. This pattern determines the type of color fringing that will appear in the image—with one chromatic pair becoming more dominant than the other—and is consistent with the behavior previously observed in the 35 mm lens. In other words, lateral chromatic aberration not only increases with distance from the optical axis but also exhibits a directional component.
Another noteworthy feature is the smooth shape of the channel profiles, which show no abrupt irregularities. This indicates that the aberration is progressive and purely lateral in nature, arising from the optical geometry of the lens rather than from focus-dependent (longitudinal) chromatic aberration. This behavior is fully consistent with the broadening and deformation of the PSF toward the image periphery: as the point spread function becomes larger and increasingly elongated, the individual color channels also become progressively displaced relative to one another, producing the measured chromatic separation.

From a visual standpoint, this means that the 50 mm lens produces a clean image at the center while introducing subtle color fringing along high-contrast edges in the peripheral regions under demanding conditions. Nevertheless, the measured values remain moderate, and because the aberration is regular and highly predictable, its visual impact is generally well controlled.

The radial chromatic aberration plot for the 50 mm lens (Fig. 32) provides a detailed view of how color-channel displacement is distributed across the entire image field and, more importantly, how it evolves with increasing distance from the image center, integrating and extending the observations previously obtained from the edge profiles.

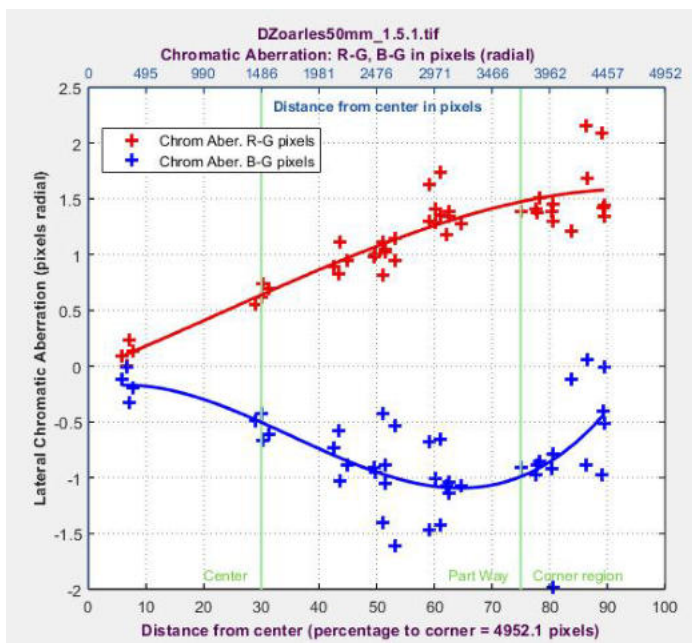

Figure 32

Within the central region (approximately 0–20% of the image radius), lateral chromatic aberration is virtually negligible. Both the R–G (red) and B–G (blue) curves remain very close to zero, confirming that the color channels are well aligned at the center of the image and that no perceptible chromatic displacement is introduced. This is fully consistent with the CA measurements obtained at the image center and with the compact PSF observed in that region.

Moving toward the outer regions of the image field, a characteristic pattern emerges: chromatic aberration increases progressively, but it does so differently for each color channel. The R–G curve rises steadily, reaching approximately 1.5–1.7 pixels near the corners of the image, whereas the B–G curve follows the opposite trend, decreasing to about –1.0 to –1.2 pixels across the mid-field before showing a slight recovery toward the outer edge.

Displacement (px)	Perceptual Level	Visual Description
< 0.3 px	Very low / negligible	Virtually invisible, even at high magnification. Excellent chromatic alignment.
0.3 – 0.8 px	Low	Barely perceptible. Visible only at high magnification or along high-contrast edges.
0.8 – 1.5 px	Moderate	Begins to be noticeable under demanding conditions (strong contrast, fine edges). Generally acceptable in motion-picture imaging.
1.5 – 2.5 px	Moderately high	Clearly visible along high-contrast edges, particularly toward the image periphery. May reduce the perceived cleanliness of the image.
2.5 – 4 px	High	Pronounced color fringing. Visible without magnification in certain areas. May become distracting in theatrical projection.
> 4 px	Very High	Dominant chromatic aberration. Clearly misregistered color edges with an obvious impact on perceived image quality.

Table 5. Reference values for lateral chromatic aberration expressed in pixels. The pixel-displacement values used as perceptual reference correspond primarily to the color-channel separation measured in the radial chromatic aberration analysis, as well as to the CA (Crossing) metric, since both directly quantify the spatial displacement between the color channels. These measurements provide the most direct indication of the visibility of color fringing in the final image.

This behavior has several important implications. First, it confirms the presence of a radial lateral chromatic aberration, in which the color channels progressively diverge in opposite directions as the distance from the optical axis increases. Second, the asymmetry between the R–G and B–G curves indicates that the red channel is displaced more strongly relative to the green channel than the blue channel, defining the characteristic pattern of color fringing that will appear in the image. Rather than being chromatically balanced, the fringing is dominated by a specific color pair.

Another important aspect is the shape of the curves themselves. The R–G curve increases progressively before tending to level off in the outermost regions of the image field, whereas the B–G curve exhibits a steeper decline across the mid-field followed by a slight recovery toward the edge. This indicates that chromatic aberration does not increase at a perfectly uniform rate. Instead, the greatest variation occurs in the intermediate region of the image field, coinciding with the reduction in MTF and the deformation of the PSF observed previously. In other words, the lens behavior is defined not only by the extreme corners but also by the transition from the image center toward the periphery.

The crosses superimposed on the curves represent the actual measurements obtained from each ROI. Their relatively small dispersion confirms that the lens exhibits consistent behavior across the image field, with no significant localized anomalies. As noted previously, the continuous lines correspond to the regression curves that describe the overall trend of the measurements.

From a visual standpoint, this pattern results in an image that is essentially free of chromatic aberration at the center, with color fringing appearing progressively toward the edges, particularly along high-contrast transitions. The measured displacement—approximately 1.0 to 1.7 pixels—falls within the moderate range, meaning that the effect becomes noticeable under demanding conditions but is not visually dominant.

Overall, this plot clearly demonstrates that the chromatic aberration of the 50 mm lens is progressive, radial, and directional, and that its evolution is closely linked to the same optical phenomena responsible for the reduction in off-axis resolution. The close agreement between these results, the MTF measurements, and the PSF analysis reinforces the overall interpretation of the lens: strong central performance combined with a gradual degradation toward the image periphery that affects both sharpness and chromatic alignment.

Geometric Distortion

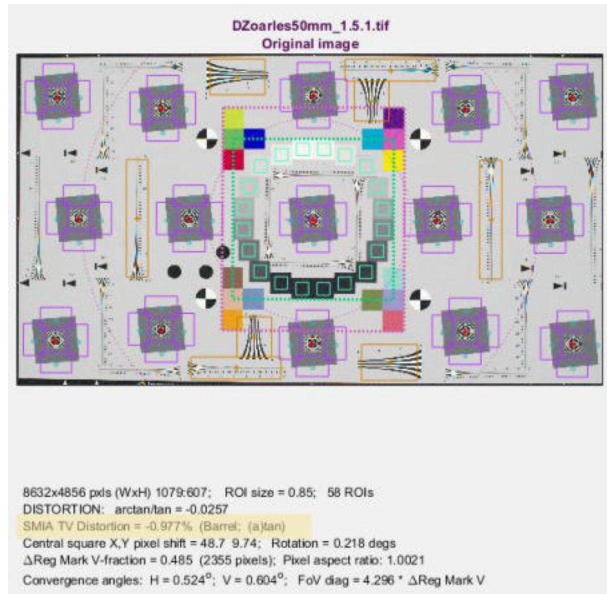

Figure 33

The geometric distortion analysis of the 50 mm lens (Fig. 33) reveals a well-controlled level of distortion, particularly when considered alongside the resolution and aberration measurements.

The primary parameter reported by Imatest is an SMIA TV distortion of –0.97%, indicating a slight barrel distortion. The negative value confirms that straight lines bend gently outward toward the edges of the frame, although the magnitude remains below 1%, a level that can be regarded as moderate in practical imaging applications.

The fitted arc-tangent (arc-tan) model yields a value of –0.0257, reinforcing the conclusion that the distortion is smooth and progressive, without complex inflections or irregular behavior. In other words, the lens does not exhibit a strongly pronounced distortion pattern, but rather a relatively uniform global geometric deviation.

Another relevant parameter is the displacement of the optical center (48.7, 9.74 pixels), indicating that the optical axis is not perfectly coincident with the geometric center of the image sensor. Although this offset is small relative to the overall image resolution, it may contribute to a slight asymmetry in the perceived distortion, a behavior that had already been suggested by the non-uniform distribution of optical performance observed in both the MTF maps and the PSF analysis.

The measured image rotation (0.218°) is essentially negligible and does not introduce any significant geometric effects.

Overall, these results are fully consistent with the previous analyses. Although the 50 mm lens exhibits a more pronounced reduction in resolution together with stronger off-axis aberrations than the 35 mm lens, geometric distortion is not a dominant factor in its optical performance. The lens maintains high geometric fidelity in the rendering of straight lines, with a slight, uniform, and predictable barrel distortion that produces a visually stable image geometry, even in wide compositions. As a result, attention is drawn primarily to the gradual loss of sharpness and the off-axis optical behavior rather than to any structural deformation of the scene, consistent with an optical design whose principal limitations lie in the spatial uniformity of its performance rather than in its geometric accuracy.

This frame is highly consistent with the optical behavior described throughout the technical analysis of the 50 mm lens. The definition of the main subject is high, yet without appearing excessively harsh, while the transition into the out-of-focus regions remains smooth and progressive, without abrupt edges. This closely reflects the MTF measurements, which show strong central performance combined with a gradual decline toward the image periphery, associated more with a reduction in fine-detail contrast than with any abrupt degradation of image quality.

The separation between depth planes also reflects this balance. The background is clearly out of focus, yet it retains sufficient structure and legibility, avoiding both complete dissolution and an overly dominant bokeh. This observation is consistent with the conclusions drawn from the defocus analysis of the 35 mm lens: although off-axis aberrations become apparent under the controlled conditions of the laboratory charts, in real-world imagery the lens exhibits a restrained rendering, where cat's-eye bokeh and other peripheral blur characteristics remain subtle unless the scene itself accentuates them.

Chromatic aberration is equally well controlled. The image remains clean even along relatively high-contrast edges, with no perceptible color fringing. This confirms the measurement results, which showed negligible aberration at the center and only a gradual increase to moderate levels toward the periphery—levels that are generally imperceptible under normal shooting conditions. Consequently, the lens introduces no chromatic artifacts that might distract from or compromise the visual clarity of the frame.

The off-axis behavior further reinforces this overall consistency. The reduction in definition toward the edges occurs smoothly and continuously, without noticeable artifacts or irregularities, in agreement with both the radial MTF analysis and the energy distribution revealed by the PSF. Rather than an abrupt loss of image quality, what is perceived is a controlled transition that naturally directs the viewer's attention toward the subject while preserving the spatial continuity of the scene.

In this frame, vignetting is more clearly apparent, shaping the image through a gradual concentration of luminance toward the center of the frame. The lateral regions and corners exhibit a noticeable falloff, although it remains smooth and naturally integrated into the visual structure of the scene rather than appearing abrupt.

At the same time, veiling glare is more evident than in lower-contrast situations. The bright exterior highlights appear gently softened, while the interior shadows remain slightly elevated, producing a compression of overall image contrast without any significant loss of structural detail.

This behavior corresponds closely to the MTF response at low spatial frequencies, which predicts a reduction in overall contrast that, in the image itself, is perceived as greater tonal cohesion. The interaction between vignetting and veiling glare prevents abrupt transitions between regions of different luminance, preserving visual continuity even in a scene with a high dynamic range.

Although the distribution of light within a narrative shot is inevitably influenced by the lighting design, several of the observed characteristics—such as the gradual falloff toward the edges and the compression of overall contrast—cannot be explained solely by the scene lighting.

The smoothness of the tonal transitions, their relative independence from the dominant lighting direction, and, above all, their close correspondence with the laboratory measurements (vignetting, veiling glare, and the MTF response at low spatial frequencies) indicate that these effects are fully consistent with the optical behavior of the lens.

Rather than isolating individual causes, this frame demonstrates how the optical characteristics measured under laboratory conditions are expressed as an integrated whole in real-world cinematographic imagery.

Adriana Bernal*: Veiling glare was definitely present, especially when strong light sources entered the frame directly or were positioned close to the optical axis. It was something we had to keep under control because the lenses reacted quite readily to bright highlights, causing the blacks to lift and the image to take on a slightly milky appearance. That was something we encountered repeatedly throughout the shoot.*

My visual approach relied heavily on silhouettes against bright backgrounds, so it was essential for me to expose the highlights with great precision. At the same time, it required extremely careful control from the camera assistants to keep unwanted flare under control.

At the same time, that behavior was also part of the Arles lenses' character. The veiling glare never looked particularly unpleasant or overly digital. Instead, it introduced a gentle veil over the image that, in certain situations, actually contributed to the atmosphere of the film. There were scenes where I deliberately wanted to preserve some of that veiling glare because it gave the image a certain fragility and helped avoid a look that felt too clean or too perfect.

Director Jairo Estrada and Director of Photography Adriana Bernal, ADFC, on the set of Indeleble.

4- 75 MM LENS

Figures 34–37 present the MTF curves at different locations across the image field.

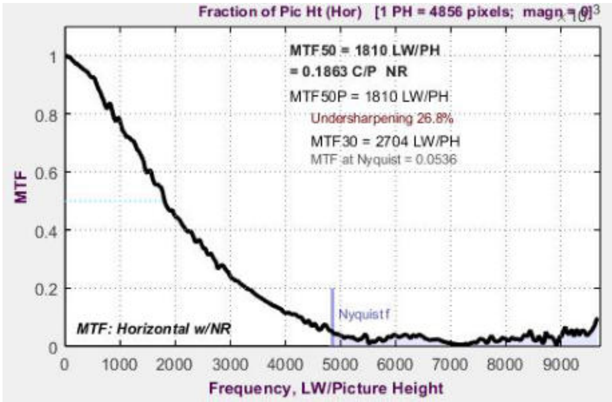

Figure 34. Center of the Image

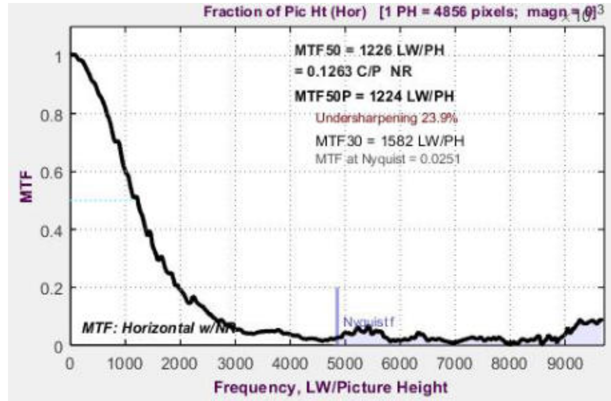

Figure 35. Left Side of the Image

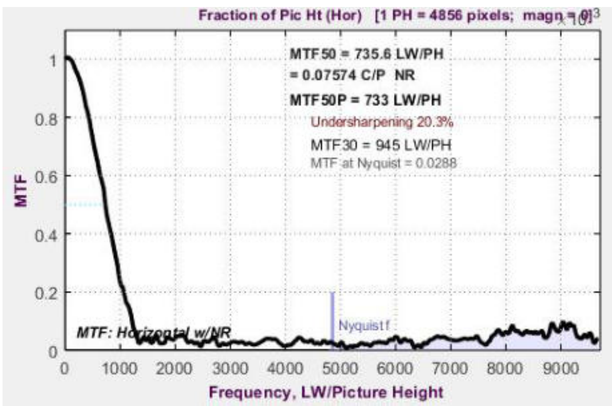

Figure 36. Upper-Left Corner of the Image

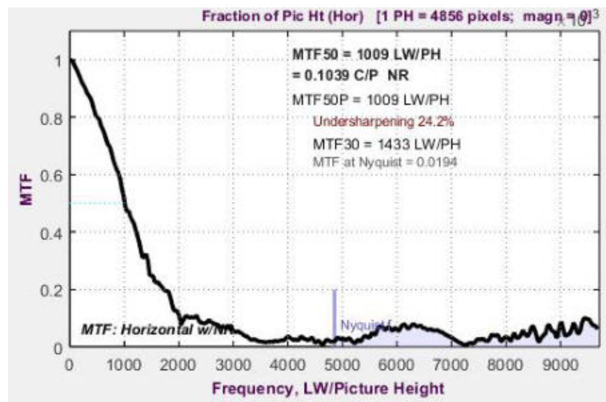

Figure 37. Lower-Right Corner of the Image

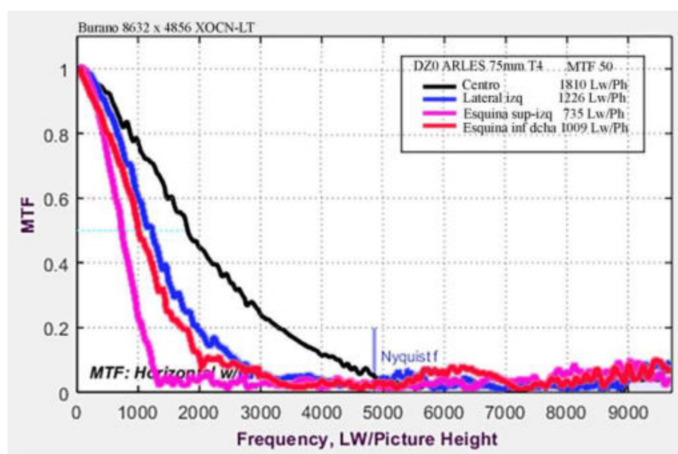

Figure 38

The comparative MTF curves (Fig. 38) of the 75 mm lens reveal a significant departure from the behavior observed in the shorter focal lengths, particularly in terms of performance uniformity across the image field.

At the center of the image, the lens achieves an MTF50 value of 1810 LW/PH, representing solid performance, although slightly lower than that of the 35 mm lens and broadly comparable to the 50 mm. The central MTF curve exhibits a relatively controlled, gradual decline while maintaining a reasonable response at mid-spatial frequencies, indicating strong contrast at these frequencies along the optical axis.

A more pronounced difference emerges, however, as the analysis moves away from the image center. In the left side of the image, the MTF50 value decreases to 1226 LW/PH, representing an approximately 32% reduction relative to the center. This decline is noticeably greater than that observed in the 50 mm lens, indicating a reduced ability to maintain optical performance away from the optical axis.

The degradation becomes substantially more pronounced in the corners. In the upper-left corner, the MTF50 value falls to 735 LW/PH, corresponding to a reduction of approximately 59%, while in the lower-right corner it reaches 1009 LW/PH, representing a loss of about 44%. The difference between the two corners also introduces an element of asymmetry, indicating that the degradation is not entirely uniform across the image field.

The MTF curves illustrate this behavior very clearly. The separation between the central curve (black) and the peripheral curves (blue, magenta, and red) is considerably greater than in the shorter focal lengths, and this divergence occurs at relatively low spatial frequencies. This indicates that the loss of performance affects not only the reproduction of fine detail but also the preservation of contrast at mid-spatial frequencies, with a direct impact on the perceived sharpness of the image.

Another noteworthy aspect is the rate at which the peripheral curves decline toward values approaching zero. This falloff is particularly abrupt in the upper-left corner (magenta curve), indicating a severe reduction in resolving power in that region. This behavior is consistent with the presence of more pronounced off-axis aberrations, particularly astigmatism and field curvature.

The three-dimensional MTF50 map of the 75 mm lens (Fig. 39) clearly confirms what was already suggested by the MTF curves: a pronounced loss of field uniformity and a more irregular spatial distribution of optical performance than in the shorter focal lengths.

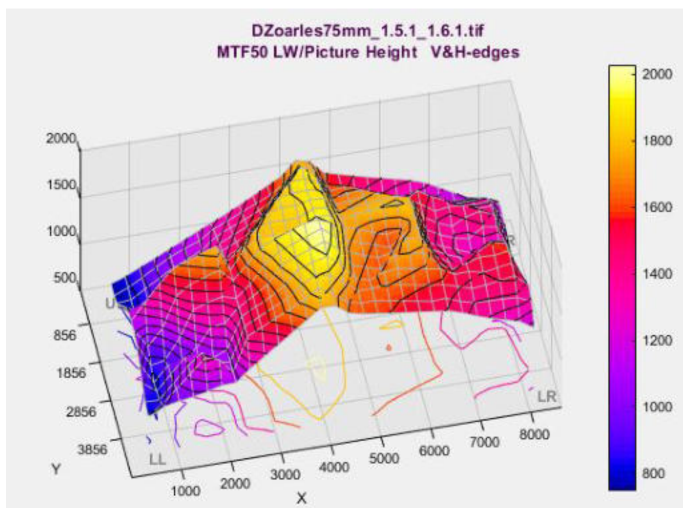

Figure 39

At the center of the image, a well-defined peak is observed, reaching approximately 1800 LW/PH and forming a relatively compact region of maximum performance. Unlike the 35 mm and even the 50 mm lens, however, this central "plateau" is considerably narrower and declines rapidly as the distance from the optical axis increases. The surface gradient is noticeably steeper, indicating a more abrupt transition between the strong central performance and the peripheral degradation.

The statistical data reinforce this interpretation. The weighted mean MTF50 is 1547 LW/PH, with representative values of 1871, 1459, and 1033 LW/PH for the center, intermediate regions, and corners, respectively. This corresponds to an overall reduction of approximately 45% from the center to the corners, consistent with the values already observed in the MTF50 curves. In addition, the minimum value falls to 709 LW/PH, indicating the presence of particularly weak regions within the image field.

One of the most significant features of the map is the asymmetry of the surface. Rather than exhibiting a uniform radial falloff, the topography displays clear irregularities and noticeable differences between various regions of the image field. Some lateral areas retain relatively high performance, whereas others—particularly one of the corners—show a much steeper decline. This lack of symmetry is consistent with the differences observed between the corners in the MTF curves and suggests the presence of non-uniform off-axis aberrations, such as astigmatism combined with minor optical alignment deviations.

In addition, the peripheral "valley" is neither flat nor uniform but exhibits gentle undulations, indicating that the degradation is not entirely regular. This observation connects directly with the radial analysis discussed in the following section: the reduction in performance toward the image periphery is not only progressive but also exhibits localized variations in magnitude.

From a practical imaging perspective, this behavior results in an image with strong central definition but a much more pronounced loss of sharpness toward the corners than that observed in the 50 mm lens. Furthermore, the asymmetry between the corners suggests that this degradation may not be perceived uniformly across the frame, introducing a degree of irregularity into the spatial response of the lens.

Overall, the 75 mm lens delivers solid central performance but exhibits a more pronounced and less uniform reduction in resolution than the shorter focal lengths. This indicates lower field uniformity and anticipates what will likely be confirmed by the remaining optical metrics: a stronger influence of off-axis aberrations together with reduced stability of optical performance across the image field.

Tables 6 and 7, along with Figures 40 and 41, present the MTF50 and MTF30 measurements, respectively.

75 MM LENS	LW/PH 50%
CENTER	1810
LEFT SIDE	1224
UPPER-LEFT CORNER	733
LOWER-RIGHT CORNER	1009

Table 6

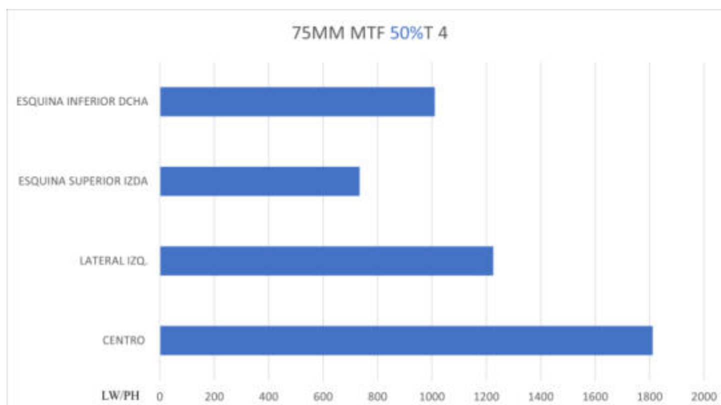

Figure 40

75 MM LENS	LW/PH 30%
CENTER	2704
LEFT SIDE	1582
UPPER-LEFT CORNER	945
LOWER-RIGHT CORNER	1433

Table 7

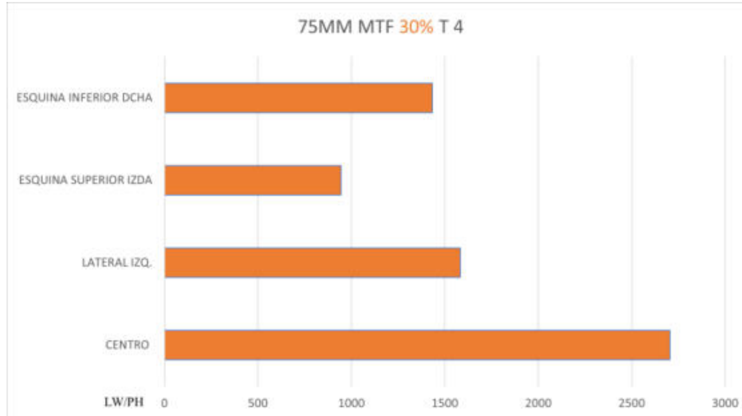

Figure 41

The comparison between the MTF50 and MTF30 results for the 75 mm lens does not reveal a different pattern of behavior; rather, it reinforces the same trend with even greater clarity. Unlike the 50 mm lens, where the MTF30 measurements partially moderated the interpretation suggested by the MTF50 results, both metrics evolve in a remarkably similar manner across the image field in this focal length.

This indicates that the loss of optical performance is not confined to the highest spatial frequencies (fine detail) but also affects contrast at mid-spatial frequencies, which forms the basis of perceived sharpness. In other words, the 75 mm lens not only loses resolving power in the peripheral regions but also becomes less capable of preserving the structural integrity of the image, making the degradation more readily apparent to the viewer.

Another important observation is that the relationship between the two metrics remains relatively stable across the different regions of the image field. There is no significant perceptual compensation: contrast at mid-spatial frequencies does not mitigate the loss of resolution but instead declines in parallel with it.

In practical terms, this places the 75 mm lens in a different position within the Arles set: the loss of performance toward the image periphery is not masked by the MTF30 response but instead becomes more directly apparent. Consequently, the image exhibits a more pronounced and less moderated reduction in sharpness away from the optical axis.

The radial MTF30 plot of the 75 mm lens (*Fig. 42*) effectively summarizes the behavior observed throughout the preceding analyses while adding an important nuance: the degradation is not only pronounced but also more uniform and sustained across the image field.

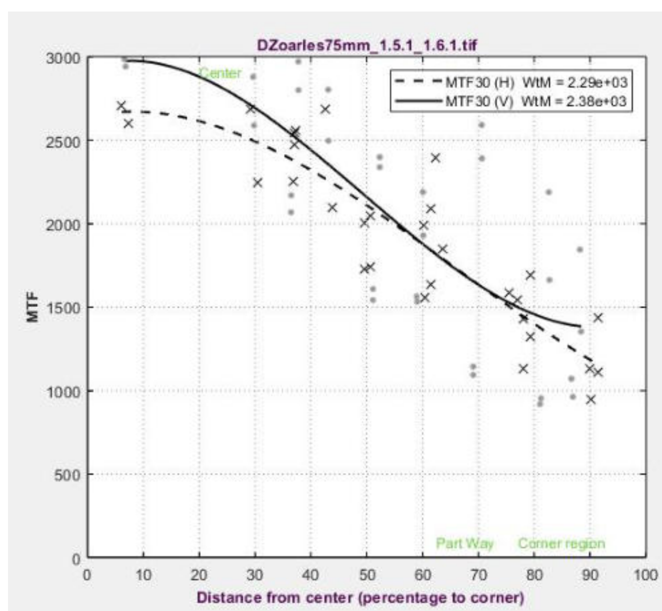

Figure 42

From the center of the image, where the highest contrast at mid-spatial frequencies is achieved, the curve begins a progressive decline that, unlike the behavior observed in the 50 mm lens, shows neither recovery regions nor significant irregularities. The decrease is continuous and consistent all the way to the periphery, indicating that the loss of performance is not confined to a particular region but extends steadily from the optical axis toward the corners.

This behavior is particularly significant because it confirms the interpretation already suggested by the comparison between the MTF50 and MTF30 measurements. In the 75 mm lens, there is no clear perceptual compensation: contrast at mid-spatial frequencies does not remain stable across the intermediate regions but declines in parallel with the reduction in resolving power, reinforcing the perception of diminishing sharpness throughout the image periphery.

Another important feature is the difference between the horizontal and vertical curves. Although not pronounced, a consistent separation between them is clearly evident, indicating that the optical response depends on the orientation of image structures. This behavior is consistent with the PSF analysis, where a marked elongation of the point spread function was already observed, confirming astigmatism as one of the principal contributors to the off-axis degradation.

The dispersion of the individual measurement points remains relatively limited, indicating that the overall behavior of the lens is reasonably stable despite some local variability. This is fully consistent with the three-dimensional MTF map: rather than exhibiting abrupt irregularities, the lens displays a generalized reduction in performance across the image field.

From a perceptual standpoint, this behavior means that image sharpness does not deteriorate only in the corners but decreases progressively from the center outward, without intermediate regions where contrast recovers. As a result, the image appears less uniform across the entire field, particularly when compared with the shorter focal lengths.

Overall, the radial MTF30 plot reinforces the general interpretation of the 75 mm lens: it delivers good central performance but exhibits continuous degradation, without perceptual compensation and with a measurable degree of directional dependence. This explains the lower field uniformity observed throughout the remaining optical metrics.

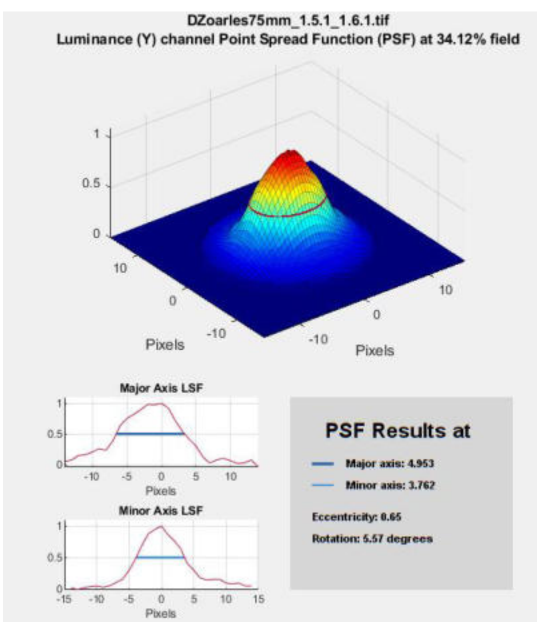

Figure 43

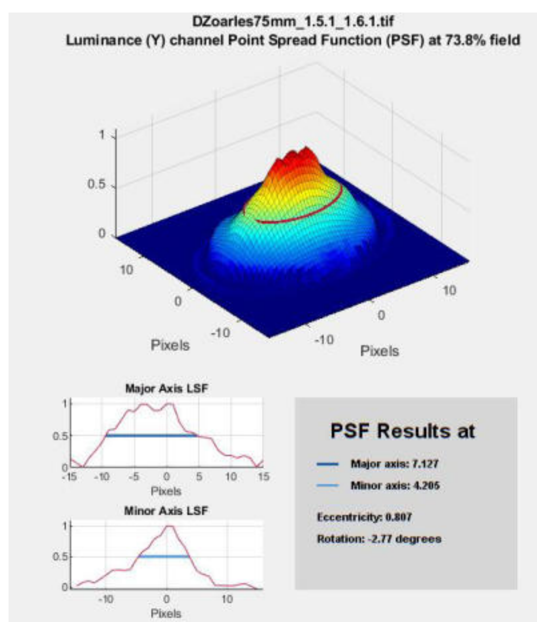

Figure 44

The PSF analysis of the 75 mm lens provides a direct physical explanation for the behavior previously observed in the MTF measurements and the three-dimensional map, confirming that this focal length is characterized not only by a reduction in optical performance but also by a change in the way light energy is distributed across the image.

Near the center of the image (approximately 34% of the image field) (Fig. 43), the PSF remains relatively compact, although it already exhibits noticeable elongation. The measured major and minor axes (4.953 px and 3.762 px, respectively), together with an eccentricity of 0.650, indicate that the response is not perfectly symmetrical. In other words, even before reaching the image periphery, the lens already exhibits a degree of directional dependence, consistent with the slight separation between the horizontal and vertical responses suggested by the MTF curves.

The most significant change, however, occurs toward the periphery of the image (approximately 74% of the image field) (Fig. 44). Here, the PSF broadens and becomes clearly more distorted, with a major axis of 7.127 px, a minor axis of 4.205 px, and an eccentricity increasing to 0.807. Rather than remaining approximately point-like, the PSF evolves into an elongated distribution with a well-defined orientation. This behavior is characteristic of astigmatism, in which light energy is no longer concentrated into a single point but is distributed differently depending on direction.

This broadening and deformation of the PSF provides a direct explanation for the behavior described in the preceding sections, but with an important distinction. In the 75 mm lens, not only is the useful light energy reduced, but it is also distributed less efficiently. Consequently, unlike the 50 mm lens—where the MTF30 measurements still exhibited a degree of stability—contrast at mid-spatial frequencies also declines significantly, because the energy is no longer sufficiently concentrated to preserve the structural integrity of the image.

Furthermore, the orientation of the PSF (5.57° in the intermediate region and –2.77° toward the periphery) indicates that this deformation is neither uniform nor aligned with the sensor axes. This contributes directly to the asymmetry in optical performance previously identified in the three-dimensional MTF map and in the differences observed between the image corners.

Another important aspect is the progressive nature of this behavior. The transition from the central PSF to the peripheral PSF is not abrupt, yet it is sufficiently pronounced to create a critical intermediate region where the degradation in image quality accelerates. This is entirely consistent with the previous interpretation: the defining characteristic of the 75 mm lens is determined not only by the extreme corners but by the gradual transition from the image center toward them.

From a perceptual standpoint, this behavior results in an image in which sharpness decreases progressively toward the edges while also acquiring an increasingly directional character in the blur, affecting the rendering of both textures and edges. The loss therefore involves not only resolution but also the spatial coherence with which fine detail is reproduced.

Overall, the PSF analysis confirms and provides the physical basis for the observations made throughout the study. In the 75 mm lens, the off-axis degradation is more pronounced than in the shorter focal lengths and, more importantly, less effectively compensated. This explains why the reductions in both MTF50 and MTF30 occur in parallel and become more readily apparent from a perceptual standpoint.

***Adriana Bernal**: The contrast of the Arles lenses is a little lower than what we usually find in other cinema lenses designed to produce a very clean, high-contrast image. In the measurements we carried out, the gap between the MTF50 and MTF30 values tended to remain relatively wide across several focal lengths. That allows the image to retain texture and tonal continuity, even when there is a lot of visual information within the frame. In practice, faces and surfaces preserve detail without the textures becoming overly pronounced or separating too aggressively.*

I think one of the most interesting qualities of these lenses is precisely that balance. They are not designed to produce an extremely contrasty image or an excessively sharp rendering of detail, but rather a smoother and more continuous reproduction of fine textures.

For Indeleble, that behavior worked particularly well because it helped maintain an image with a strong sense of density and atmosphere without sacrificing definition or spatial depth. My lighting approach, on the other hand, was intentionally very high in contrast. The first visual reference I proposed to Jairo was Sin City—an image that was almost monochrome, with only a few selectively saturated colors associated with the victims. Jairo felt that approach was too extreme, so we pulled it back. In that context, the lower native contrast of the Arles lenses helped temper the contrast created by the lighting, allowing us to preserve density while maintaining definition and a convincing sense of depth.

Lateral Chromatic Aberration

The analysis of lateral chromatic aberration in the 75 mm lens (Figs. 45–47) confirms a behavior consistent with the resolution and PSF analyses, while introducing an important nuance: the increase in chromatic aberration is not merely quantitative but also structural, particularly as the distance from the optical axis increases.

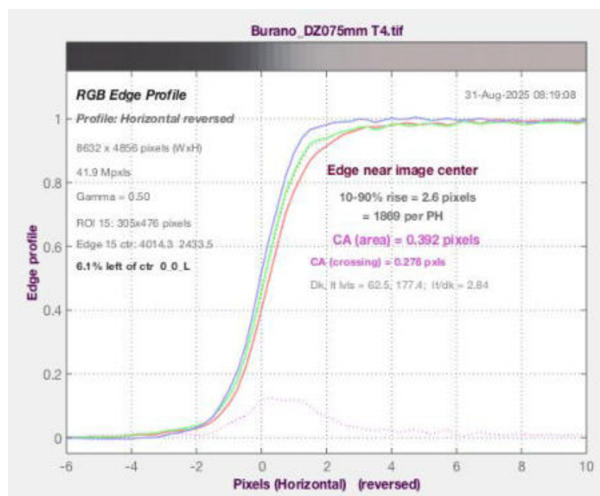

Figure 45

Near the center of the image, the behavior remains well controlled. The RGB channel profiles remain closely aligned, and the edge transition is clean, with CA (Area) values of approximately 0.39 pixels and CA (Crossing) values of 0.278 pixels. This indicates that, although lateral chromatic aberration is present, its visual impact remains moderate and does not significantly compromise on-axis image definition.

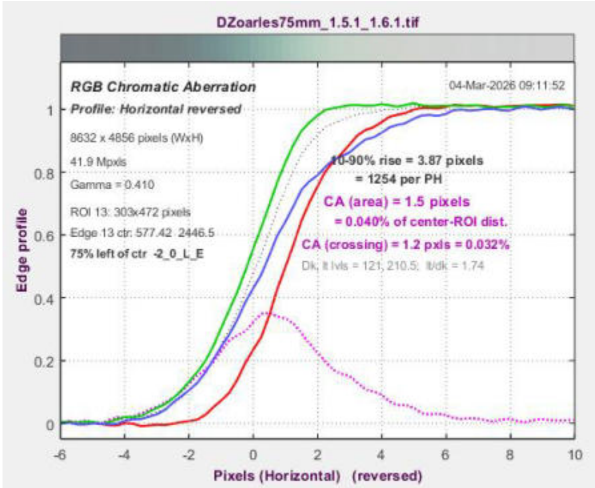

Figure 46. Left Side of the Image

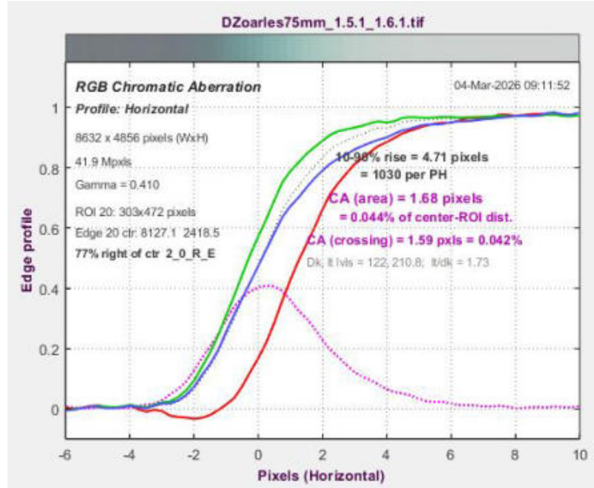

Figure 47. Right Side of the Image

However, as we move toward the intermediate regions of the image field (approximately 75% of the image field), the situation changes noticeably. The separation between the color channels becomes more evident, particularly across the edge transition, where a progressive displacement develops between the red, green, and blue channels. At this location, the CA (Area) values reach approximately 1.5 pixels (about 0.040% of the distance from the image center), while the CA (Crossing) values are approximately 1.2 pixels, indicating a clearly measurable displacement at the geometric edge position.

Toward the periphery (approximately 77% of the image field), this behavior becomes even more pronounced. The edge transition becomes distinctly asymmetrical, and the chromatic separation is more apparent, with CA (Area) values of 1.68 pixels (approximately 0.044%) and CA (Crossing) values of 1.59 pixels (approximately 0.042%). At this point, chromatic aberration is no longer merely a subtle optical effect but becomes a factor that directly contributes to the perceived loss of sharpness, particularly along high-contrast edges (see *Table 5*).

This progressive increase is fully consistent with the PSF analysis. The elongation and spreading of the point spread function away from the optical axis not only reduce resolving power but also cause increasing separation of the color channels, producing directional color fringing. This behavior is likewise reflected in the MTF curves, where the parallel decline of the MTF50 and MTF30 measurements indicated the absence of perceptual compensation at mid-spatial frequencies. Another noteworthy aspect is that the chromatic aberration does not increase symmetrically across the color channels. As suggested by the previous analyses, the separation between the different color-channel pairs is not equivalent, giving rise to a characteristic pattern of color fringing in which certain chromatic pairs become more prominent than others. This forms part of the chromatic signature of the lens and influences the way edges and contours are perceived in the final image.

From a visual standpoint, the 75 mm lens exhibits a clear pattern: lateral chromatic aberration remains well controlled at the center of the image but increases progressively and perceptibly toward the periphery, contributing to a loss of definition that is not only optical (resolution) but also chromatic in nature. This reinforces the overall interpretation of the 75 mm within the lens set: a lens with strong on-axis performance but a more pronounced and less effectively compensated off-axis degradation than the shorter focal lengths.

The radial chromatic aberration plot (*Fig. 48*) completes the previous analysis by introducing a key dimension: how chromatic aberration increases continuously from the image center toward the corners and the characteristic chromatic dominance that it assumes.

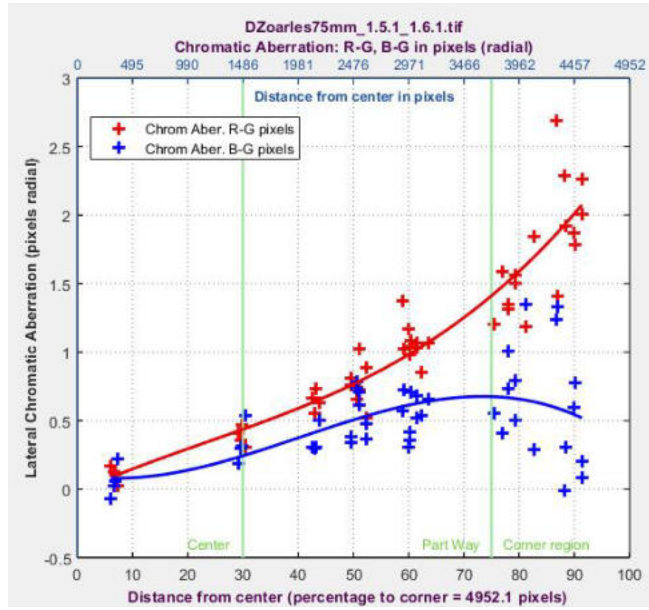

Figure 48

First, the progressive nature of the phenomenon is clearly confirmed. Within the central region (approximately 0–30% of the image field), the values remain low and relatively stable for both chromatic pairs. Beyond this point, chromatic aberration increases steadily, with the most pronounced growth occurring in the transition toward the periphery (approximately 60–80% of the image field), particularly for the R–G channel pair.
One of the most significant features of the plot is the difference between the red (R–G) and blue (B–G) curves. The R–G curve exhibits a considerably steeper slope, reaching values close to or exceeding 2 pixels in the outermost regions of the image field, whereas the B–G curve remains at substantially lower levels, increasing more gradually and even showing a tendency to stabilize—or decline slightly—toward the extreme edge.

This divergence has a direct impact on the image. The chromatic aberration is not neutral but is dominated by the red–green channel pair, defining the characteristic pattern of color fringing produced by the lens. In practical terms, this results in edges where chromatic displacement is more pronounced along that specific chromatic axis, producing characteristic color fringes along high-contrast boundaries.

The crosses shown on the plot represent the individual measurements obtained at different locations across the image field. Their dispersion—particularly toward the periphery—indicates that, although the overall trend is clear, localized variations are present. This is consistent with the behavior observed in both the three-dimensional MTF map and the PSF analysis: the degradation is not perfectly uniform but exhibits small regional variations.

The continuous curves correspond to regression fits that summarize the overall trend of the measurements. They clearly reveal the characteristic evolution of the aberration: minimal near the image center, increasing more rapidly through the intermediate regions, and eventually tending to stabilize—albeit at relatively high values—toward the image periphery.

In relation to the edge-profile plots, this diagram provides complementary information. Whereas the edge profiles describe the local behavior at specific measurement locations, the radial plot illustrates the overall growth of lateral chromatic aberration across the image field. Most importantly, it confirms that in the 75 mm lens the aberration not only increases toward the edges but does so in a structured and progressive manner, with a pronounced asymmetry between the color channels, thereby reinforcing its perceptual impact on the final image.

Geometric Distortion

The geometric distortion analysis of the 75 mm lens (Fig. 49) reveals a relatively well-controlled behavior, particularly when considered alongside the aberrations and the reduction in resolution discussed in the preceding sections.

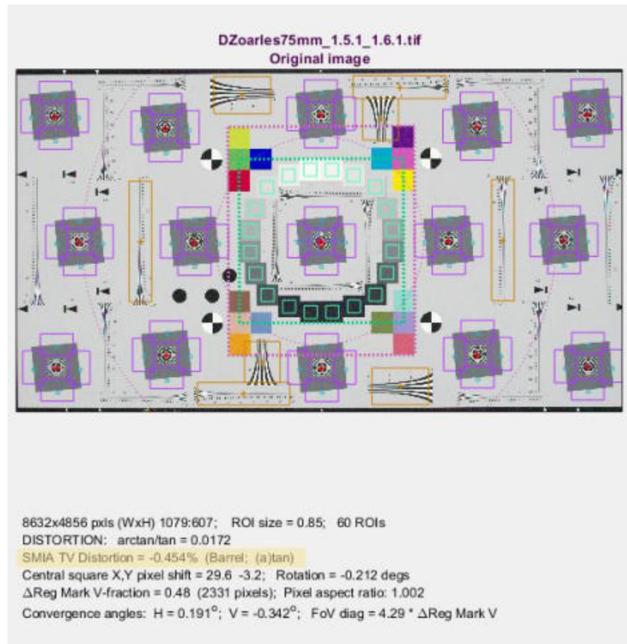

Figure 49

The primary parameter reported by Imatest, SMIA TV = –0.454%, indicates the presence of slight barrel distortion. The negative sign confirms that straight lines tend to bow gently outward from the center of the image, although the magnitude remains below half a percent, placing it within a low perceptual range.

This result is supported by the arc-tangent (arc-tan) distortion coefficient of 0.0172, which describes the deviation from an ideal geometric projection. The small magnitude of this parameter confirms that the overall image deformation is limited and highly regular, with no evidence of complex or compound distortion patterns.

Another relevant parameter is the optical center displacement (Center Square X, Y Shift = 29.6, –3.2 pixels). Although the optical axis is slightly offset from the geometric center of the image sensor, the magnitude of this displacement is small relative to the overall image resolution, and its practical impact is therefore negligible. Likewise, the measured image rotation of –0.212° indicates only a minor misalignment, well within acceptable limits.

The convergence angles (H = 0.191°, V = –0.342°) further support this interpretation. They indicate only a slight tendency for horizontal and vertical lines to converge or diverge, without reaching levels that would produce visible geometric distortion under normal shooting conditions.

Overall, and in contrast to the findings from the resolution, PSF, and chromatic aberration analyses, the geometric distortion of the 75 mm lens can be considered well controlled, smooth, and highly regular. It introduces no significant irregularities or pronounced asymmetries, allowing the lens to maintain a high degree of geometric fidelity in its spatial rendering.

This is particularly significant because it indicates that the limitations observed in this focal length arise not from image geometry but primarily from off-axis optical phenomena—namely the spreading of the point spread function, astigmatism, and lateral chromatic aberration. This distinction helps isolate more clearly the physical mechanisms responsible for the degradation of image quality toward the periphery.

This frame is fully consistent with the optical behavior of the 75 mm lens described throughout the technical analysis. The greater spatial compression and the more pronounced defocus enhance the separation of the subject from its surroundings, while the slight loss of uniformity in the background and the less homogeneous transition of fine detail reflect the peripheral falloff observed in the MTF curves together with the increased complexity of the PSF. Compared with the more neutral rendering of the 50 mm lens, the 75 mm produces a more selective and expressive image, in which the out-of-focus rendering plays a more prominent role at the expense of spatial uniformity.

Adriana Bernal*: The Arles lenses are not particularly forgiving when it comes to very intense light sources or uncontrolled highlights. During the shoot, I had to be very careful with the white levels. I almost never allowed the highlights to rise above 70%, and at most they reached around 80%. Beyond that point, veiling glare became quite noticeable, lifting the blacks and reducing the tonal separation within the image.*

That behavior was also related to the lenses' relatively moderate contrast and to the way they respond to flare and internal light scatter. The tests showed that tonal transitions were smooth and that the contrast was never particularly aggressive. But precisely because of that, whenever very strong light sources entered the frame—or whenever areas became excessively overexposed—the image could lose depth quite quickly.

I never regarded this as a flaw, but rather as a characteristic that required conscious control. The visual language of the film called for very carefully managed exposure, and under those conditions the lenses performed much better. When the highlights were properly contained, the image retained excellent texture, solid blacks, and a rich sense of atmosphere. But if the whites were allowed to climb too far, veiling glare appeared very quickly and the image began to wash out.

5- 100 MM LENS

Once again, the MTF curves at different locations across the image field are presented in Figures 50–53.

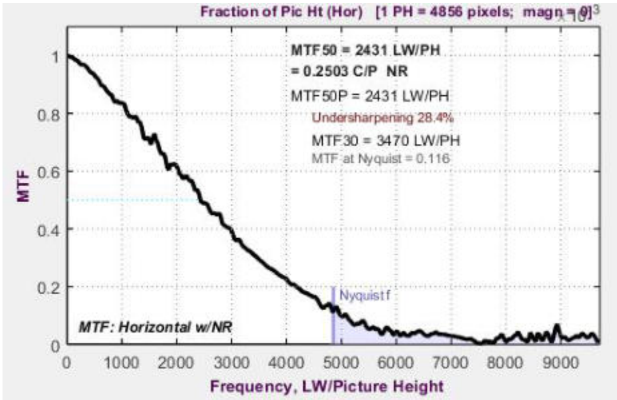

Figure 50. Center of the Image

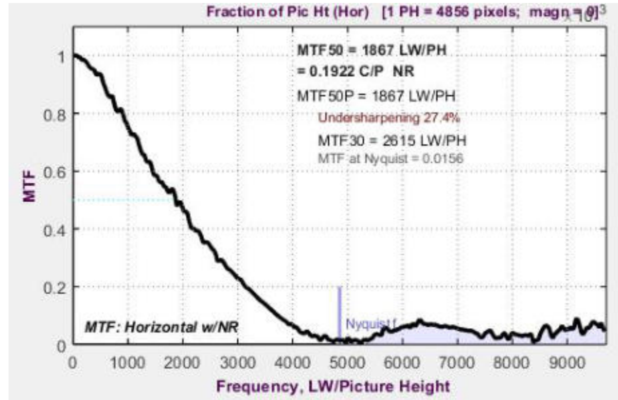

Figure 51. Left Side of the Image

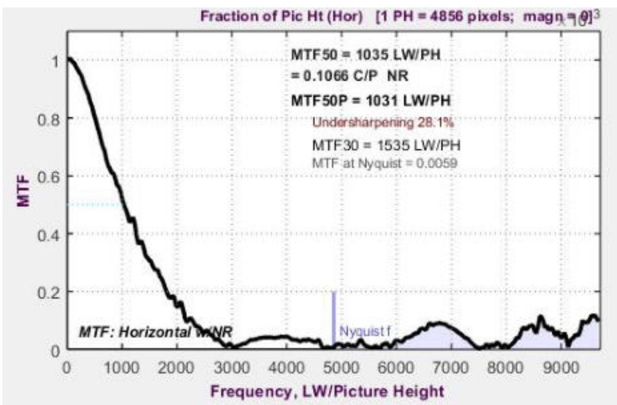

Figure 52. Upper-Left Corner of the Image

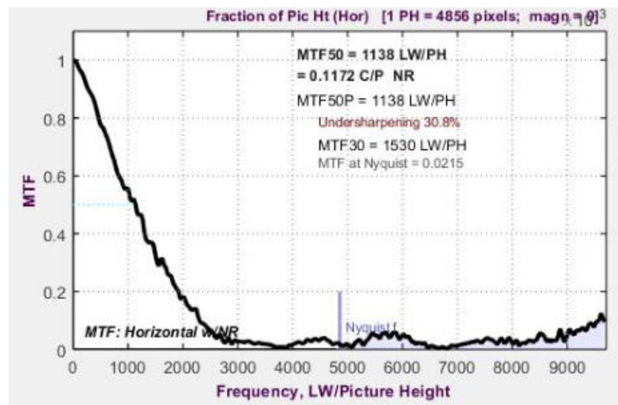

Figure 53. Lower-Right Corner of the Image

The 100 mm lens introduces an interesting change compared with the shorter focal lengths: central performance is clearly superior, but the loss of performance toward the image periphery is also more pronounced, reinforcing a balance between higher on-axis contrast and reduced field uniformity.

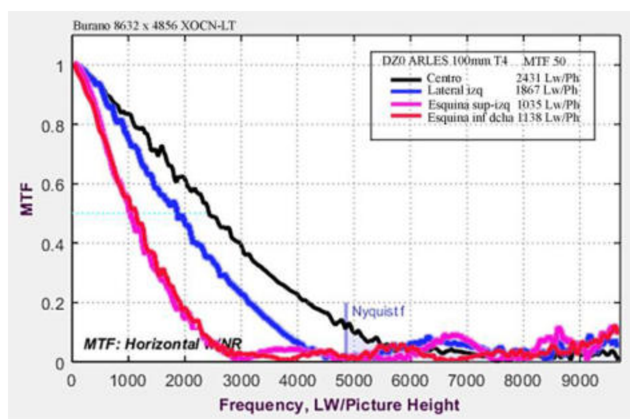

Figure 54. Comparative MTF Curves

At the center of the image (*Fig. 54*), the black curve starts from a high level and maintains contrast over a broader range of mid-spatial frequencies than the 75 mm lens, reaching an MTF50 value of 2431 LW/PH. This indicates excellent resolving power for fine detail and, more importantly, superior preservation of contrast at mid-spatial frequencies in the central region. The decline is progressive and relatively well controlled through approximately the middle of the spatial-frequency spectrum.

Moving toward the lateral region, however, the blue curve already shows a clear separation from the central response. With an MTF50 value of 1867 LW/PH, the reduction is approximately 23%, indicating that off-axis degradation begins earlier and is more pronounced than in the shorter focal lengths. The steeper slope of the curve reflects a reduced ability to preserve contrast at mid-spatial frequencies.

This trend becomes even more evident in the corners. The magenta and red curves (upper-left and lower-right corners, respectively) decline much more rapidly, reaching MTF50 values of 1035 and 1138 LW/PH. These correspond to reductions of approximately 53–57% relative to the image center, demonstrating a substantial degradation in optical performance. Moreover, both curves converge to low values at relatively low spatial frequencies, indicating that the loss affects not only fine detail but also the fundamental structural content of the image.

An important observation is that, although slight differences exist between the two corners, the overall behavior remains highly consistent. Rather than isolated anomalies, the lens exhibits a continuous and systematic degradation from the center toward the edges. The wide and persistent separation between the curves results in lower field uniformity than that of the 50 mm lens and, in some respects, an even more pronounced non-uniformity than that observed in the 75 mm lens.

From a physical standpoint, this pattern is consistent with the presence of stronger off-axis aberrations—primarily astigmatism and field curvature—which predominantly affect the peripheral regions of the image. The more rapid decline of the MTF curves indicates that the point spread function becomes increasingly dispersed, reducing both resolving power and contrast in those areas.

The three-dimensional MTF50 map of the 100 mm lens (Fig. 55) provides a further level of interpretation beyond the MTF curves, as it not only confirms the reduction in optical performance but also reveals how this degradation is distributed spatially across the image field.

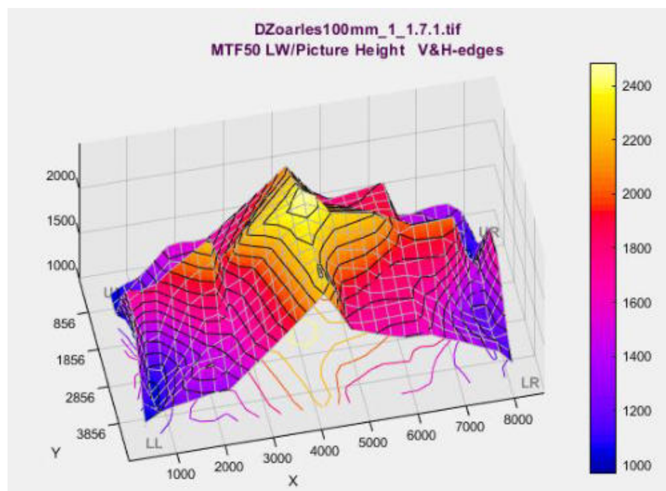

Figure 55

The first notable feature is that the region of maximum performance does not form a broad plateau but rather a relatively compact and somewhat irregular peak. This refines the interpretation of the MTF curves: although the central performance is excellent, it does not extend uniformly into the surrounding regions but is confined to a smaller area than might be inferred from a one-dimensional analysis alone.

Beyond this central peak, the surface descends toward the image periphery, but the falloff is not radially uniform. Lateral variations and gentle undulations become apparent, particularly in the intermediate regions of the image field, indicating that the reduction in resolving power is not entirely regular. This observation complements the radial MTF analysis: the degradation is characterized not only by a progressive decline and directional dependence but also by localized variations within the same region of the image field.

Another important feature is the asymmetry between different regions of the image field. Although not pronounced, it is sufficiently evident to confirm that optical performance is not distributed perfectly evenly across the four quadrants. This finding is entirely consistent with both the MTF curves and the PSF analysis: the off-axis degradation is not isotropic but depends on both direction and position within the image field.

From a visual standpoint, the 100 mm lens behaves as an optic with excellent central definition but a pronounced loss of sharpness toward the edges, particularly in wide compositions or in scenes containing important visual information near the corners of the frame. This combination—strong on-axis performance together with substantial peripheral degradation—defines the character of the lens within the Arles set: an optic that performs exceptionally well along the optical axis but is less consistent in maintaining uniform image detail across the entire field.

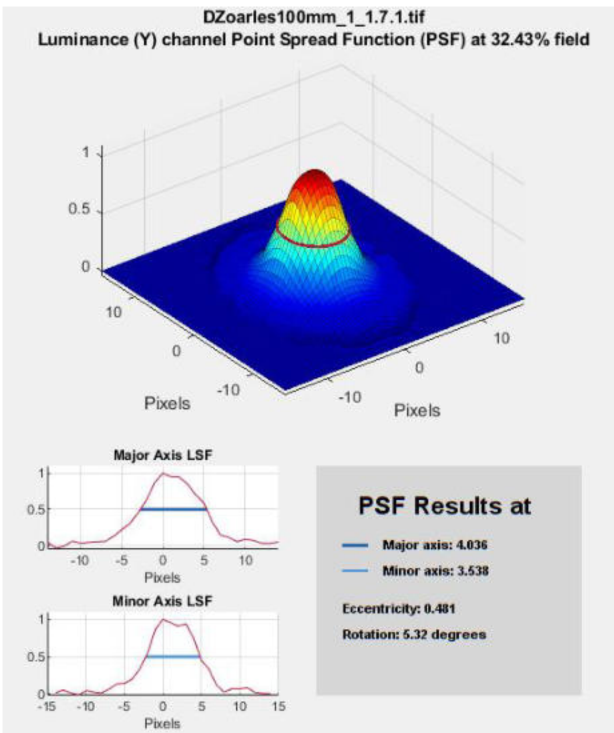

Figure 56

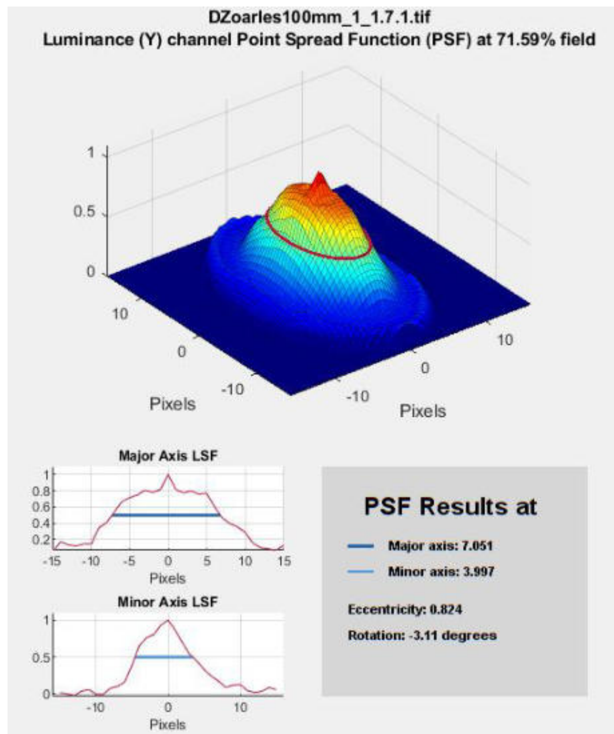

Figure 57

The PSF analysis of the 100 mm lens (Figs. 56 and 57) provides a clear physical explanation for the behavior previously observed in the MTF curves and the three-dimensional map: the difference between the center and the periphery is not merely one of magnitude but also of the shape of the optical response.

Near the center of the image (approximately 32% of the image field), the PSF remains relatively compact and well confined. Although it is not perfectly circular, it retains a fairly regular shape, with a moderate difference between the major and minor axes (4.036 px and 3.538 px, respectively) and an eccentricity of 0.481. This indicates that the light energy remains reasonably well concentrated, explaining why the center achieves such a good balance between resolving power and contrast at mid-spatial frequencies.

Toward the image periphery (approximately 72% of the image field), however, the transformation is substantial. The PSF broadens and becomes markedly distorted, with the major axis increasing to

7.051 px while the minor axis reaches 3.997 px, raising the eccentricity to 0.824. Rather than remaining approximately point-like, the distribution becomes distinctly elongated and directionally oriented.

This change is not merely quantitative but structural. The light energy that is concentrated within a compact volume at the image center becomes increasingly spread along a preferred direction toward the periphery, meaning that image detail is no longer reproduced equally in all orientations. This directly reveals the same phenomenon already suggested by the MTF curves and by the separation between the horizontal and vertical responses: an anisotropic optical response characteristic of astigmatism.

The rotation of the PSF (from 5.32° in the intermediate region to –3.11° toward the periphery) further supports the conclusion that this deformation is not aligned with the sensor axes, contributing to the spatial asymmetry observed in the three-dimensional MTF map. Rather than a uniform degradation, the lens exhibits a complex redistribution of light energy that depends on image position.

From a practical standpoint, this explains why the reductions in MTF50 and MTF30 are not perceptually compensated in the 100 mm lens. The issue is not simply that less useful light energy reaches the image, but that it is distributed less efficiently and with a stronger directional component. The broader and more elongated peripheral PSF reduces both the ability to resolve fine detail and the ability to preserve contrast at mid-spatial frequencies.

Overall, the PSF analysis confirms that the 100 mm lens maintains a high-performance core at the image center but exhibits a more complex off-axis degradation than the shorter focal lengths, characterized by greater spreading of the point spread function, stronger directional dependence, and reduced energy concentration. The result is a more pronounced loss of field uniformity in the final image.

The comparison between the MTF50 and MTF30 measurements for the 100 mm lens (Tables 8 and 9; Figs. 58 and 59) reinforces—but also refines—the interpretation derived from the MTF curves.

100 MM LENS	LW/PH 50%
CENTER	2431
LEFT SIDE	1867
UPPER-LEFT CORNER	1035
LOWER-RIGHT CORNER	1138

Table 8

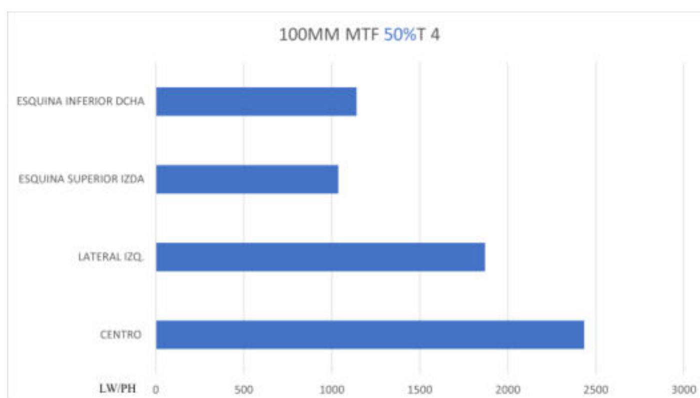

Figure 58

100 MM LENS	LW/PH 30%
CENTER	3470
LEFT SIDE	2615
UPPER-LEFT CORNER	1535
LOWER-RIGHT CORNER	1530

Table 9

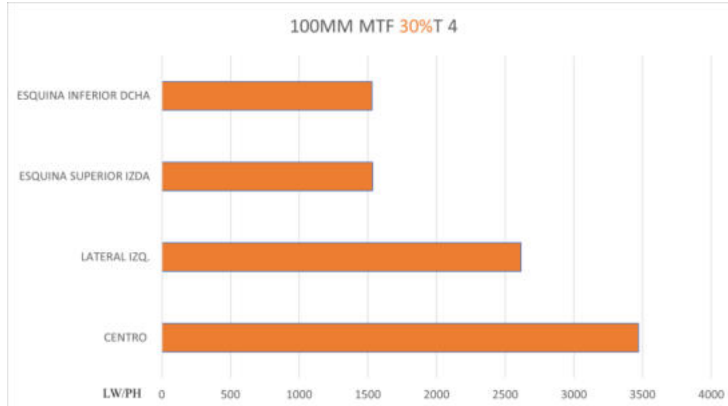

Figure 59

The most significant observation is that the transition from MTF50 to MTF30 produces a substantial proportional increase across all regions of the image field, indicating that the lens retains a considerable amount of energy at mid-spatial frequencies even where fine-detail resolution has already declined. In other words, although resolving power decreases rapidly away from the optical axis, the overall image structure is preserved better than the MTF50 values alone would suggest.

This apparent "recovery," however, is not uniform. At the image center, the increase from MTF50 to MTF30 is particularly pronounced, confirming an exceptionally strong response in terms of both contrast and overall image definition. In the lateral regions, the behavior remains relatively consistent: the MTF30 response closely follows that of the center, suggesting that the image retains good coherence across this intermediate portion of the field.

The critical difference appears in the corners. Although the MTF30 values improve substantially relative to the MTF50 measurements, the relative gap with respect to the image center remains considerable. This indicates that the degradation in these regions is not confined to high spatial frequencies but also affects mid-spatial frequencies. In other words, there is no sufficient perceptual compensation: the increase in MTF30 is not enough to offset the reduction observed in MTF50.

This behavior places the 100 mm lens in an intermediate position between the characteristics observed in the 50 mm and the 75 mm lenses. Like the 75 mm, the degradation affects both resolving power and contrast at mid-spatial frequencies; yet, like the 50 mm, the image still retains a certain degree of structural integrity. The result is a lens with an outstanding central region, while the image periphery shows some improvement when evaluated through the MTF30 response but still fails to achieve the same level of uniformity.

From a visual standpoint, this translates into an image with a very strong center and excellent tonal richness, while the edges, although not completely degraded, continue to exhibit a noticeable loss of consistency.

The radial MTF30 plot of the 100 mm lens (*Fig. 60*) refines the interpretation of optical performance from a more perceptual perspective, focusing on how contrast at mid-spatial frequencies is preserved across the image field. In the central region, the response is both high and stable, confirming that the lens not only delivers excellent on-axis resolving power but also maintains a strong foundation of contrast at mid-spatial frequencies capable of preserving the structural integrity of the image.

As the analysis moves away from the image center, the curve declines progressively, but an important nuance emerges: the behavior is not identical in all directions. The horizontal response is maintained over a longer portion of the image field, whereas the vertical response decreases more rapidly, producing a clear separation between the two. This difference is not constant but evolves across the image field to the point where the two curves eventually intersect.

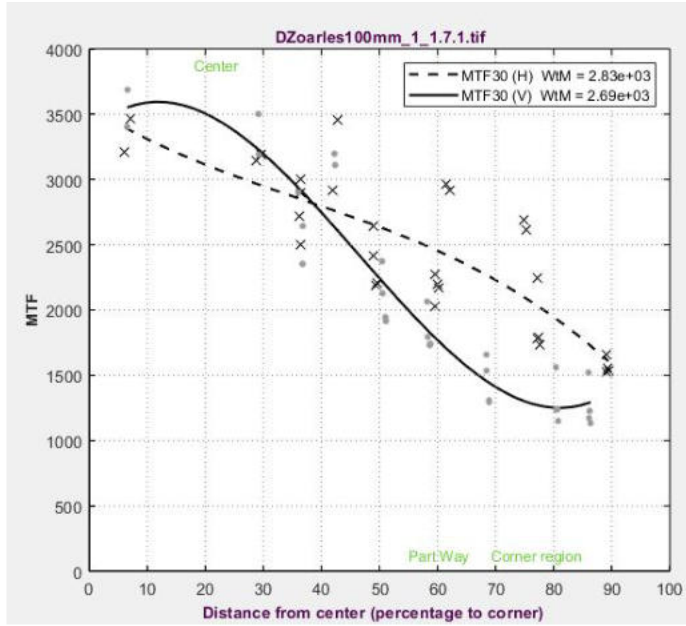

Figure 60

This intersection is particularly significant from an interpretative standpoint. It indicates that the relative performance of the lens changes depending on image position: in some regions, one orientation (sagittal or horizontal) reproduces detail more effectively, whereas in others the opposite orientation (meridional or vertical) provides superior performance. This is therefore not simply a reduction in resolving power but a directional variation in optical performance.

Such behavior is characteristic of off-axis aberrations, particularly astigmatism, in which the optical system does not focus all detail orientations equally. As a result, the point spread function is no longer distributed uniformly, and the plane of best focus varies with orientation, introducing a degree of directional inconsistency in image reproduction.

From a visual standpoint, this means that sharpness not only decreases toward the image periphery but does so in a manner that depends on the orientation of image structures. Certain edges and contours may therefore retain better definition than others according to their direction. This affects the consistency of texture reproduction and reinforces the loss of field uniformity already observed in both the MTF curves and the spatial analysis.

Overall, the radial MTF30 plot confirms that the 100 mm lens delivers strong on-axis performance but exhibits a progressive degradation that is not only pronounced but also directional and position-dependent. This further defines its character as a lens with excellent central performance but reduced consistency away from the optical axis.

Lateral Chromatic Aberration

The analysis of lateral chromatic aberration in the 100 mm lens introduces an interesting nuance compared with the resolution measurements. While the lens maintains relatively good chromatic correction at the image center, chromatic aberration increases progressively toward the lateral regions of the image field. At the center of the image (Fig. 61), the measured values are low, and the RGB channel profiles remain closely aligned, indicating excellent channel convergence. With a CA (Area) value of approximately 0.262 pixels and a CA (Crossing) value of approximately 0.095

pixels, lateral chromatic aberration remains at a very low level and is essentially imperceptible under normal viewing conditions. This is fully consistent with the relatively compact PSF observed on-axis: the light energy is not only well concentrated but also exhibits excellent chromatic alignment. Moving toward the lateral regions of the image (Figs. 62 and 63), however, the behavior changes markedly. The separation between the color channels increases, and the edge transition becomes progressively more staggered across the RGB channels. At these locations, the measured values rise to approximately 1.74 pixels for CA (Area) and 1.23 pixels for CA (Crossing), indicating clearly measurable lateral chromatic aberration. This increase is not insignificant: it means that the individual color channels no longer coincide at the same edge position, producing visible color fringing under high-contrast conditions.

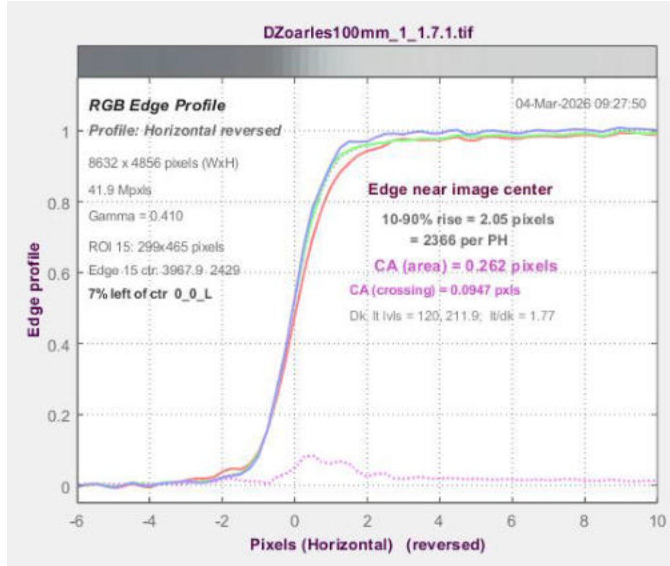

Figure 61

On the opposite side of the image field (right side), the values remain of a similar magnitude (approximately 1.5 pixels for CA (Area) and 1.15 pixels for CA (Crossing)), suggesting a highly consistent behavior between both sides of the image. In other words, unlike the resolution measurements, the chromatic aberration exhibits much less overall asymmetry, although it still shows a clear dependence on the distance from the image center.

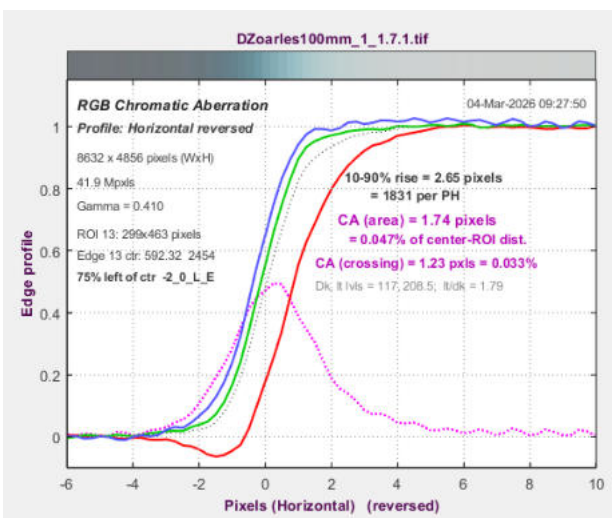

Figure 62. Left Side of the Image

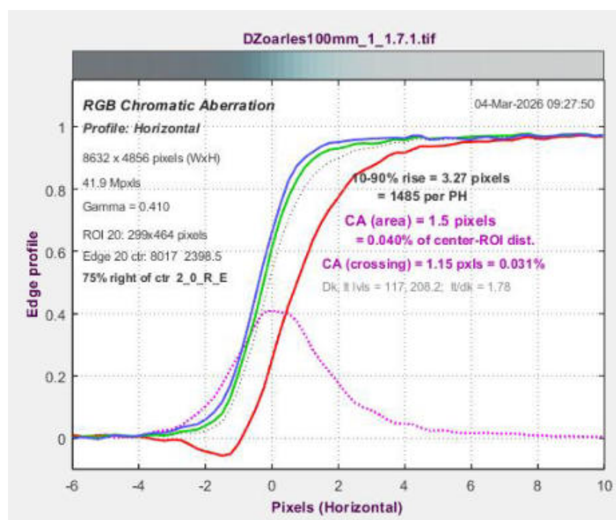

Figure 63. Right Side of the Image

From the edge-profile perspective, this behavior is reflected in a progressive separation of the RGB channel curves. The red channel generally exhibits the greatest displacement, while the blue and green channels remain comparatively closer together. This difference defines the characteristic pattern of color fringing, which tends to appear with specific chromatic dominance along image edges.

When considered together with the rest of the analysis, a consistent interpretation emerges:

- The reduction in MTF together with the deformation of the PSF indicated a loss of sharpness and image coherence away from the optical axis.
- The present analysis shows that this degradation is accompanied by a progressive increase in chromatic misalignment.

Overall, the 100 mm lens combines a clean, well-corrected image center with a peripheral region where lateral chromatic aberration becomes increasingly significant. Although the measured values do not reach extreme levels, they are sufficient to become visible under demanding conditions, reinforcing the overall character of this focal length: excellent on-axis performance combined with a progressive degradation—both spatial and chromatic—toward the edges of the image field.

The radial chromatic aberration plot of the 100 mm lens (*Fig. 64*) provides a clear visualization of how chromatic displacement increases and is distributed across the image field, while introducing an important nuance compared with the shorter focal lengths: the aberration not only increases with distance from the optical axis but also develops asymmetrically between the different color-channel pairs.

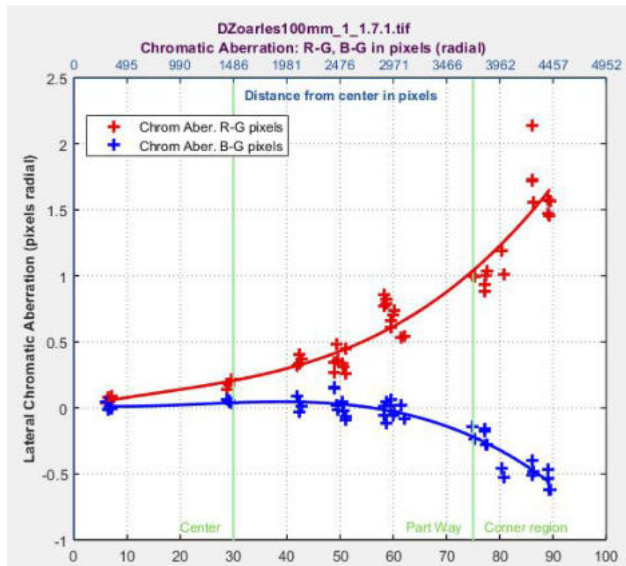

Figure 64

Within the central region of the image field (approximately 0–30%), both curves remain very close to zero. The measured chromatic displacements are on the order of ≤0.2 pixels, corresponding to a very low perceptual level. This confirms excellent chromatic alignment along the optical axis, consistent with the results obtained from the edge-profile analysis.

Beyond this region, the two curves begin to diverge progressively. The R–G channel pair (red curve) increases steadily, reaching values of approximately 0.5–1.0 pixels in the intermediate region of the image field (approximately 40–60%), corresponding to a low-to-moderate perceptual level. The transition is smooth and continuous, without abrupt discontinuities, indicating that the chromatic aberration develops as an inherent characteristic of the optical design rather than as a localized anomaly.

The most significant behavior appears toward the image periphery (approximately 70–90% of the image field). Here, the R–G curve rises more rapidly, reaching values of approximately 1.5–2.0 pixels, placing it within the moderate to moderately high perceptual range, where color fringing becomes visible under high-contrast conditions. This increase is not linear but exhibits a progressively steeper slope, indicating that lateral chromatic aberration intensifies rapidly over the outermost portion of the image field.

In contrast, the B–G channel pair (blue curve) exhibits a different behavior. After remaining close to zero throughout the central region, it begins to shift in the opposite direction, reaching values of approximately –0.5 pixels near the image corners. This does not indicate a lower degree of chromatic aberration but rather a displacement in the opposite direction. The result is a differential chromatic separation: the color channels not only diverge but do so in opposite directions (see *Table 5*).

Figure 65. Lateral chromatic aberration of the 100 mm lens. ×1500 magnified detail of a lateral perforation on the Via Stellae test chart, with slight increases in contrast and color saturation to highlight the separation of the color channels.

From a chromatic standpoint, this pattern is clearly anisotropic. The aberration does not affect all color channels equally, with the red channel becoming the dominant contributor to the chromatic displacement. This has a direct impact on the final image: rather than producing neutral color fringing, the lens generates fringes with a characteristic chromatic bias—typically reddish-yellow on one side of an edge and cyan-blue on the other (*Fig. 65*).

The crosses on the plot, which represent the individual measurements, also exhibit moderate dispersion, particularly toward the image periphery. This indicates that, although the overall trend is well defined, localized variations exist across different regions of the image field. This observation further reinforces the interpretation derived from the three-dimensional MTF map: the degradation is not perfectly uniform across the field.

Overall, the radial chromatic aberration plot confirms that the 100 mm lens maintains excellent chromatic correction at the image center, while lateral chromatic aberration increases progressively toward the image periphery in a channel-dependent manner, reaching perceptible levels in the corners. This increase—more pronounced for the R–G channel pair—defines the chromatic signature of the lens and is consistent with the loss of spatial and directional uniformity observed throughout the other optical performance metrics.

Geometric Distortion

The geometric distortion analysis (*Fig. 66*) reveals an essentially neutral optical behavior, with a barrel distortion of –0.257%. This value lies well below the perceptual threshold under normal viewing conditions, resulting in faithful

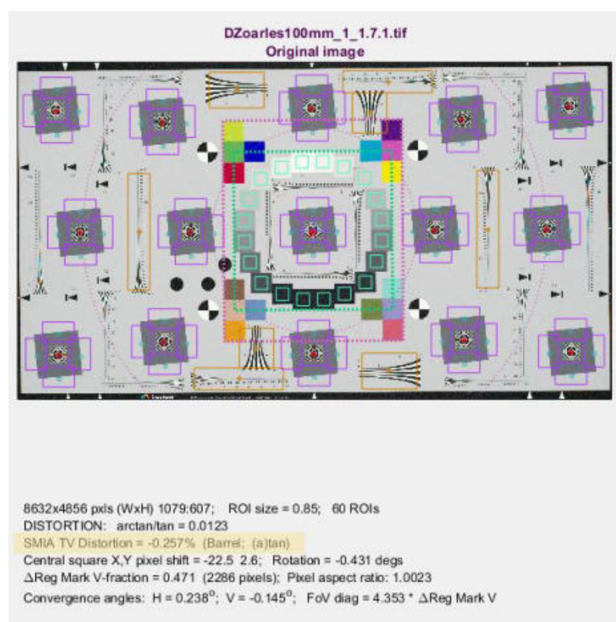

Figure 66

reproduction of straight lines without noticeable geometric deformation. The supporting parameters—including a pixel aspect ratio very close to unity and minimal convergence angles—further confirm the reliability of the measurements. Overall, the lens exhibits excellent geometric stability, consistent with its telephoto design, where the perceived spatial compression arises from perspective rather than optical distortion.

Adriana Bernal*: I did notice slight geometric distortion with the wider focal lengths, but never to a degree that felt excessive or problematic.*
In practice, the distortion was mainly visible near the edges of the frame, particularly in interior scenes or whenever strong architectural lines were present. Even then, I never had the impression that the space became distorted or that vertical lines bent in an exaggerated way. The image always felt quite natural and remained easy to control compositionally.
As the focal length increased, the geometry became much more neutral. With the normal focal lengths—and especially with the telephoto lenses—geometric distortion virtually disappeared, and the spatial impression depended far more on the natural perspective compression of the focal length than on any optical deformation introduced by the lens itself.
I think one of the most interesting qualities of the Arles set is precisely the consistency of the transition from one focal length to the next. Although the wider lenses produce a slightly greater sense of spatial expansion and a modest amount of edge curvature, there is never an abrupt change when moving to the normal or longer telephoto focal lengths. That consistency contributed greatly to maintaining the visual continuity of the film.

Light Falloff

or the 100 mm lens, and as a representative reference, light falloff was evaluated at T1.4 in addition to the T4 aperture used throughout the remainder of the analysis. The variation in image illumination as a function of aperture is representative of the behavior observed across the entire lens set; however, for the sake of brevity, only the results obtained with the 100 mm lens are presented here.

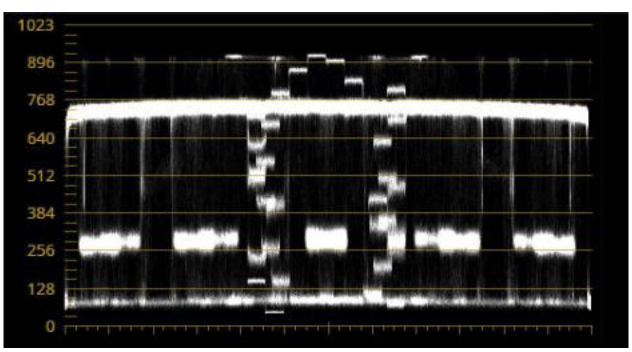

Figure 67. 100mm T4

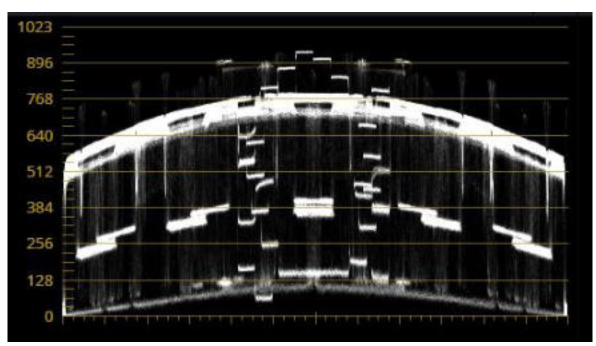

Figure 68.100mm T 1.4

The waveform monitor provides a perceptual estimate of the luminance falloff across the image field. At T4 (*Fig. 67*), the luminance difference between the center and the periphery is approximately 10–15%, corresponding to about 0.2–0.3 EV. When the aperture is opened to T1.4 (Fig. 68), this difference increases to approximately 25–30% (about 0.45–0.5 EV), reflecting the expected increase in optical vignetting at maximum aperture, although it remains within a moderate range.

The analysis of flare (veiling glare) introduces an important nuance to the interpretation of luminance uniformity. Whereas vignetting describes the progressive reduction in illumination toward the image periphery, veiling glare reveals a complementary phenomenon: the redistribution of light within the image caused by internal reflections inside the optical system.
This stray light raises the black level and reduces overall image contrast, producing an image that—particularly in the presence of intense light sources adjacent to dark regions—acquires a characteristic creamy quality.

Adriana Bernal: *This was definitely an important issue during the shoot, particularly with the longer focal lengths. We relied heavily on the telephoto lenses, and they were not always easy for the focus puller to work with. The characteristic softness of the Arles lenses—especially when combined with low-light scenes and moderate contrast—made it more difficult than usual to identify the exact point of critical focus.*
The technical tests reflected the same behavior. Although the lenses provide sufficient resolving power, the finest detail and contrast at mid-spatial frequencies are not especially pronounced, particularly away from the center of the image. As a result, the image does not "snap" into focus as immediately or as decisively as it does with lenses that have higher native contrast or a more clinically sharp rendering of fine detail.
In addition, Indeleble was conceived as a film built around darkness, with many scenes taking place in low light and a deliberately restrained visual atmosphere. For that reason, I never worked at extreme apertures. During the first days of the shoot, I gradually refined my exposure strategy without altering the tonal placement I had established for the scenes on the grayscale. I consistently worked at T4, and often at T5.6, while keeping my characters in the penumbra, typically between Zones I and II. Even under those conditions, the lighting remained demanding for focus pulling, particularly with the telephoto lenses, where depth of field is naturally much shallower.
It was never an issue of the mechanical precision of the lenses. Rather, it resulted from the combination of the gentle rendering of the optics, the relatively low contrast of many scenes, and the particular visual language we were pursuing. Together, these factors required a great deal of attention and sensitivity from the focus puller throughout the production.

A comparison with the MTF curves suggests that the effect of veiling glare is not directly reflected in the low-spatial-frequency response. The curves maintain high values at their origin, particularly at the image center, indicating that local edge contrast is largely preserved. However, this representation does not fully capture the elevation of the black level or the reduction in global image contrast introduced by stray light.

This characteristic originates in the way the lens itself distributes light. The PSF analysis shows that, in addition to the portion of light that accurately defines image contours, there is a fraction that spreads around them in the form of diffuse halos. Although this light does not contribute directly to image formation, it envelops the image by raising the black level, softening tonal transitions, and reducing the separation between image planes. It is within this subtle diffusion that veiling glare originates—not as an isolated optical defect, but as an inherent characteristic that modulates the image, imparting a softer rendering, particularly in high-contrast scenes.

The comparison of the three-dimensional MTF50 maps (*Figs. 69 and 70*) reveals a significant change in the spatial distribution of resolving power as a function of aperture. At T4, the lens exhibits a more homogeneous surface, characterized by a broad central plateau and a gradual decline toward the image periphery. At T1.4, by contrast, resolving power becomes concentrated in a more pronounced central peak, with a faster and more irregular degradation toward the edges of the image field.

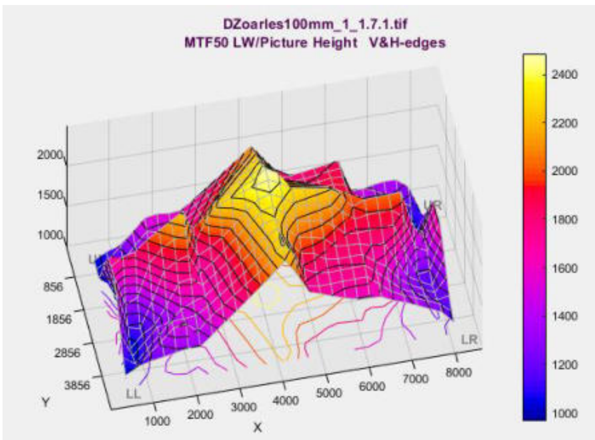

Figure 69. 100mm T 4

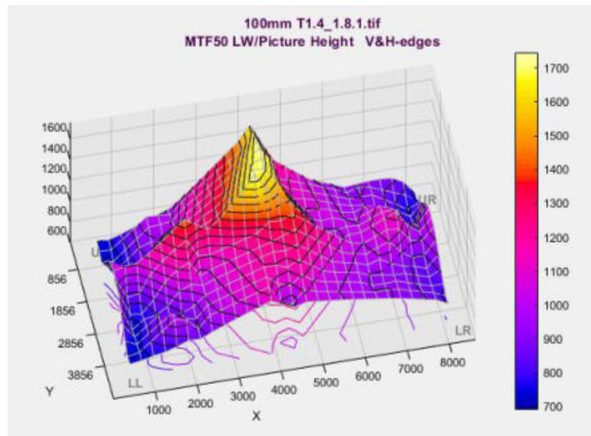

Figure 70.100m T 1.4

Although the three-dimensional MTF50 maps and the waveform monitor represent different quantities—spatial resolution and luminance distribution, respectively—they provide complementary descriptions of the lens's behavior across the image field. At maximum aperture, the concentration of resolving power at the image center and its rapid decline toward the periphery are accompanied by reduced luminance uniformity, as veiling glare and the redistribution of stray light diminish overall tonal separation. Although there is no direct causal relationship between these two measurements, they exhibit a clear perceptual correspondence: the loss of spatial uniformity is reflected in an image that appears both less sharply defined and lower in overall contrast.

In this frame, photographed with the 100 mm lens, the image exhibits moderate perspective compression, bringing the background—vegetation and gravestones—closer to the characters without either separating them excessively or flattening the scene. Everything remains contained within a unified visual space, reinforcing the relationship between the characters and their surroundings.

The focal length makes it possible to work with clearly defined layers: an out-of-focus foreground that enters the frame like a subtle veil, the characters rendered in sharp focus, and a background that remains present yet visually restrained. This spatial organization does not distract from the scene but instead supports its narrative.

This behavior is fully consistent with the optical characteristics observed throughout the technical analysis of the lens. The MTF maintains a high level of image detail across the usable portion of the image field, producing well-defined faces without excessive harshness. The PSF and the out-of-focus rendering reveal a smooth and consistent blur, evident in the foreground, which integrates naturally without interfering with the readability of the image. Lateral chromatic aberration remains low and increases only gradually toward the image periphery, so no visible color fringing appears in high-contrast areas. Geometric distortion is virtually negligible, preserving the straight lines of the bench and the surrounding forms without noticeable deformation.

Overall, the visual strength of the frame does not rely on conspicuous optical effects but on a balanced combination of characteristics: perspective compression organizes the spatial relationships, the out-of-focus rendering separates the planes without isolating them excessively, and the image retains its structural coherence without geometric distortion.

6- 135 MM LENS

Figures 71–74 present the MTF curves at different locations across the image field.

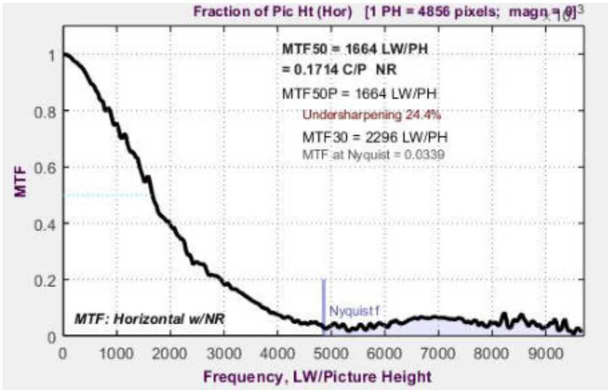

Figure 71. Center of the Image

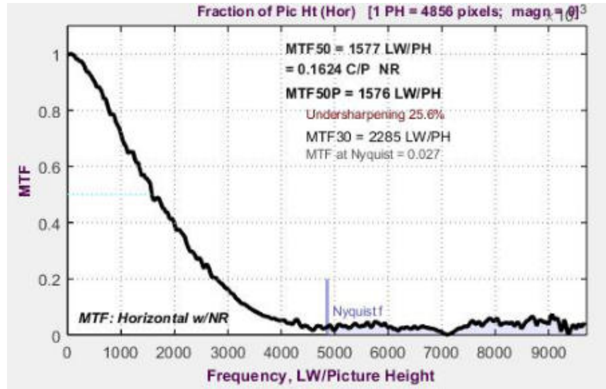

Figure 72. Left Side of the Image

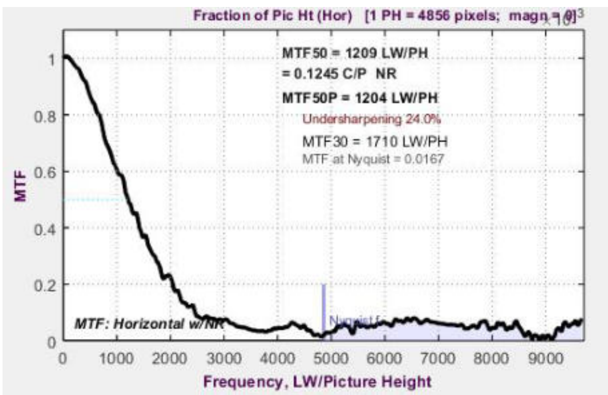

Figure 73. Upper-Left Corner of the Image

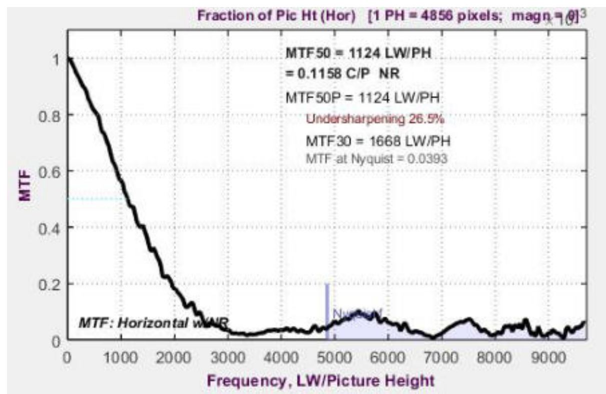

Figure 74. Lower-Right Corner of the Image

The MTF curves of the 135 mm lens at T4 (*Fig. 75*) exhibit remarkably uniform performance across the entire image field. At the image center, the MTF50 reaches 1664 LW/PH, decreasing only slightly toward the lateral region (1577 LW/PH) and more gradually toward the corners (1209 and 1124 LW/PH). This relatively modest reduction—particularly between the center and the lateral region—already indicates a high degree of spatial uniformity across the image field.

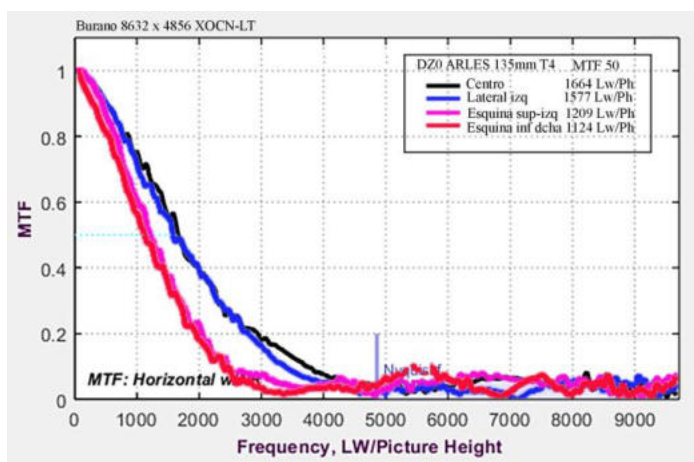

Figure 75.MTF curves compared

Beyond the individual measurement values, the shape of the MTF curves is particularly revealing. Throughout the low- and mid-spatial-frequency range (up to approximately 2000–2500 LW/PH), the curves exhibit similar, nearly parallel slopes, without abrupt divergence or premature collapse in the corners. The reduction in contrast occurs in a smooth and continuous manner, providing a gradual transition from the center toward the image periphery.

Within the mid-spatial-frequency range, which contributes most strongly to the perception of image sharpness, the center retains a slight advantage. Nevertheless, both the lateral regions and the corners maintain a useful level of response, avoiding any structural breakdown of image quality away from the optical axis. This continuity extends into the higher spatial frequencies, where all of the curves converge progressively toward lower values without significant irregularities.

Overall, both the close agreement between the measured values and the regularity of the curve slopes indicate a stable optical performance, with a well-controlled reduction in contrast across the entire image field. In contrast to lenses whose performance is more heavily concentrated at the image center, the 135 mm lens produces a more balanced image, with resolving power distributed more uniformly across the field and a gradual, consistent transition toward the image periphery.

The three-dimensional MTF50 map (*Fig. 76*) confirms the interpretation derived from the MTF curves, revealing a relatively uniform distribution of resolving power across the image field. The central region reaches approximately 1600–1700 LW/PH, decreasing progressively toward values of about 1400–1200 LW/PH in the image periphery, in agreement with the point-based MTF measurements. Beyond this overall trend, however, the surface is not perfectly uniform but exhibits subtle undulations that reveal localized variations in optical performance. Although these irregularities do not represent a structural discontinuity, they do qualify the apparent parallelism of the MTF curves, indicating that the reduction in contrast, while globally smooth, is not identical in every direction. Overall, the lens produces a continuous and stable field of resolving power, yet with a subtle spatial texture that prevents the response from appearing completely uniform.

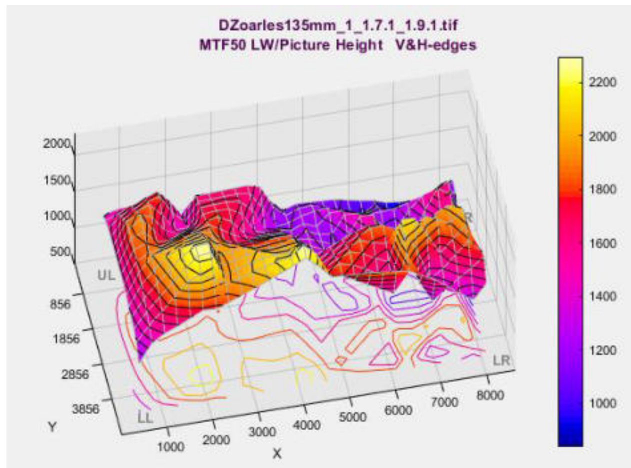

Figure 76

135 MM LENS	LW/PH 50%
CENTER	1664
LEFT SIDE	1577
UPPER-LEFT CORNER	1209
LOWER-RIGHT CORNER	1124

Table 10

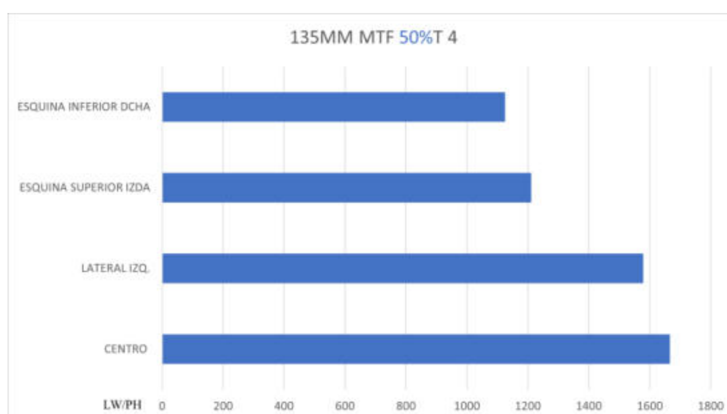

Figure 77

135 MM LENS	LW/PH 30%
CENTER	2296
LEFT SIDE	2285
UPPER-LEFT CORNER	1710
LOWER-RIGHT CORNER	1668

Table 11

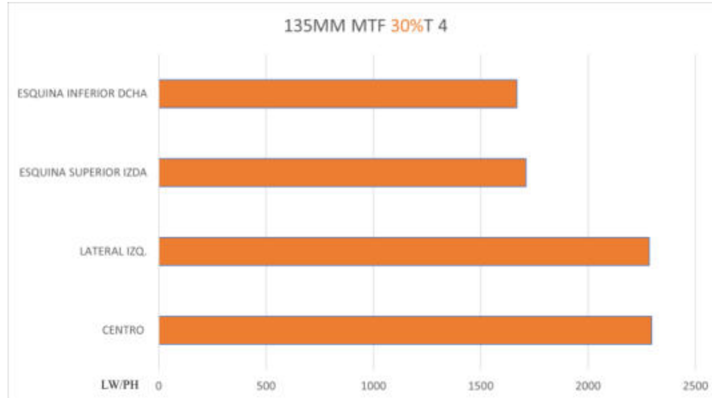

Figure 78

The comparison between the MTF50 and MTF30 values for the 135 mm lens at T4 (Tables 10 and 11; Figs. 77 and 78) provides a more nuanced interpretation of its optical performance. While the MTF50 reaches approximately 1660 LW/PH at the image center and decreases to around 1200–1100 LW/PH in the corners, the corresponding MTF30 values increase to approximately 2300 LW/PH at the center and 1650–1700 LW/PH toward the image periphery.

This difference reveals a relatively steep decline in contrast with increasing spatial frequency: the lens preserves contrast at mid-spatial frequencies more effectively than it preserves the finest image detail. At the same time, the smaller spread of the MTF30 values indicates greater overall image uniformity, in contrast to the more pronounced degradation of fine detail away from the optical axis. Overall, the optical behavior suggests a lens that prioritizes structural coherence and overall image contrast over maximum resolving power, maintaining image readability while introducing a gradual softening toward the edges of the frame.

The relationship between the MTF measurements and the out-of-focus rendering of the 135 mm lens is particularly coherent. The stronger preservation of contrast at mid-spatial frequencies (MTF30), together with the more pronounced decline in fine-detail resolution (MTF50), produces an out-of-focus rendering that favors tonal continuity over the precise definition of blurred shapes. Near the image center, the blur discs remain relatively uniform, whereas toward the image periphery they become compressed and increasingly directional, producing the characteristic cat's-eye bokeh. Rather than disrupting the image, this transition introduces a gradual variation: the background retains its tonal density and overall coherence while becoming less uniform in the shape of the blur. Overall, the lens preserves the structural integrity of the composition while allowing the out-of-focus rendering to become more expressive, reinforcing an aesthetic that is more organic than analytical.

The radial MTF30 plot of the 135 mm lens (Fig. 79) reveals a distinctive behavior within the lens set, in which useful resolving power is not only maintained but also exhibits a subtle spatial redistribution across the image field.

At the image center, the response begins at a relatively high level, although not the highest within the measured range, indicating a moderate transfer of contrast at mid-spatial frequencies. As the analysis moves toward the intermediate regions of the image field, however, the curve shows a slight increase, reaching its maximum at approximately 40–60% of the image field. This behavior—

unusual when compared with the more typical progressive decline—suggests that the lens does not concentrate its highest performance exclusively along the optical axis but instead distributes it more uniformly across the usable image area.

Beyond this intermediate region, as the analysis progresses toward the image periphery, the response declines gradually, with a more pronounced reduction in the sagittal component than in the meridional one. The separation between the two curves becomes increasingly evident across the outer third of the image field, indicating the onset of off-axis aberrations that affect the two orientations differently. Nevertheless, the degradation is progressive rather than abrupt, suggesting well-controlled optical behavior even at the extreme edges of the field.

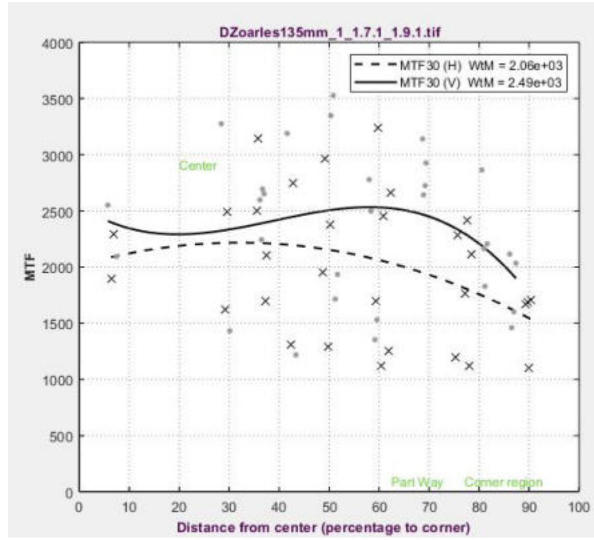

Figure 79

This profile—with its subtle broadening of performance across the intermediate region and its restrained decline toward the image borders—characterizes a lens that prioritizes consistency across a wide portion of the image field rather than concentrating its highest performance exclusively at the optical axis. From a cinematographic perspective, this translates into an image in which perceived sharpness remains remarkably stable throughout the intermediate regions of the frame, avoiding an excessive hierarchy between the center and the periphery while still introducing a gentle softening toward the edges.

Overall, the radial MTF30 profile of the 135 mm lens describes an optic with a well-balanced distribution of resolving power at mid-spatial frequencies, whose region of maximum performance is shifted toward the intermediate image field rather than being confined to the center. The progressive peripheral falloff imparts character to the image without compromising its overall coherence.

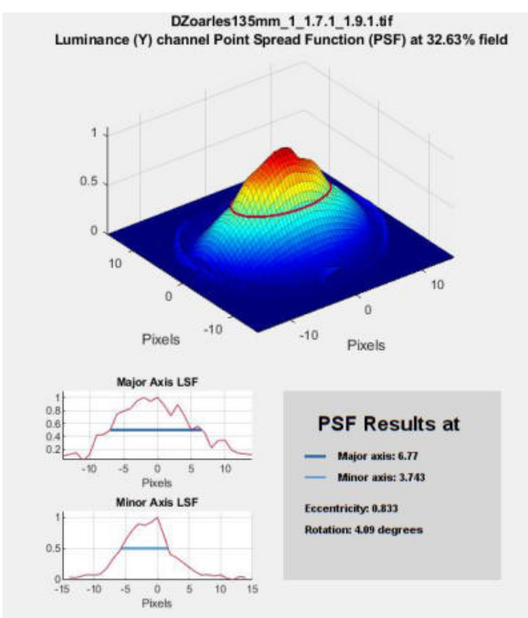

Figure 80

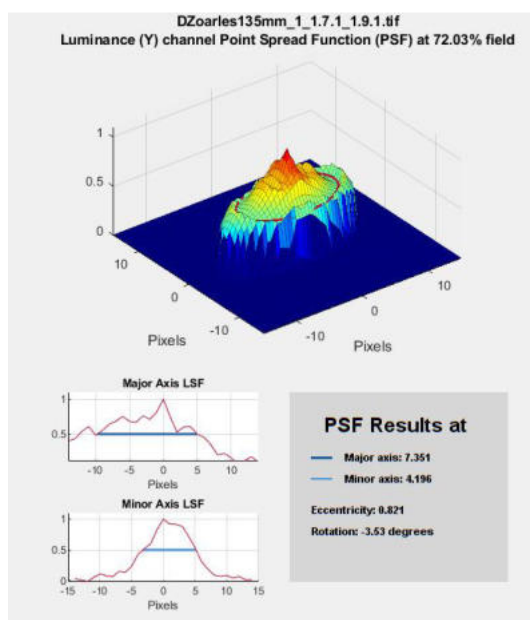

Figure 81

The PSF analysis of the 135 mm lens is highly consistent with the behavior previously suggested by both the radial MTF curve and the overall optical performance of the lens, while adding an essential dimension: how image energy is distributed spatially across the image field.
In the intermediate region of the image field (approximately 30%; Fig. 80), the PSF already exhibits a distinctly anisotropic shape, with pronounced elongation (major and minor axes of approximately 6.8 and 3.7 pixels, respectively; eccentricity ≈ 0.83). This indicates that, even well away from the optical axis, the lens does not distribute light energy in a perfectly circular manner. Nevertheless, the central core of the PSF remains compact and relatively well defined, explaining the slight increase observed in the radial MTF curve across the intermediate region: the light energy remains well concentrated, although not perfectly isotropically.
Toward the image periphery (approximately 70%; Fig. 81), the PSF undergoes a more pronounced transformation. The elongation persists (major and minor axes of approximately 7.3 and 4.2 pixels, respectively), but, more importantly, the distribution develops a more irregular and truncated profile, with less continuous and more sharply defined boundaries. At this stage, the light energy is not only more widely dispersed but also redistributed in a distinctly directional and less uniform manner. This behavior directly explains both the progressive decline of the MTF30 response and the increasing separation between the sagittal and meridional components observed in the radial MTF plot.
Importantly, this is not a chaotic degradation but a structured one. In the intermediate region, the lens redistributes light energy while preserving overall coherence; toward the image periphery, the energy becomes increasingly elongated and fragmented, introducing both directionality and a distinctive optical character.
This behavior is also fully consistent with the observations derived from the bokeh analysis and the out-of-focus test charts. The tendency toward elliptical, compressed blur away from the optical axis is not merely an aesthetic characteristic but the direct manifestation of the progressive deformation of the PSF across the image field. Likewise, the increasing difference between the major and minor axes of the PSF reinforces the previous interpretation of astigmatism and other off-axis aberrations, already suggested by the divergence between the sagittal and meridional MTF responses.
Overall, the PSF analysis confirms that the 135 mm lens maintains a relatively well-confined energy core throughout the central and intermediate regions of the image field, while exhibiting progressively greater deformation toward the edges. This behavior not only explains the evolution of the measured resolving power but also relates directly to the visual appearance of the image: clarity and presence are preserved across the useful image area, whereas the image periphery acquires a degree of directional softness that contributes to the distinctive rendering of the lens. Rather than an abrupt deterioration in image quality, what emerges is a transformation in the way the lens renders light, entirely consistent with the optical behavior described throughout the preceding analyses.

Lateral Chromatic Aberration

The chromatic aberration analysis of the 135 mm lens both confirms and refines the interpretation suggested by the MTF and PSF results. Rather than behaving as a perfectly neutral optic, the lens exhibits excellent chromatic correction along the optical axis while introducing character in a gradual and well-structured manner toward the image periphery.

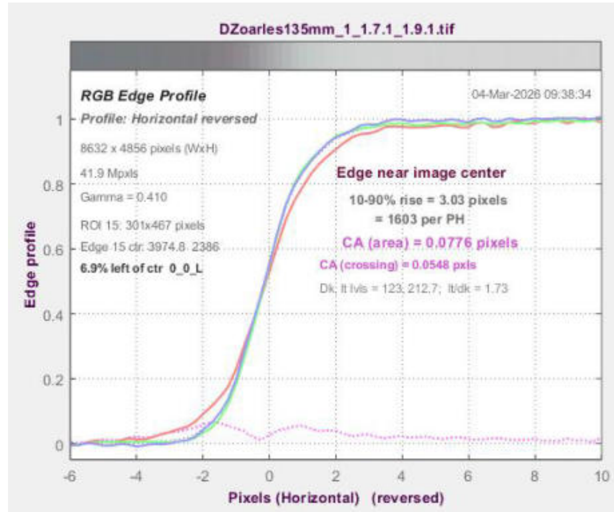

Figure 82. Center of the Image

At the image center (*Fig. 82*), chromatic aberration is virtually negligible. The measured values (approximately 0.08 pixels for CA area and 0.05 pixels for CA crossing) lie well below the perceptual threshold, and the RGB channels exhibit excellent alignment. This is entirely consistent with the MTF and PSF analyses: a well-confined central core with no appreciable chromatic dispersion, where image sharpness is preserved without color contamination.

Moving toward the lateral regions (approximately 75% of the image field; *Figs. 83 and 84*), chromatic aberration increases to values of approximately 2 pixels (about 1.97 pixels on the left side and 2.04 pixels on the right). This represents a clear and progressive increase relative to the image center, where chromatic aberration is essentially absent. Although there is a slight difference between the two sides—more pronounced in the CA crossing values—the overall behavior remains consistent and free of abrupt variations. This is significant because it closely parallels the transformation observed in the PSF: as the light energy becomes increasingly dispersed and directional, the chromatic component evolves in the same progressive manner.

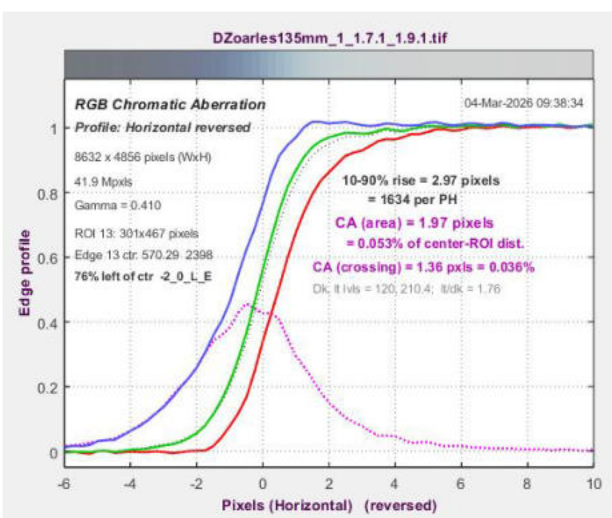

Figure 83. Left Side of the Image

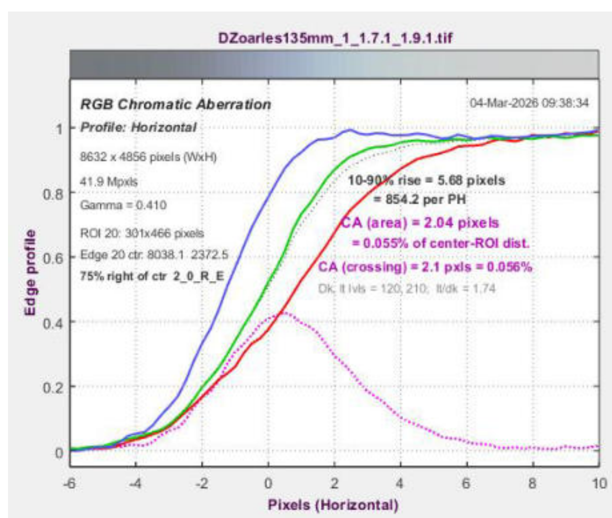

Figure 84. Right Side of the Image

An especially important point is that chromatic aberration must be understood as one component of the lens's overall optical performance. In other words, the reduction in image quality toward the edges is not attributable to chromatic aberration alone, but rather to the combined effect of several off-axis aberrations—including astigmatism, PSF deformation, and the decline in MTF—of which the chromatic component constitutes only one element within a broader optical system.

From a visual standpoint, this behavior translates into an image in which:

- the image center remains clean and chromatically neutral;
- the intermediate image field retains good clarity and readability; and
- the image periphery introduces a subtle degree of chromatic fringing that reinforces the perceptual transition toward the edges of the frame.

Overall, the 135 mm lens exhibits excellent chromatic correction along the optical axis, with chromatic aberration increasing gradually toward the image periphery, consistent with an optical design that prioritizes central stability while allowing a degree of expressive character at the edges. Rather than constituting a dominant optical defect, chromatic aberration forms part of the same behavior already described by the MTF and PSF analyses: a lens that does not deteriorate abruptly at the image extremes but instead modulates its optical performance progressively, maintaining a strong correspondence between the technical measurements and the resulting visual perception.

The radial chromatic aberration analysis of the 135 mm lens (*Fig. 85*) provides a clear representation of how chromatic separation is distributed across the image field. From the image center, where chromatic deviation is virtually negligible, both curves evolve in a smooth and continuous manner: the R–G component increases progressively to approximately +1.2 pixels at the image periphery, while the B–G component diverges in the opposite direction, reaching approximately –1.4 pixels. This symmetrical divergence, without abrupt changes in trend, characterizes a stable and highly predictable optical behavior.

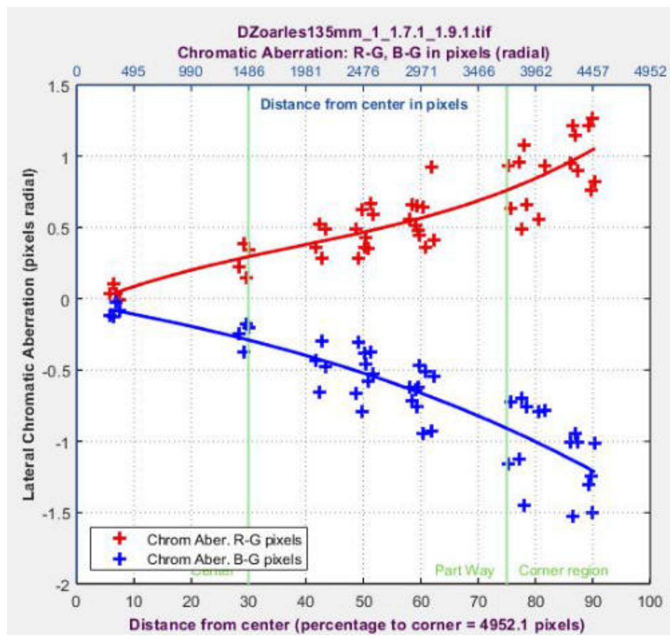

Figure 85

What is particularly significant is not merely the final magnitude of the aberration, but the manner in which it develops. Chromatic aberration does not appear suddenly; rather, it accumulates progressively with increasing distance from the optical axis. Even in the outermost regions of the image field, where the channel separation becomes most apparent, the transition remains smooth and continuous, without irregularities or anomalous scatter in the measured data.

This interpretation is fully consistent with the lateral measurements discussed previously. At the image center, the virtually negligible chromatic aberration corresponds directly to the origin of the radial curves. In the intermediate regions, where chromatic aberration first becomes perceptible, the radial plot already exhibits a clear yet well-controlled slope. Finally, at the image periphery, where the highest values are recorded, the plot confirms that this increase results from a sustained and orderly progression rather than from erratic optical behavior.

Overall, the 135 mm lens does not completely eliminate lateral chromatic aberration at the image periphery, but it manages it in a highly coherent manner. Color separation remains orderly and well controlled, integrated into the overall optical behavior of the system and fully consistent with the findings of the MTF and PSF analyses. Rather than introducing abrupt discontinuities, the lens modulates its optical performance progressively toward the image periphery while maintaining a structurally coherent image.

Geometric Distortion

The geometric distortion analysis of the 135 mm lens (*Fig. 86*) reveals extremely well-controlled behavior, entirely consistent with a well-corrected telephoto optic.

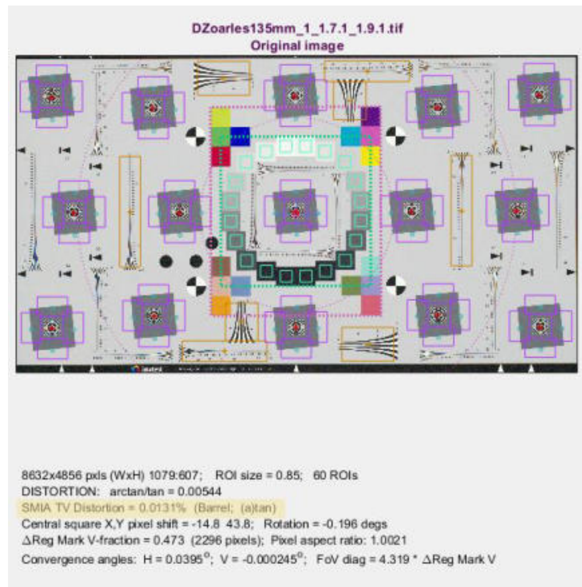

Figure 86

The primary value reported by Imatest (approximately 0.054% using the arctan/tan model) places geometric distortion within an exceptionally low range. From a visual standpoint, this means that straight lines remain essentially straight throughout the image field, with no perceptible curvature even near the edges. There is no clear signature of either barrel or pincushion distortion; if present at all, it remains well below the threshold of perceptibility under normal cinematographic viewing conditions.

The SMIA value (approximately 0.013%) further supports this interpretation, indicating only a negligible tendency toward barrel distortion. This produces no visible bowing of architectural elements or structural lines, an especially important characteristic in a telephoto lens, where even minor geometric deviations could become more apparent in compressed compositions.

Another noteworthy aspect is the absence of localized irregularities or asymmetric deformation. The distortion remains smooth, global, and highly consistent across the image field, with no regions exhibiting abrupt changes in behavior. This reflects careful optical design and, above all, highly predictable geometric performance.

The pixel aspect ratio (approximately 1.002), together with the absence of significant angular deviations, further confirms that no additional geometric deformation is introduced either by the image acquisition system or by the measurement pipeline.

In practical imaging terms, this translates into a very specific characteristic: the 135 mm lens does not intervene in the geometry of the scene. The spatial compression perceived in the resulting images is produced exclusively by the natural perspective associated with the focal length, rather than by optical distortion. In other words, the lens compresses perspective without deforming geometry.

Within the broader context of the MTF, PSF, and chromatic aberration analyses, this behavior is entirely consistent. The lens derives its character from the way it renders out-of-focus regions and from the gradual evolution of image quality from the center toward the periphery—with sharpness declining progressively and the blur becoming increasingly elliptical and directional rather than perfectly circular and homogeneous toward the image edges. At the same time, it preserves the geometric integrity of the frame. This combination of gradual image rendering and exceptional geometric stability is precisely what makes the 135 mm lens such a compelling tool for cinematographic applications.

This frame corresponds remarkably well with the optical behavior measured for the 135 mm lens, to the extent that the image appears to be a practical manifestation of the technical results. First, the spatial compression defines both the composition and the visual structure of the frame: the subject is clearly isolated, while the background is brought visually closer without sacrificing continuity or coherence among its elements. This continuity is entirely consistent with the MTF30 analysis, which showed that the lens does not concentrate its performance exclusively at the image center but instead maintains a consistent response across the intermediate image field, allowing background elements to remain legible even when rendered out of focus.

At the same time, the rendering of the background blur closely reflects the behavior observed in the PSF analysis. Rather than producing a completely neutral or homogeneous bokeh, the lens generates a blur with a certain visual density, subtle internal structure, and a slight directional character. This is fully consistent with the progressive elongation of the PSF across the intermediate and peripheral regions of the image field: the light energy is not distributed in a perfectly circular manner but instead exhibits a mild anisotropy that adds texture to the background without disrupting its visual coherence.

With regard to chromatic aberration, its effect in this frame is virtually imperceptible on the main subject, in agreement with the measured values along the optical axis, where lateral chromatic aberration remains extremely low. In the background, although chromatic separation may become apparent under more demanding conditions, it is effectively masked by the out-of-focus rendering, reinforcing the overall impression of a clean and well-controlled image.

Most importantly, none of these characteristics appear as isolated phenomena; rather, they operate as components of a single, coherent optical system. The gradual decline in resolving power toward the image edges, the progressive deformation of the PSF, and the controlled increase in lateral chromatic aberration all converge to produce an image in which the center remains stable and well defined, while the remainder of the frame softens progressively in a smooth and visually coherent manner.

In this respect, the frame photographed with the 135 mm lens clearly expresses its optical character: a lens that builds the image around central stability and perspective compression while introducing a gradual transition toward a more structured out-of-focus rendering at the image periphery. The result is an image with both consistency and a distinctive visual identity, in which visual perception directly confirms what the technical analysis had anticipated.

Adriana Bernal: *That very softness we've been discussing was one of the qualities that benefited skin tones the most. Although the Arles lenses maintain a solid level of resolving power, fine detail never becomes excessively pronounced, allowing skin texture to appear more natural and less overly delineated.*

As I mentioned when discussing the technical tests, another interesting characteristic also became apparent: the lenses preserve good definition at the image center, but the transition in contrast is remarkably gradual, and fine detail is never rendered in an overly aggressive manner. This allows skin to retain both texture and volume without appearing harsh, particularly in close-ups or in scenes with high-contrast lighting.

In practice, faces retained more than enough detail, yet without the hyper-defined appearance that can sometimes make every pore or skin imperfection overly conspicuous. The image remained precise, but with a rendering that felt gentler, more organic, and ultimately more flattering.

7- 180 MM LENS

Figures 87–90 show the MTF curves at different locations across the image field.

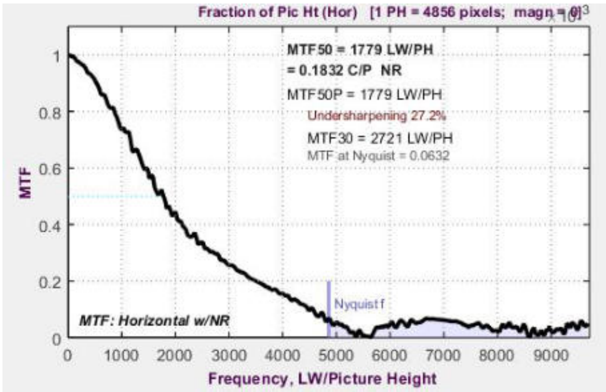

Figure 87. Center of the Image

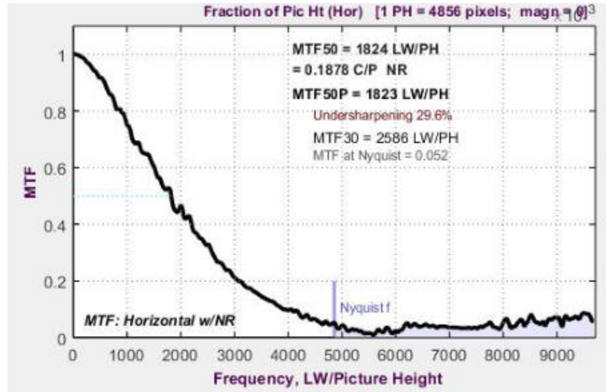

Figure 88. Left Side of the Image

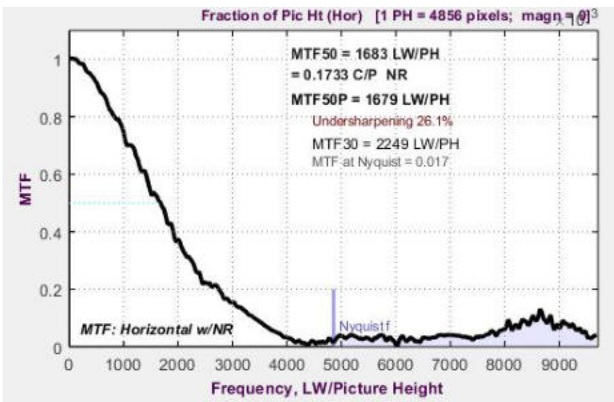

Figure 89. Upper-Left Corner of the Image

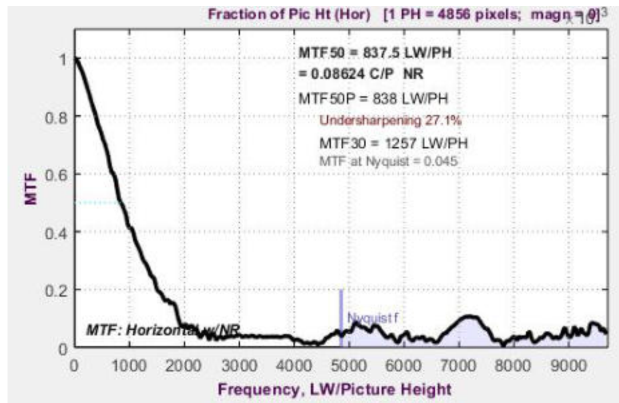

Figure 90. Lower-Right Corner of the Image

The comparison of the MTF curves across different regions of the image field (Fig. 91) reveals an optical performance that is non-uniform yet well structured. The image center and the intermediate regions—extending from the optical axis toward the image borders—maintain very similar levels of performance, with no significant degradation, confirming excellent stability throughout most of the usable image area. Toward the corners, the response declines progressively, although with a marked asymmetry: while one corner retains performance relatively close to that of the center, the opposite corner exhibits a considerably more pronounced reduction.

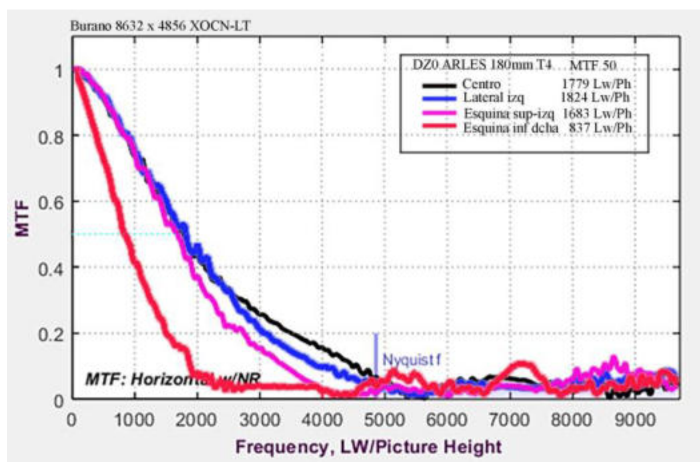

Figure 91

This difference does not result from a simple, uniform loss of performance but rather from a localized variation in the off-axis optical behavior, most likely associated with residual aberrations or slight optical misalignment. Nevertheless, the overall shape of the MTF curves remains coherent, indicating that the lens preserves the fundamental structure of its optical response while modulating it unevenly across the image field.

From a visual standpoint, this translates into an image that remains robust along the optical axis and throughout the intermediate field, with localized degradation confined to peripheral regions. Although this behavior rarely compromises the overall readability of the frame, it may become perceptible in particularly wide compositions where image information extends into the extreme corners.

The three-dimensional MTF map (Fig. 92) provides a precise visualization of the spatial distribution of the lens's optical performance. At the image center, the response reaches approximately 1779 LW/PH and extends into the intermediate regions with values remaining within a comparable range of roughly 1800–1600 LW/PH, without any abrupt decline. This confirms the stability of both the central region and a substantial portion of the usable image field, as already indicated by the MTF curve analysis.

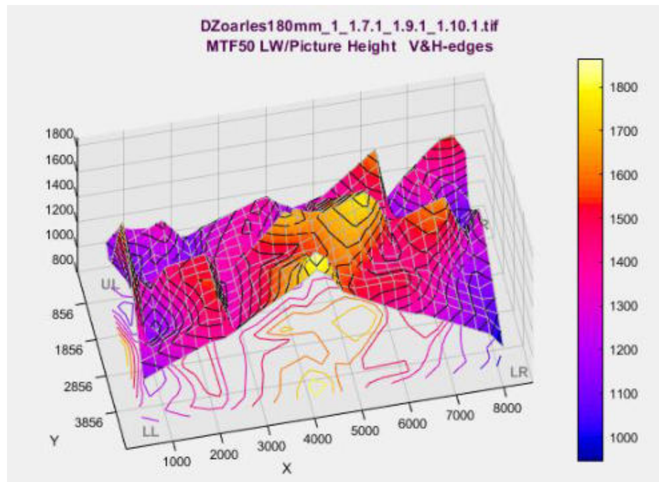

Figure 92

As the analysis moves toward the image periphery, optical performance declines progressively, reaching approximately 1500–1300 LW/PH in the better-preserved edge regions, consistent with the 1683 LW/PH measured in one of the corners. This decline, however, is not entirely uniform. The three-dimensional map reveals a localized region of the image field where performance decreases more markedly, reaching values of approximately 837 LW/PH, in agreement with the measurements obtained in the lower-right corner.

This asymmetry does not reflect a general deterioration of the optical system but rather a localized variation in off-axis performance. Even so, the overall structure of the response remains coherent: the lens preserves a solid level of performance at the image center and across much of the usable image field, while modulating its response progressively toward the edges without introducing abrupt discontinuities.

Overall, the 180 mm lens exhibits a spatial distribution of optical performance that combines excellent axial stability with a gradual, directional decline toward the image periphery, fully consistent with both the MTF curves and the preceding analysis of its optical behavior.

The comparison between the MTF50 and MTF30 measurements (*Tables 12 and 13; Figs. 93 and 94*) further confirms the consistency of the lens's performance across the entire image field. Although the absolute values decrease toward the periphery—most noticeably in one of the corners—the relationship between the two metrics remains remarkably stable, maintaining an approximately constant proportion. This indicates that the reduction in performance does not occur abruptly or in a structurally irregular manner, but rather through a gradual decline in contrast as spatial frequency increases.

From a visual standpoint, this relationship results in an image that, although exhibiting reduced microcontrast in the most demanding regions of the frame, continues to preserve the definition of forms and the overall readability of the scene. Even in those areas where optical performance is at its lowest, the lens maintains a coherent image structure without introducing disruptive discontinuities. This behavior further reinforces the interpretation of a controlled and progressive degradation, fully consistent with the findings of the preceding optical analyses.

FOCAL 180MM	LW/PH 50%
CENTER	1779
LEFT SIDE	1824
UPPER-LEFT CORNER	1683
LOWER-RIGHT CORNER	837,5

Table 12

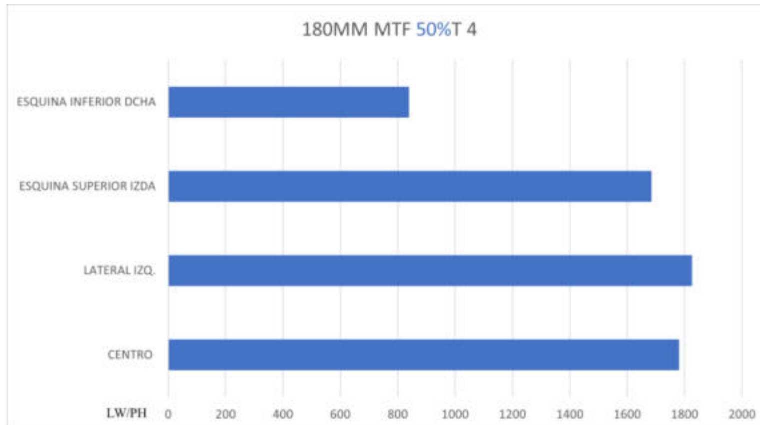

Figure 93

FOCAL 180MM	LW/PH 30%
CENTER	2721
LEFT SIDE	2586
UPPER-LEFT CORNER	2249
LOWER-RIGHT CORNER	1257

Table 13

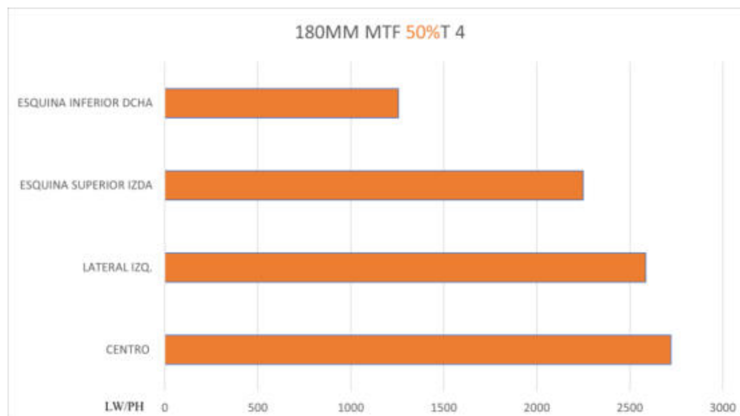

Figure 94

The radial MTF30 plot in the horizontal and vertical orientations (*Fig. 95*) provides a more detailed view of how optical performance is distributed across the image field. The curves exhibit a gradual decline from the image center toward the periphery, decreasing from values close to 2500 LW/PH to approximately 1800–2000 LW/PH in the outer regions of the field, without any abrupt discontinuities.

This decline, however, is not entirely uniform between the two orientations. From approximately the midpoint of the image field onward, a separation becomes evident between the horizontal and vertical

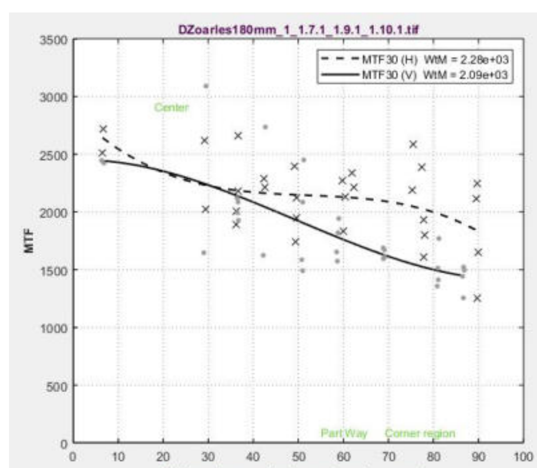

Figure 95

curves, with one orientation maintaining slightly higher performance than the other. This divergence becomes increasingly pronounced toward the image corners, suggesting the presence of direction-dependent off-axis aberrations, consistent with residual astigmatism or the combined effects of field curvature.

This behavior reinforces the previous observations: the lens maintains a robust level of performance along the optical axis, while introducing a gradual peripheral degradation that is not only spatially progressive but also dependent on image orientation.

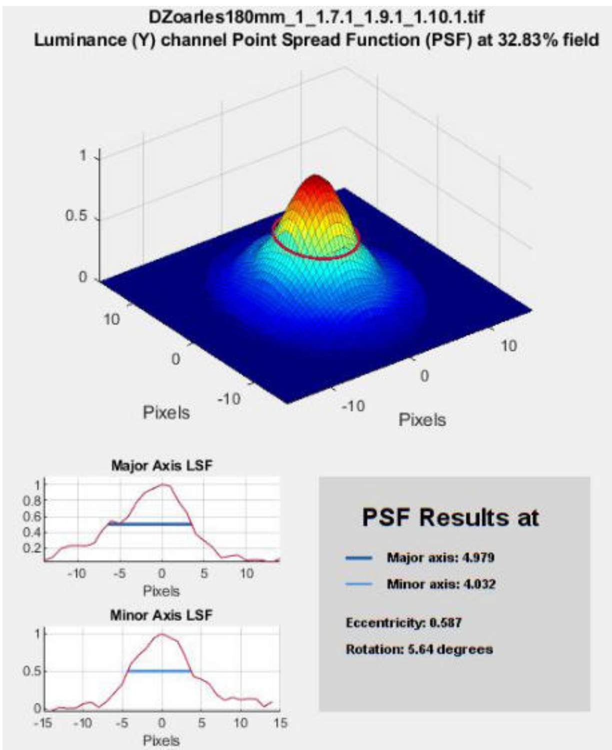

Figure 96

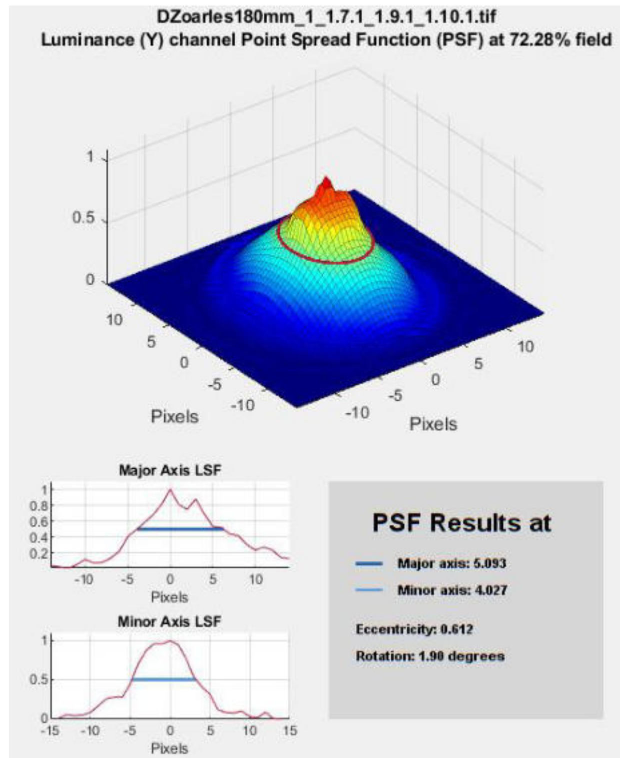

Figure 97

The analysis of the Point Spread Function (PSF) (*Figs. 96 and 97*) confirms the physical origin of the variations observed throughout the other optical metrics. As the analysis progresses toward the image periphery, the PSF retains a relatively compact structure while exhibiting a gradual increase in eccentricity, rising from approximately 0.58 to about 0.61. This change is reflected in a progressive elongation of the point image, with a major axis of approximately 5 pixels compared with a minor axis of about 4 pixels.

This difference between the principal axes explains the divergence observed between the horizontal and vertical MTF curves, revealing an increasing degree of anisotropy away from the optical axis. Rather than representing an abrupt deterioration of image quality, this behavior corresponds to a directional redistribution of light energy: the lens preserves its structural coherence while no longer responding in a completely uniform manner across different image orientations.

The orientation of the PSF provides a further refinement of this interpretation. Although the elongation increases toward the image periphery, its principal axis remains closely aligned with the horizontal and vertical axes of the imaging system, without any significant rotation toward the radial direction of the image field. This suggests that the observed anisotropy cannot be attributed solely to classical radial astigmatism but instead includes a more stable directional component inherent to the optical design itself.

This behavior has a direct counterpart in the out-of-focus rendering. The elongation of the PSF corresponds to the elliptical shape of the blur discs, whose orientation follows the same directional pattern. At the same time, mechanical vignetting produces the characteristic compression associated with cat's-eye bokeh, aligned with the radial geometry of the image field. The combination of these two effects—the radial deformation of the light bundle and the internally oriented elongation of the PSF—produces an out-of-focus rendering that varies not only in shape but also in its internal structure.

Overall, the lens does not exhibit a purely radial degradation of optical performance but rather a superposition of distinct behaviors: a geometric component associated with the optical system itself and a progressively increasing directional anisotropy toward the image periphery. This evolution preserves the overall coherence of the image while defining an optical character in which the out-of-focus rendering evolves in a controlled and progressive manner, without abrupt degradation.

Lateral Chromatic Aberration

The chromatic aberration analysis reveals behavior that is clearly dependent on position within the image field. At the image center, the measured values are essentially negligible (approximately 0.38 pixels for CA area and 0.10 pixels for CA crossing), with the RGB channels exhibiting almost complete superposition. This results in a clean image, free from any perceptible chromatic artifacts (*Fig. 98*).

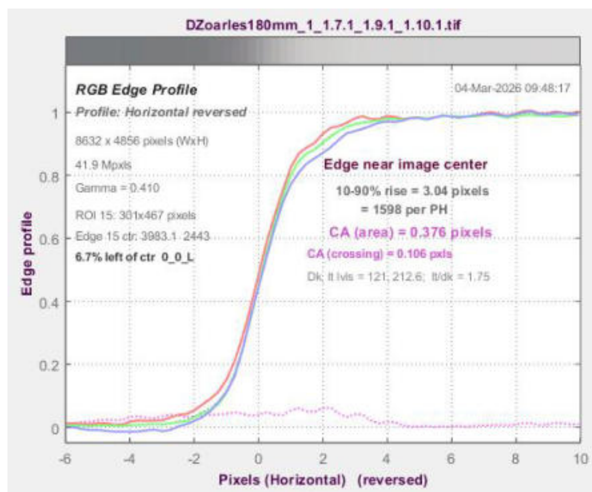

Figure 98. Center

As the analysis moves toward the image periphery, chromatic aberration increases progressively. In the lateral regions of the image field, the measured values reach approximately 1.2–1.4 pixels, with a clear separation of the RGB channels that becomes particularly evident along high-contrast edges. This increase is gradual, orderly, and highly consistent, with no signs of irregular or erratic behavior (*Table 14 Figs. 99 and 100*).

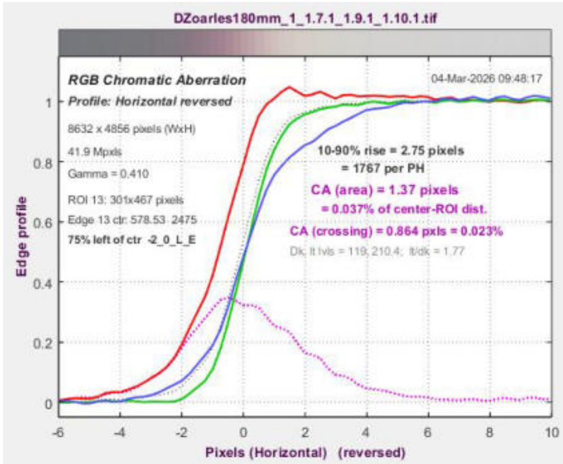

Figure 99. Left Side of the Image

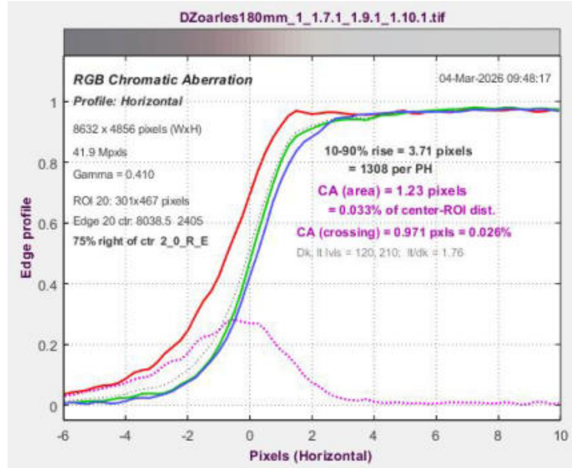

Figure 100. Right Side of the Image

Zone	CA area	CA crossing	Interpretation
Center	0.376 px	0.106 px	Virtually negligible
Left side	1.37 px	0.864 px	Visible
Right side.	1.23 px	0.971 px	Visible

Table 14

Comparison of the two sides of the image field reveals no significant differences, indicating a high degree of symmetry in the lateral chromatic response. Overall, the lens exhibits excellent chromatic correction along the optical axis and only moderate levels of lateral chromatic aberration away from the center, fully consistent with the behavior previously observed in the MTF and PSF analyses. From a visual perspective, this results in an image that remains chromatically stable at the center, with only a subtle appearance of chromatic fringing toward the edges of the frame, without significantly affecting the image as a whole.

The radial analysis of lateral chromatic aberration reveals a progressive increase from the image center toward the periphery (Fig. 101). In the central region, channel separation is virtually negligible.

As the distance from the optical axis increases, the first clearly defined pattern emerges: the blue curve (B–G) rises progressively to positive values of approximately 0.3–0.4 pixels, while the red curve (R–G) decreases toward negative values of approximately –0.6 to –0.9 pixels. In other words, the color channels diverge in opposite directions (see *Table 5*).

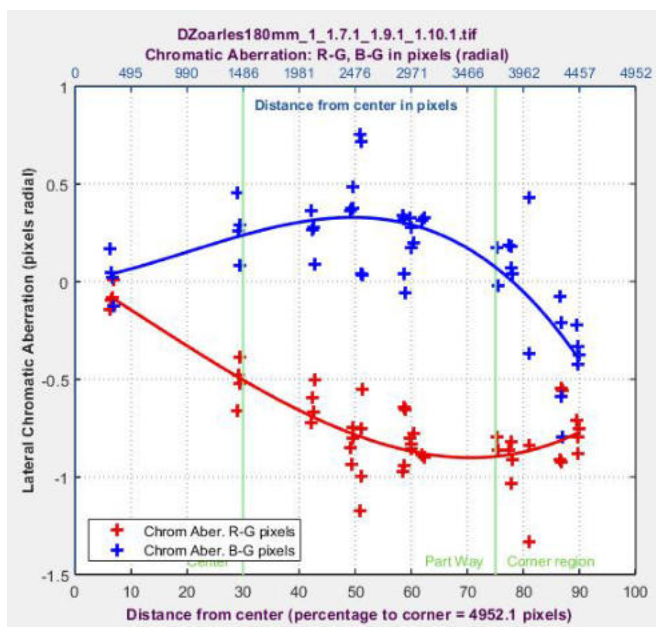

Figure 101

In the transition zone toward the image periphery (approximately 60–80% of the image field), an inflection point becomes evident. The blue curve reaches its maximum value and then begins to decline, while the red curve reaches its minimum—approximately –1 pixel—and subsequently tends to stabilize. This change indicates that chromatic aberration no longer continues to increase but instead enters a more stable and controlled regime.

In the outermost regions of the image field, the measured values remain within this regime, although the individual measurements exhibit greater scatter, a behavior commonly observed near the image boundaries.

This behavior is fully consistent with the other optical metrics. The progressive decline in MTF and the slight elongation of the PSF describe the same underlying evolution, in which image resolution decreases gradually and with a degree of directional dependence, but without any abrupt degradation.

Overall, lateral chromatic aberration increases progressively with distance from the optical axis, but it does so in an orderly and predictable manner, remaining well controlled throughout the entire image field.

Geometric Distortion

The geometric distortion analysis of the 180 mm lens (*Fig. 102*) reveals exceptionally well-controlled behavior. The overall distortion value (0.00508, arctan model) together with the SMIA measurement (0.0167%) indicates a very slight barrel distortion, although its magnitude remains extremely low. In practical terms, it is imperceptible in the final image.
Straight lines remain accurately rendered across the entire image field, with no visible deformation at the frame edges. This allows the lens to be used confidently in scenes containing architectural subjects or other geometrically structured elements without requiring additional distortion correction.

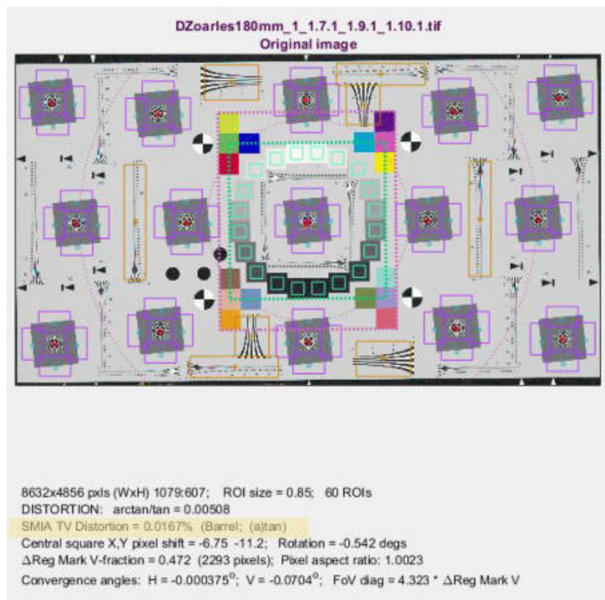

Figure 102

The alignment parameters (center shift of –6.75 and –11.2 pixels, and a rotation of –0.542°) correspond to the measurement alignment procedure rather than to the optical behavior of the lens itself, and therefore have no perceptible effect on the recorded image. Likewise, the pixel aspect ratio (1.0023) and the virtually negligible convergence angles confirm the absence of any significant geometric deviation.

Overall, the 180 mm lens introduces no perceptible geometric distortion. Straight lines remain straight, object shapes are faithfully preserved, and the structural integrity of the scene is maintained. The visual character of the image is therefore determined by the natural perspective compression associated with the focal length and by the out-of-focus rendering, rather than by any alteration of the scene's geometry.

8- Overall Evaluation of the DZO Arles Lenses Tested

Having examined each focal length individually, we now turn to the performance of the lens set as a whole in order to identify common trends and significant differences across the different focal lengths.

Resolution

For this comparative analysis, we have included the 14 mm, 21 mm, and 25 mm focal lengths, together with those examined in detail in the preceding sections. Here, the comparison is based on the center-of-image response expressed in cycles per pixel (cycles/pixel).

Focal (mm)	MTF50 (C/P)	MTF30 (C/P)
14	0.1455	0.202
21	0.2312	0.323
25	0.1578	0.224
35	0.2278	0.352
50	0.1746	0.252
75	0.1863	0.278
100	0.2503	0.357
135	0.1714	0.236
180	0.1832	0.28

Table 15

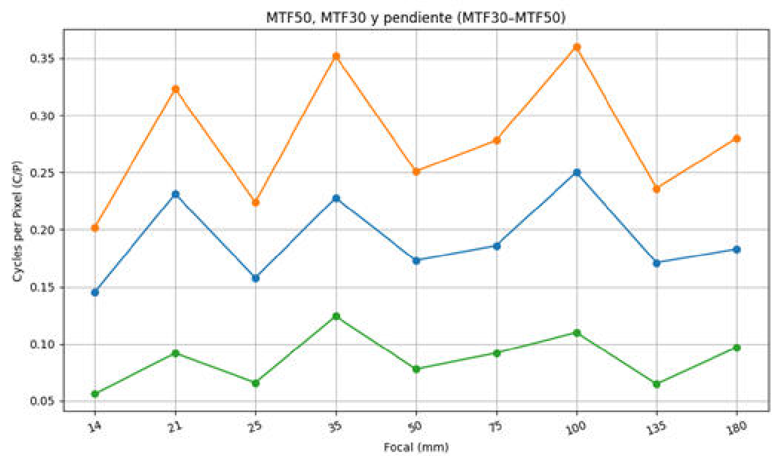

Figure 103

Figure 103 and *Table 15* present the MTF50 (blue), MTF30 (orange), and their difference (green), expressed in cycles per pixel (cycles/pixel). This latter parameter (MTF30–MTF50) may be used as a comparative indicator of the rate at which image contrast declines.

Whereas MTF50 defines the spatial frequency at which contrast falls to 50% and is closely associated with perceived image sharpness, MTF30 reflects the lens's ability to preserve contrast at medium and high spatial frequencies. The difference between these two values (green curve) does not directly measure resolving power or the complete slope of the MTF curve; rather, it serves as a comparative reference between two contrast thresholds.

Among the wide-angle focal lengths, such as the 14 mm (≈ 0.056 cycles/pixel) and the 25 mm (≈ 0.066 cycles/pixel), the relatively small differences indicate a more rapid transition between MTF50 and MTF30. This suggests an earlier loss of contrast at medium-to-high spatial frequencies, producing an image with a softer rendering and a less aggressive reproduction of fine detail. The 21 mm exhibits a somewhat distinct behavior within this group. Although it retains the spatial rendition and depth characteristic of a wide-angle lens, its MTF50 (≈ 0.231 cycles/pixel) and MTF30 (≈ 0.323 cycles/pixel) values are among the highest in the series. The difference between these two thresholds (≈ 0.092 cycles/pixel) indicates a more gradual decline in contrast than that observed in the 14 mm and 25 mm lenses, resulting in greater persistence of fine detail and a more stable, well-defined image texture.

By contrast, focal lengths such as the 35 mm (≈ 0.124 cycles/pixel) and the 100 mm (≈ 0.110 cycles/pixel) exhibit larger differences between MTF50 and MTF30, indicating a more gradual decline in contrast. In these lenses, useful image contrast is preserved over a broader range of spatial frequencies, promoting a more continuous rendering of textures and smoother tonal transitions.

The intermediate focal lengths, such as the 50 mm (≈ 0.078 cycles/pixel) and the 75 mm (≈ 0.092 cycles/pixel), occupy a balanced position, combining good resolving power with a relatively smooth decline in contrast. Among the longer telephoto lenses, the 135 mm (≈ 0.065 cycles/pixel) continues to exhibit a more rapid transition between the MTF50 and MTF30 thresholds, whereas the 180 mm (≈ 0.097 cycles/pixel) partially recovers a more gradual contrast transition, although without reaching the levels observed in the 35 mm and 100 mm lenses.

When this interpretation is considered alongside the absolute MTF50 values, the overall picture becomes more complete. The various focal lengths remain within a relatively homogeneous range of central resolving power—approximately 0.145 to 0.25 cycles/pixel—with no critical declines or significant discontinuities across the lens series.

However, similar resolving power does not necessarily imply identical visual rendering. Two lenses with comparable MTF50 values may produce noticeably different images depending on how they distribute contrast across the medium and high spatial frequencies. The rate of contrast decline therefore introduces a qualitative dimension that is more closely related to microcontrast, texture, and tonal transitions than to sharpness alone.

From a cinematographic perspective, these variations help explain why certain focal lengths are perceived as softer and more continuous, whereas others produce an image with greater definition and stronger contrast. Taken together, the combined analysis of MTF50 and MTF30 reveals a highly coherent optical system in which the differences between focal lengths do not appear as discontinuities, but rather as distinct ways of organizing image contrast, texture, and tonal rendering (*Fig. 104*).

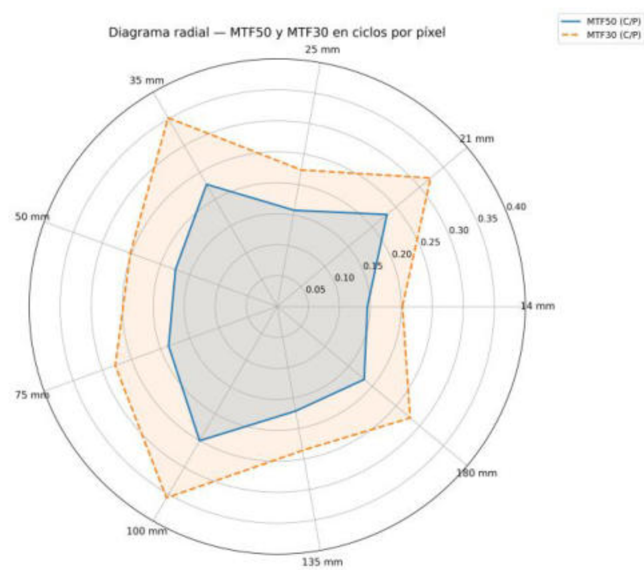

Figure 104. Radial Diagram

Tables 16 and 17 relate the absolute MTF50 and MTF30 values presented in Table 15 to a range of visual characteristics commonly encountered in digital cinematography. These classifications should not be interpreted as absolute scales of optical quality, but rather as indicative references for understanding the visual behavior of the lenses.

Approx. MTF50 (cycles/pixel).	Perceived Resolving Power	Microcontrast	Visual Impression	Perceived Image Rendering	Cinematographic Interpretation
0.10 – 0.14	Low–Moderate	Low	Soft	Less pronounced edges, reduced texture separation, smooth tonal transitions, fine detail less apparent	Organic rendering, less aggressive appearance, more atmospheric and immersive image
0.14 – 0.18	Moderate	Moderate	Balanced	Good level of detail without making the image appear harsh; natural texture separation and controlled definition	Classic cinematographic rendering, balancing sharpness and softness
0.18 – 0.22	High	High	Well-defined / Crisp	Clearly defined edges, visible microdetail, strong texture separation, immediate perception of sharpness	Clean, precise rendering with an enhanced sense of definition and dimensionality
0.22 – 0.26	Very High	Very High	Highly Crisp / Clinical Tendency	Extremely visible texture, sharply delineated edges, very high fine-detail contrast, highly analytical rendering	Modern, highly defined aesthetic with the potential to make skin and materials appear overly harsh
> 0.26	Extremely High	Extremely High	Highly Analytical / Clinical Tendency	Hyper-defined rendering, minimal optical softness, consistently pronounced fine detail	Highly technical or "surgical" rendering that may sacrifice organicity and accentuate the digital character of the image

Table 16

Approx. MTF30 (cycles/pixel)	Fine-Detail Retention	Contrast Persistence	Visual Impression	Perceived Image Rendering	Cinematographic Interpretation
0.18 – 0.24	Low	Low	Soft / Delicate	Fine detail disappears relatively early, textures become simplified, and the image exhibits lower visual density.	A more atmospheric, less analytical rendering with smooth tonal transitions.
0.24 – 0.30	Moderate	Moderate	Natural	Texture remains present without becoming dominant, preserving good continuity between planes and materials.	A well-balanced cinematographic rendering, with detail that remains visible without becoming aggressive.
0.30 – 0.36	High	High	Rich in Texture	Surfaces retain relief and tonal separation, while fine detail remains clearly visible.	An image with a strong sense of visual density and tonal separation.
0.36 – 0.42	Very High	Very High	Highly Defined	Textures are strongly differentiated, contrast remains highly consistent across medium and high spatial frequencies, and the image conveys an exceptional sense of clarity.	A modern, highly precise rendering in which fine detail becomes particularly prominent.
> 0.42	Extremely High	Extremely High	Analytical / Clinical Tendency	Fine detail dominates the visual impression, with minimal loss of texture and a highly pronounced rendering.	A rendering that risks excessive definition, reducing the image's sense of organicity.

Table 17

Beyond the differences in focal length and perspective, the lens series exhibits remarkable optical coherence in the way it distributes contrast and texture. The variations between individual lenses do not appear as abrupt shifts in optical character, but rather as gradual transitions within a shared visual language. Each focal length subtly rebalances resolving power, tonal transitions, and spatial rendering while maintaining a sufficiently consistent optical response to allow changes of focal length without disrupting the overall visual identity of the image.

21 mm lens

21 mm lens

75 mm lens

25 mm lens

Selected frames from Indeleble. Cinematography by Adriana Bernal, ADFC.

The comparison of these four frames illustrates how the lens set establishes a coherent visual identity across markedly different focal lengths, maintaining continuity in texture and contrast while fundamentally reshaping the relationship between space, subject, and depth.

In the wide-angle frames—the hospital room, the industrial exterior, and the scene beside the vehicle—space assumes a clear narrative function and remains structurally integral to the composition. The image does not merely record the character but incorporates the surrounding environment as an active dramatic element within the frame. In the hospital scene, depth is articulated through successive spatial layers: the out-of-focus flowers, the hospital bed, the character, and the corridor coexist within a continuous spatial arrangement without becoming optically fragmented. In the industrial exterior, the pipes, steel structures, and humid atmosphere all remain simultaneously legible without producing a hyper-defined appearance; textures remain cohesive, and the environment preserves a strong sense of atmospheric density. In the vehicle scene, the wide-angle lens introduces a more pronounced spatial tension: the subject's proximity to the camera expands the perceived space and heightens the sense of threat, while the well-controlled geometric distortion prevents the face from appearing caricatured or excessively distorted.

Across all three examples, a common characteristic of the wide-angle lenses becomes evident: the image preserves spatial structure and depth without rendering fine detail excessively harsh. The relatively rapid decline in contrast at medium-to-high spatial frequencies softens microcontrast and promotes a more continuous perception of space. Textures remain integrated within the scene rather than becoming separated in an overly clinical manner.

The fourth frame—the telephone close-up—reorganizes this spatial logic entirely. Here, the surrounding environment recedes in importance, and visual contrast is concentrated on the subject's face. Depth is no longer established through spatial breadth but instead through tonal separation and out-of-focus rendering. Skin texture, wrinkles, and hair retain clear definition without appearing overly delineated or harsh. The background remains smooth and coherent, free from visible halos or abrupt blur transitions, directly reflecting the more progressive optical behavior observed in the normal and short telephoto focal lengths.

What is particularly significant is that, despite these differences in spatial organization, the series maintains a clear visual continuity. Contrast never becomes excessive, tonal transitions remain gradual, and optical aberrations never assume a visually dominant role. The individual focal lengths do not appear to belong to different optical systems but rather to different expressions of the same underlying optical philosophy. Some prioritize spatiality and the coexistence of multiple image planes, while others concentrate visual attention and simplify spatial relationships. Yet all of them share the same approach to distributing contrast, moderating the transition of fine detail, and shaping the overall texture of the image.

Comparison of corner sharpness degradation across the different focal lengths.

Focal Length (mm)	**Upper-Left Corner MTF50 (LW/PH)**	**Upper-Left Corner MTF30 (LW/PH)**	**Lower-Right Corner MTF50 (LW/PH)**	**Lower-Right Corner MTF30 (LW/PH)**	**Center MTF50 (LW/PH)**	**Center MTF30 (LW/PH)**
35	1244	1728	1203	1660	2212	3417
50	1271	1785	1206	1670	1696	2447
75	733	945	1009	1433	1810	2704
100	1035	1535	1138	1530	2431	3470
135	1209	1710	1124	1668	1664	2296
180	1683	2249	837,5	1257	1779	2721

Table 18

The graph compares the resolving performance of the lens series between the image center and two opposite corners—the upper-left and lower-right—using MTF50 and MTF30 values expressed in LW/PH (*Table 18 and Fig. 105*). The solid lines represent the central performance, while the dashed and dotted lines illustrate the degradation toward the image periphery.

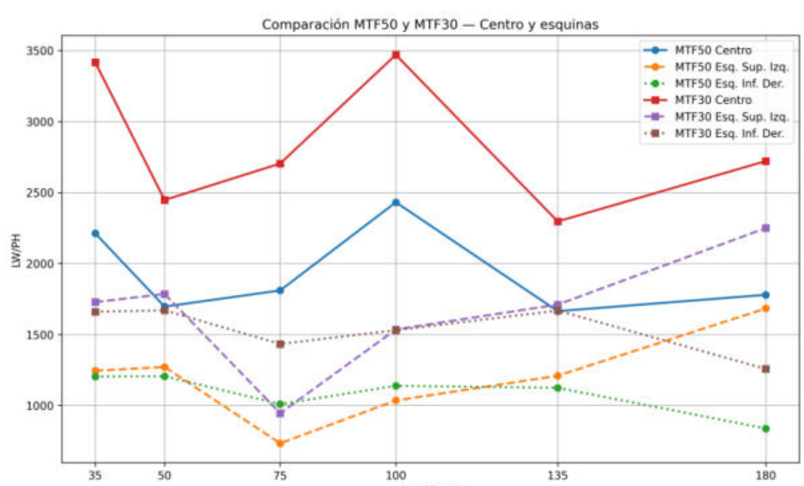

Figure 105

The first observation is immediately apparent: all of the lenses exhibit a reduction in resolving power away from the image center, but neither the magnitude nor the pattern of this decline is the same across the different focal lengths. The spatial performance of the lens series is therefore heterogeneous rather than uniform.

The **100 mm** lens emerges as the strongest performer within the series. It exhibits the highest central values for both MTF50 and MTF30, reaching approximately 2430 LW/PH and 3470 LW/PH, respectively. Although a significant decline in performance is observed toward the image periphery, the transition from the center to the corners remains more controlled than in other focal lengths displaying steeper or more asymmetric degradation. This confirms the conclusions of the preceding analyses: the 100 mm combines high resolving power with a gradual decline in contrast, resulting in an image of exceptional overall stability.

The **35 mm** lens likewise demonstrates highly balanced behavior. Although its central values are slightly lower than those of the 100 mm, it maintains excellent consistency between the image center and the corners. Peripheral degradation is present but remains gradual rather than abrupt, explaining the strong sense of spatial continuity and homogeneous texture observed in the representative image frames.

The **50 mm** occupies an intermediate position within the series. Its central resolving power is satisfactory, but the separation between the center and the corners becomes more evident. The image remains clear along the optical axis, although fine-detail contrast declines more rapidly outside the central region.

The **75 mm** exhibits a less uniform behavior. While maintaining relatively high central values, the upper-left corner shows a pronounced decline, particularly in MTF30. This indicates an earlier loss of contrast in certain peripheral regions of the image field, resulting in a less spatially uniform image.

The **135 mm** displays moderate central values, but the difference between the two corners is less pronounced than in the 75 mm. Peripheral resolving power remains clearly lower than at the image center, although the transition is more gradual and better controlled.

The **180 mm** is arguably the least spatially balanced lens in the series. Although the image center retains a respectable level of resolving power, peripheral degradation is considerably more pronounced, particularly in the lower-right corner. The difference between the center and the edge is greater than in the other focal lengths, suggesting an image that is more directional in character: highly effective at concentrating visual attention along the optical axis, but less uniform toward the extremes of the frame.

Several focal lengths also exhibit noticeable differences between opposite corners, indicating that the spatial response is not entirely uniform across the image field.

Another important aspect of the graph is the relationship between MTF50 and MTF30. In the most consistent focal lengths—particularly the 35 mm and the 100 mm—the separation between the two curves remains relatively large and stable even away from the image center. This indicates that contrast does not collapse abruptly as spatial frequency increases, but instead declines more gradually. From a visual standpoint, this behavior generally translates into images with greater tonal continuity, stronger volumetric rendering, and richer textural density.

By contrast, the focal lengths exhibiting the strongest peripheral degradation show a progressive convergence of the MTF50 and MTF30 curves toward the image corners. This suggests a more rapid loss of microcontrast and a less stable transition of fine detail toward the image periphery.

Overall, the graph demonstrates that the lens series is organized not only by absolute levels of resolving power, but also by the way each focal length distributes that resolving power across the image field. Certain lenses—such as the 35 mm—prioritize spatial uniformity and visual continuity, whereas others—most notably the 100 mm—stand out for their exceptionally high central resolving power and stable contrast transfer. Still others, particularly the 180 mm, concentrate their performance around the optical axis while allowing a more pronounced degradation toward the image periphery.

Adriana Bernal, ADFC, preparing a shot during the production of Indeleble.

From a cinematographic perspective, these differences should not be interpreted as a hierarchy of optical quality, but rather as distinct approaches to directing visual attention, shaping spatial depth, and rendering image texture. The variations between focal lengths primarily affect the spatial distribution of resolving power and contrast rather than the overall visual identity of the image. Throughout the series, the lenses maintain a remarkably consistent optical signature in terms of texture, tonal transitions, and contrast rendering, allowing changes in focal length that are perceptible yet remain visually organic and coherent.

Comparison of Lateral Chromatic Aberration Across the Lens Series

Focal Length (mm)	Center CA Area (px)	Center CA Crossing (px)	Left Side CA Area (px)	Left Side CA Crossing (px)	Right Side CA Area (px)	Right Side CA Crossing (px)
35	0,148	0,158	1,94	1,63	1,83	1,54
50	0,302	0,172	2,84	2,3	2,94	2,36
75	0,392	0,278	1,5	1,2	1,68	1,59
100	0,262	0,0947	1,74	1,23	1,5	1,15
135	0,0776	0,0548	1,97	1,36	2,04	2,1
180	0,376	0,106	1,37	0,864	1,23	0,971

Table 19

The two graphs (*Figs. 106 and 107, and Table 19*) provide a clear overview of how lateral chromatic aberration is distributed across the lens series and, more importantly, how it varies spatially between the image center and the peripheral regions of the frame. The distinction between *CA Area* and *CA Crossing* is particularly valuable because it avoids conflating two different aspects of optical behavior: the overall magnitude of chromatic aberration and the way in which the color channels converge or diverge across the image field.

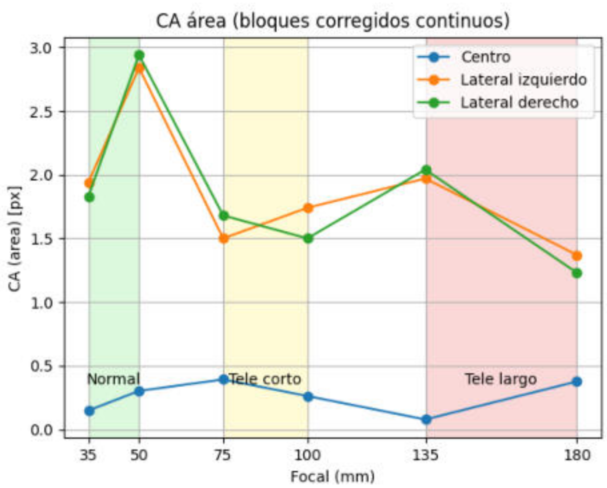

Figure 106

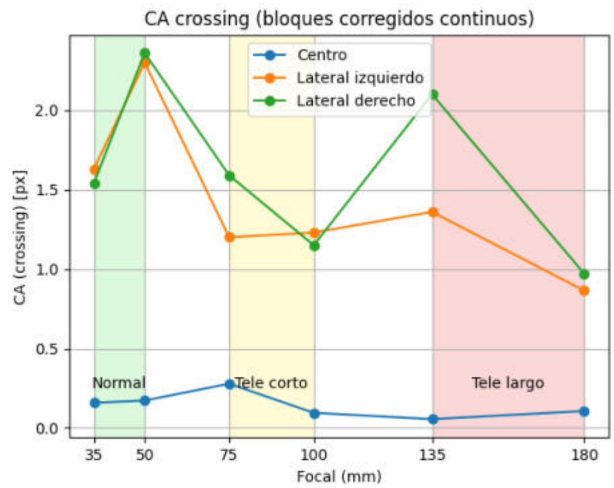

Figure 107

The graphs reveal that the image center maintains consistently low levels of lateral chromatic aberration across all focal lengths. In both *CA Area* and *CA Crossing*, the central values remain clearly separated from those measured in the lateral regions. This confirms that the lens series provides excellent chromatic correction along the optical axis, with lateral chromatic aberration becoming significant primarily toward the edges of the image field. From a cinematographic perspective, this is particularly important, as the principal subject—typically positioned near the center of the frame—retains a clean image, free from noticeable chromatic halos or pronounced channel separation.

The most significant differences emerge in the lateral regions of the image. The **50 mm lens** represents the point of maximum chromatic aberration within the series. Both *CA Area* and *CA Crossing* reach their highest lateral values at this focal length, approaching 3 pixels for *CA Area* and exceeding 2 pixels for *CA Crossing*. This indicates the potential for more visible chromatic separation toward the image periphery. Nevertheless, the behavior remains highly symmetrical between the left and right sides of the frame, suggesting a well-structured and uniform aberration pattern rather than an irregular optical defect or mechanical decentering. Visually, this is generally expressed as subtle chromatic fringing along high-contrast edges near the frame boundaries, particularly in scenes containing fine structures or visually complex backgrounds.

The **75 mm** lens still exhibits relatively high levels of lateral chromatic aberration, although both metrics show a reduction compared with the peak observed in the 50 mm, particularly in the *CA Crossing* graph. This transition places the 75 mm in an intermediate position within the series: it retains some of the chromatic expansion characteristic of the normal focal lengths while beginning to approach the more controlled behavior of the longer telephoto lenses.

The **100 mm** occupies an interesting position within the series. In terms of *CA Area*, the lateral values remain moderate, whereas *CA Crossing* reveals a certain asymmetry between the two sides of the frame. This suggests that, although the overall magnitude of the chromatic aberration is not excessive, the spatial distribution of chromatic displacement is not entirely uniform. Even so, the measured values remain well within a controlled range and are fully consistent with the overall behavior of the lens series.

The **135 mm** lens displays perhaps the most distinctive chromatic behavior of the group. In *CA Area*, the lateral values increase again, particularly on the right side of the image, while *CA Crossing* exhibits the greatest asymmetry between opposite corners. The right side clearly exceeds the left, once again approaching relatively high *CA Crossing* values. This suggests a more complex spatial redistribution of chromatic aberration than that observed in the other focal lengths. Although this does not necessarily translate into a significant issue in practical cinematographic imaging, it does indicate that the image periphery may respond somewhat less uniformly.

The **180 mm** substantially reduces lateral *CA Crossing* compared with both the 135 mm and the 50 mm, while still maintaining moderate *CA Area* values. The result is an image that, although retaining a degree of peripheral chromatic expansion, avoids overly aggressive chromatic separation. Its chromatic behavior is therefore more restrained and more stable than might typically be expected from a long telephoto lens.

Overall, the graphs depict a remarkably coherent optical system. Although clear differences exist among the focal lengths—particularly toward the image periphery—no abrupt discontinuities in chromatic behavior are observed. Chromatic aberration remains very well controlled at the image center and increases progressively toward the lateral regions, following a relatively continuous pattern throughout the lens series. The greatest variations occur among the normal and short telephoto lenses—especially the 50 mm and, to a lesser extent, the 75 mm—whereas the longer telephoto lenses tend to redistribute chromatic aberration in a more spatially irregular, though not necessarily more intense, manner.

From a cinematographic standpoint, these differences are likely to be perceived primarily as subtle variations in texture and spatial rendering rather than as obvious optical defects. The overall coherence of the lens series is preserved because chromatic aberration never reaches extreme levels nor introduces major discontinuities between focal lengths.

Despite the differences revealed by the measurements, the analysis of the actual motion-picture frames does not reveal lateral chromatic aberration that would be considered visually problematic, even in areas of high contrast. This suggests that, although chromatic channel separation is measurable, its magnitude remains within a visually well-controlled range under normal cinematographic conditions. In practice, the chromatic behavior of the lens series proves to be stable and coherent, without conspicuous chromatic halos or discontinuities that would significantly affect the overall perception of the image.

Each lens retains a subtly distinct personality in the way it distributes chromatic aberration toward the image periphery, yet all remain faithful to the same underlying optical philosophy: a clean optical axis, a gradual transition toward the edges, and well-controlled chromatic degradation.

Adriana Bernal: *I was very pleased with the color rendering of the lenses. I never noticed any problematic color casts or significant differences between focal lengths that would have affected our workflow during production. We had not yet reached the final color grade, but this was something we were already able to evaluate through the workflow we established for the dailies and stills generated during the shoot. Overall, the lens series behaved in a highly consistent manner.*
It is also worth remembering that Indeleble was conceived from the outset with a deliberately desaturated visual style, at times approaching black-and-white. Even so, neither on the production

monitor, nor on the vectorscope, nor in the still frames we generated each day did we observe color tendencies that required constant correction or forced us to reconsider our imaging strategy.
The laboratory tests likewise revealed a well-controlled chromatic response. Lateral chromatic aberration is certainly present, particularly toward the image periphery, but in real motion-picture frames it is rarely perceptible. The image maintains a highly stable chromatic rendering, and that consistency was instrumental in preserving the overall visual coherence of the film.
The Arles lenses exhibit a remarkably neutral color response—or, at the very least, one that is sufficiently transparent to allow the color grading and the film's visual concept to become the primary factors defining the final look of the image.

Geometric Distortion

The graph (*Fig. 108*) illustrates the evolution of the lens series' SMIA geometric distortion from the 35 mm to the 180 mm focal length. Negative values correspond to barrel distortion, whereas positive values indicate a slight tendency toward pincushion distortion. The dashed horizontal line marks the zero-distortion reference.

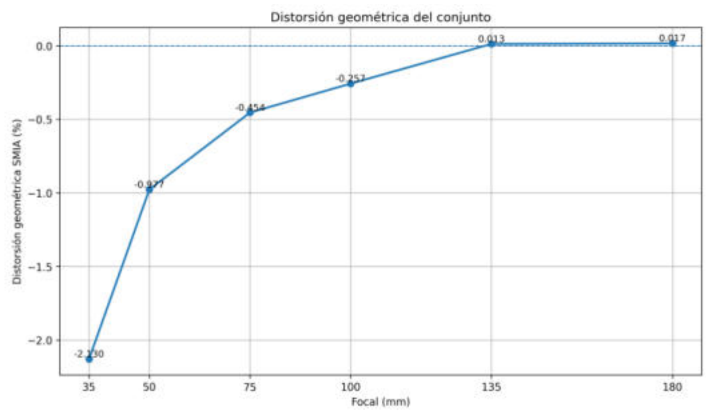

Figure 108

The first observation is straightforward: geometric distortion decreases progressively as focal length increases. The 35 mm lens exhibits the greatest geometric distortion in the series, at approximately –2.13%, a relatively high value but one that remains entirely consistent with the expected behavior of a moderately wide-angle lens. Visually, this is expressed as a slight expansion of space and a gentle outward curvature of straight lines toward the edges of the frame, particularly noticeable in architectural subjects, interior scenes, or objects positioned close to the camera.

The 50 mm lens reduces this distortion substantially, with a value close to –1%. Although a slight barrel distortion is still present, the image already appears considerably more geometrically stable. This behavior reflects the natural transition from the wide-angle group toward the more neutral focal lengths.

The 75 mm and 100 mm continue this gradual progression toward geometric neutrality. With distortion values of approximately –0.45% and –0.25%, respectively, geometric distortion becomes visually very well controlled. Under normal cinematographic conditions, these levels are rarely perceptible except in scenes containing strongly defined architectural lines or highly symmetrical compositions.

The most interesting behavior appears in the 135 mm and 180 mm lenses. Both lie essentially on the zero-distortion axis, with values only slightly above 0%. This indicates an exceptionally stable and virtually neutral geometric rendering. From a visual standpoint, straight lines remain natural, and any geometric deformation becomes effectively imperceptible. At these focal lengths, the visual character of the image is therefore determined far more by the natural perspective compression associated with the focal length than by any geometric distortion introduced by the lens itself.

The most significant aspect of the series is not merely that distortion decreases toward the longer focal lengths—a behavior that is largely expected—but the smooth and continuous manner in which this transition occurs. No abrupt changes or erratic behavior are observed between consecutive focal lengths. This provides the lens series with a high degree of geometric consistency and allows changes of focal length within the same sequence without producing abrupt alterations in the spatial structure of the image.

From a cinematographic perspective, the overall behavior of the series is particularly well balanced. Even the 35 mm lens, despite exhibiting the highest level of distortion within the group, remains sufficiently well controlled to provide a natural spatial representation in the vast majority of narrative situations. From the 75 mm onward, distortion is substantially reduced, while in the longer telephoto lenses geometric deformation becomes virtually imperceptible.

Overall, the graph reveals an optical system whose geometric rendering becomes progressively more stable as focal length increases. Although measurable differences exist among the individual lenses, they remain fully consistent with a coherent and continuous optical design, facilitating smooth transitions between focal lengths while preserving a stable spatial representation throughout the entire lens series.

Adriana Bernal: *I found the lens series to be remarkably consistent across the entire focal-length range. We worked with a very broad set—from 14 mm to 180 mm—and, overall, the lenses maintained a coherent visual identity throughout. There was clear continuity in texture, contrast, and in the way they rendered the image toward the edges of the frame.*

That consistency was also reflected in the technical tests. Although there were the expected differences between focal lengths—for example, greater geometric distortion in the wide-angle lenses or a more noticeable fall-off in resolving power with some of the telephoto lenses—the overall behavior of the series followed a continuous and coherent pattern. None of the lenses felt as though they belonged to a different optical system, nor were there abrupt changes in color, contrast, or optical character when moving from one focal length to another.

The only lens with which I never felt completely comfortable was the 75 mm. That was not because of any optical limitation, but rather a matter of habit and visual language. To me, it felt slightly too short to occupy the role that an 85 mm traditionally fills in many cinema lens sets.

I honestly don't remember which focal lengths we used the most, perhaps because no single focal length dominated the production. We relied extensively on the longer telephoto lenses—particularly the 135 mm and the 180 mm—but we also used the wide-angle lenses very frequently, especially the 14 mm, 21 mm, and 25 mm.

I think that choice was closely tied to the way we wanted to construct cinematic space throughout the film. The telephoto lenses helped us convey the characters' sense of isolation by compressing space and separating them from their surroundings without relying on extremely shallow depth of field. Conversely, the wide-angle lenses were essential for creating the spatial unease that defines many of the film's scenes. The 14 mm and the 21 mm, in particular, allowed us to work very close to the characters while maintaining a powerful relationship with the surrounding environment. And although the laboratory tests showed a certain amount of geometric distortion together with a

gradual loss of resolving power toward the edges of the frame, I never felt that these focal lengths distorted space in an excessive or distracting way.
In the end, I think the film constantly moved between those two visual extremes: one built around an intimate, spatially expansive perspective created with the wide-angle lenses, and another built around the compression and isolation produced by the telephoto lenses.
Throughout the film, we paid close attention to the way spatial planes were organized, particularly in depth, and that was closely connected to both the lighting design and our choice of focal lengths. We frequently staged scenes in which the characters moved through gradients of light or crossed multiple layers of depth within the frame, so it was essential that the lenses could faithfully sustain that spatial construction. I believe the Arles lenses performed exceptionally well in that respect.

Acknowledgments

Adriana Bernal ADFC, Jairo Estrada, Juan Pablo Bonilla
https://bernaladriana.com/
https://www.alfonsoparra.com/

All behind-the-scenes photographs are reproduced courtesy of Sagitario Film.

In Collaboration With